



Technische Universiteit Delft
Faculteit Elektrotechniek, Wiskunde en Informatica
Delft Institute of Applied Mathematics

**Bepalen van het massatraagheidsmoment
met behulp van een bifilar pendulum**
**(Determining the moments of inertia using a
bifilar pendulum)**

Verslag ten behoeve van het
Delft Institute of Applied Mathematics
als onderdeel ter verkrijging

van de graad van

BACHELOR OF SCIENCE
in
TECHNISCHE WISKUNDE

door

WOUTER SWART

Delft, Nederland
Mei 2016



BSc verslag TECHNISCHE WISKUNDE

“Bepalen van het massatraagheidsmoment met behulp van een bifilar pendulum”

(Determining the moments of inertia using a bifilar pendulum)

WOUTER SWART

Technische Universiteit Delft

Begeleider

Dr.ir. D.R. van der Heul

Overige commissieleden

Drs. E. M. van Elderen

Dr. H. M. Schuttelaars

Mei, 2016

Delft

Contents

1	Introduction	7
2	Equations of motion of the solar boat	9
3	Determination of moments of inertia	13
4	Equations of motion with constraints	17
4.1	Newtonian mechanics	17
4.2	'Smart' Newtonian mechanics	18
4.3	Lagrangian mechanics	18
4.4	Kane's Method [4]	21
4.5	Example: Spherical pendulum	24
5	Bifilar pendulum	31
5.1	Kane's method	32
5.2	Lagrangian mechanics	40
6	Verification equations of motion	45
6.1	Side-Sway	45
6.2	Torsional movement	47
6.3	Suspended object with dimensions	51
6.4	Comparison paper: cylinder	53
7	Applications equations of motion	57
7.1	Linearization	57
7.2	Tensional forces	61
8	Solar Boat	67
8.1	Geometric model	67
8.2	Suspension	69
8.3	Motion of configurations	70
8.4	Tensional forces	73
9	Conclusion & Discussion	77
10	Appendix A	79
11	Appendix B	87

1. Introduction

The TU Delft Solar Boat Team participates in the *Dong Energy Solar Challenge* and the *Solar1 Cup* for high-speed solar powered boats. Their current design utilizes two T-shaped hydrofoils. The forward hydrofoil is equipped with flaps, which can be actively controlled to lift the hull from the water, decreasing drag. Although this design results in high speeds, the boat is easily turned over due to the lack of roll stability. The stability analysis to overcome this problem requires the input of the three moments of inertia along the main axes of rotation.

In an earlier bachelors project a start was made with the stability analysis of the Solar boat. In this project, six nonlinear second-order differential equations were formulated to describe the motion of the boat, three for the position and three for the orientation. These were subsequently reformulated as a system of twelve nonlinear first-order ordinary differential equations. After linearization around one of the pseudo-equilibrium points, the stability of the boat can be assessed by computing the eigenvalues of the matrix of the dynamical system. The accuracy of this analysis relies heavily on the input parameters; the lift and drag coefficients of the hydrofoils and control surfaces, but also on the moments of inertia.

As stated by Newton's first law of motion, 'an object either remains at rest or continues to move at a constant velocity, unless acted upon by an external force'. Inertia is a measure for this resistance of an object to change its current linear movement. The rotational counterpart of this is moment of inertia, which describes an object's resistance to change to its current rotational movement. Using a bifilar pendulum, a two-suspension wire pendulum, this moment of inertia can be determined experimentally. For a given configuration of the pendulum, that is; the relevant lengths and angles of the suspension wires along with the orientation of the object, the period of the rotational motion of the object can be directly related to the moment of inertia around the axis of rotation. This project aims at designing an optimal procedure to suspend the Solar Boat using a bifilar pendulum and to measure the moments of inertia.

The project will aim at answering two main research questions:

- How should the Solar Boat be suspended to measure the three moments of inertia taking into consideration the accuracy of the measured moments of inertia and the practicality of the procedure?
- Is it possible to quantitatively predict the accuracy of the determined moments of inertia?

2. Equations of motion of the solar boat

In a previous project, a start was made with analyzing the motion stability of the Solar boat. This project used Newton's second law of motion to derive the equations of motion of the boat:

$$M \frac{d^2 \mathbf{x}}{dt^2} = \sum_i F_i. \quad (2.0.1)$$

In this equation, M is the mass of the object, \mathbf{x} its position and F_i are the forces working on the object. This equation requires all the forces acting on the boat to be known. These forces can be described either in a earth-fixed or a body-fixed reference frame, respectively $[x, y, z]$ and $[x', y', z']$ as illustrated in the figure below.



Figure 2.0.1: Earth- and body-fixed frames of reference

In a earth-fixed reference frame, the axes do not change with the movement of the boat and stay stationary relative to earth. In a body-fixed reference frame, the axes change with the rotation of the boat such that they stay stationary relative to the boat. Since all forces, except the gravitational force, are stationary relative to the boat it is convenient to describe them in a body-fixed reference frame. The origin of the reference frame is chosen to be the center of mass of the boat. For each of the axes, all forces can be explicitly expressed in terms of the boat's

speed. Doing so results in the following three nonlinear second-order differential equations:

$$\begin{aligned} M \frac{d^2 x'}{dt^2} &= F_{x'} , \\ M \frac{d^2 y'}{dt^2} &= F_{y'} , \\ M \frac{d^2 z'}{dt^2} &= F_{z'} , \end{aligned} \tag{2.0.2}$$

here $F_{x'}, F_{y'}, F_{z'}$ capture all the forces working in that particular direction. The solution to this system of differential equations gives the motion of the boat in the body-fixed reference system. In order to get the motion in the earth fixed reference system, a translation has to be made between the two systems. In the project, a rotation matrix $R(\phi_1, \phi_2, \phi_3)$ is constructed which describes a rotation around the x -, y - and z -axis respectively along angles ϕ_1 , ϕ_2 and ϕ_3 . To make a translation from a body-fixed reference system to a earth-fixed reference system, the inverse of this matrix can be used. All forces (except gravity) captured in equations (2.0.2) are working along the axes in a body-fixed coordinate system. Writing these equations in matrix form, writing the system as a system of first-order differential equations and multiplying with the inverse rotation matrix yields a system of differential equations of which the solution describes the position in a earth-fixed reference system:

$$\begin{aligned} \frac{d\mathbf{x}_1}{dt} &= \mathbf{x}_2 , \\ M \frac{d\mathbf{x}_2}{dt} &= R^{-1}(\boldsymbol{\phi}) \sum_i F'_i \left(\frac{dR(\boldsymbol{\phi})}{dt} \mathbf{x}_1 + R(\boldsymbol{\phi}) \mathbf{x}_2 \right) - Mg\hat{z} , \end{aligned} \tag{2.0.3}$$

where $\mathbf{x}_1 = [x, y, z]^T$, $\mathbf{x}_2 = \frac{d\mathbf{x}_1}{dt}$ and it has been used that:

$$F_i = R(\boldsymbol{\phi})^{-1} F'_i \left(\frac{d\mathbf{x}'}{dt} \right) .$$

These differential equations give expressions for the position of the boat, and its time derivatives. However, these depend on the angles of rotation $\boldsymbol{\phi}$ of the boat, which are therefore also calculated.

To calculate the angles of rotation, a torque balance is used to derive expressions for the orientations along the three body-fixed axes. Euler's equations are used to describe the rotation along the three principle axes:

$$\begin{aligned} I_1 \dot{\omega}_1 + (I_3 - I_2) \omega_2 \omega_3 &= M_1 = \sum_i (r_i \times F'_i)_1 , \\ I_2 \dot{\omega}_2 + (I_1 - I_3) \omega_3 \omega_1 &= M_2 = \sum_i (r_i \times F'_i)_2 , \\ I_3 \dot{\omega}_3 + (I_2 - I_1) \omega_1 \omega_2 &= M_3 = \sum_i (r_i \times F'_i)_3 . \end{aligned} \tag{2.0.4}$$

In these equations, the angular speed ω_i is given by the time derivative of the angle around the corresponding axis; $\dot{\theta}_i$, and the moments of inertia I_1, I_2, I_3 are those around the axes x' , y' and z' of the body-fixed reference system respectively. Furthermore, the orientations of the forces relative to the body-fixed reference system do not change. The same holds for the radius r_i , and as a result $r_i \times F'_i$ has a constant direction $c_i F'_i$, where c_i is the effective arm of force F'_i .

Substitution of all this results in the equations:

$$\begin{aligned}
I_{x'} \frac{d^2 \phi_1}{dt^2} + (I_{z'} - I_{y'}) \frac{d\phi_2}{dt} \frac{d\phi_3}{dt} &= \sum_i (c_i F'_i)_{x'} , \\
I_{y'} \frac{d^2 \phi_2}{dt^2} + (I_{x'} - I_{z'}) \frac{d\phi_3}{dt} \frac{d\phi_1}{dt} &= \sum_i (c_i F'_i)_{y'} , \\
I_{y'} \frac{d^2 \phi_3}{dt^2} + (I_{y'} - I_{x'}) \frac{d\phi_1}{dt} \frac{d\phi_2}{dt} &= \sum_i (c_i F'_i)_{z'} .
\end{aligned} \tag{2.0.5}$$

Finally, these equations are written in matrix form and transformed to a first-order system by defining $\boldsymbol{\rho}_1 = \boldsymbol{\phi}$, $\boldsymbol{\rho}_2 = \frac{d\boldsymbol{\phi}}{dt}$ in (2.0.5) and combined with equation (2.0.3), the following system of differential equations is obtained:

$$\begin{aligned}
\frac{d\mathbf{x}_1}{dt} &= \mathbf{x}_2 , \\
M \frac{d\mathbf{x}_2}{dt} &= R^{-1}(\boldsymbol{\rho}_1) \sum_i F'_i \left(\frac{dR(\boldsymbol{\rho}_1)}{dt} \mathbf{x}_1 + R(\boldsymbol{\rho}_1) \mathbf{x}_2 \right) - Mg\hat{z} , \\
\frac{d\boldsymbol{\rho}_1}{dt} &= \boldsymbol{\rho}_2 , \\
\mathbf{I} \frac{d\boldsymbol{\rho}_2}{dt} + \boldsymbol{\rho}_2 \times (\mathbf{I}\boldsymbol{\rho}_2) &= \sum_i \left(c_i F'_i \left(\frac{dR(\boldsymbol{\rho}_1)}{dt} \mathbf{x}_1 + R(\boldsymbol{\rho}_1) \mathbf{x}_2 \right) \right) ,
\end{aligned} \tag{2.0.6}$$

where F'_i has been defined as:

$$F'_i = \begin{pmatrix} F_m + D_B + D_b + D_f + \sum_{i=1}^4 D_i \\ F_s + L_b + L_f \\ \sum_{i=1}^4 L_i \end{pmatrix} ,$$

such that all terms are forces resulting from lift and drag. The solution to the system of equations given in (2.0.6) describes the position and orientation of the Solar boat as a function of time. A numerical integration method of choice can be used to solve this system. The accuracy of this solution depends heavily on the accuracy of the input parameters; the resistance coefficients and moments of inertia. Therefore, in order to be able to describe the motion of the boat accurately it is imperative to have a good estimation of these input parameters.

In this previous project, the moments of inertia $I_{x',y',z'}$ of the Solar Boat have been approximated using a geometric approximation method for the Solar Boat. The accuracy of the moments of inertia obtained in this way is low, since the boat was very coarsely approximated. This project will focus on a procedure to determine the mass moments of inertia $I_{x',y',z'}$ of the Solar Boat more accurately and aims at designing an optimal procedure to determine these quantities using a bifilar pendulum. The next section will discuss several methods for obtaining the moments of inertia of an object. Furthermore, the tensional forces the Solar Boat will experience while suspended by the bifilar pendulum will be determined. These are of practical interest to check whether the solar deck of the boat will be able support itself. The results obtained for the Solar Boat will be presented in section 8.

3. Determination of moments of inertia

Intuitively, the moment of inertia of an object is a measure for an object's resistance to change to its angular speed. More formally it is the torque required for an angular acceleration along a chosen axis of $1 \frac{\text{rad}}{\text{s}^2}$. The moment of inertia, I , can be calculated by summing over the product of mass m and its perpendicular distance to the rotation axis squared r^2 : mr^2 for every particle in the object. For objects which consist of a finite number of particles, this results in a finite sum. If the object is continuous, this summation becomes an integration over $r^2 dm$ over all the infinitesimally small mass elements where r is the perpendicular distance from mass element dm to the axis of rotation:

$$I = \int_V r^2 dm .$$

This definition states that mass with a large perpendicular distance to the axis of rotation contributes more to the moment of inertia than that mass with a smaller perpendicular distance. The above formula requires integrating over the volume of an object. For most simple geometries this integration can be easily done. However, once an object takes on a complex shape, such as the Solar boat, this becomes nearly impossible. In these cases, an approximation method can be used to estimate the value of the moment of inertia.

One method for approximating the moment of inertia is by approximating the geometry of the object with a combination of basic geometries such as cylinders, beams and rectangular blocks. An example of such an approximation can be seen in the figure below.

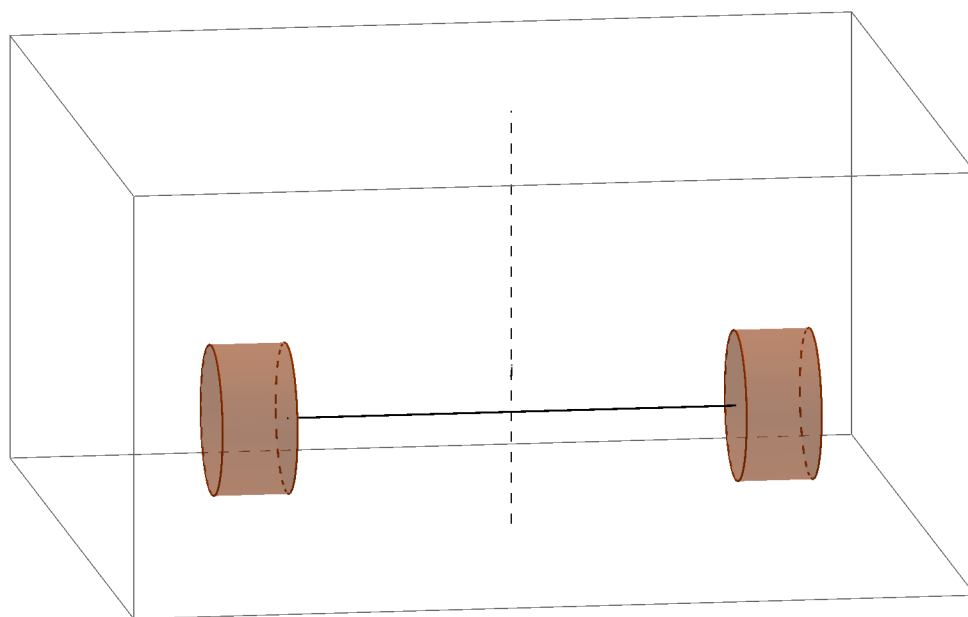


Figure 3.0.1: Approximation of a dumbbell by two solid cylinders.

In this figure, the weights of the dumbbell, with massless handle, have been approximated using two solid cylinders. The estimated moment of inertia of the dumbbell about the dotted axis is the sum of the two moments of inertia of the cylinders about that axis.

For each of these basic geometries the moment of inertia I_i can be determined using the definition given above or calculated using known expressions for these geometries. Adding all these values yields an estimation for the moment of inertia of the original object I :

$$I = \sum_i I_i.$$

The moment of inertia is calculated along the rotational axes through the center of mass of the solar boat. This center of mass can be determined by taking the weighted average of the centers of mass of all approximation geometries i :

$$r_{CM} = \frac{\sum_i m_i r_i}{M},$$

in which M is the total mass of the boat and m_i , r_i respectively the mass and distance to the rotational axis for element i . When calculating the moment of inertia of each element i , it has to be taken into account that the required moment of inertia is along a different axis than the axis going through element i 's center of mass. For this, the Parallel axis theorem can be applied to calculate the moment of inertia along the correct rotational axis.

As an example of the above described procedure, consider the dumbbell from figure (3.0.1). Assume each weight of the dumbbell has a weight of $m = 10$ kilograms, the distance from the middle of the handle to the center of mass of each weight is $d = 0.06$ meters and the weights have a radius of $r = 0.10$ meters and width of $l = 0.05$. The moment of inertia will be calculated about the dotted line; the perpendicular bisector of the handle. Since this problem is symmetric around this axis, the moment of inertia of the dumbbell can be written as:

$$I = 2I^*,$$

where I^* is the moment of inertia of one weight about the dotted axis. For a cylinder it is known that the moment of inertia about an axis perpendicular to the central axis and through the center of mass is given by:

$$\begin{aligned} I_p^* &= \frac{1}{4}mr^2 + \frac{1}{12}ml^2 \iff \\ &= \frac{13}{480}. \end{aligned}$$

Now, to calculate the moment of inertia about the dotted axis, the Parallel Axis Theorem can be applied:

$$\begin{aligned} I^* &= I_p^* + md^2 \iff \\ &= \frac{757}{12000}. \end{aligned}$$

The moment of inertia of the dumbbell about the dotted axis thus becomes:

$$I = \frac{1514}{12000}.$$

Obviously, the accuracy of this approach relies on how accurate an object's shape can be approximated with basic geometries. It is clear that the accuracy of the estimate increases as

the size of the approximating geometries decrease, as a result of the shape of the object more accurately being approximated. On the other hand, decreasing the size of the approximating geometries results in more of these geometries. Therefore, a consideration has to be made between the desired accuracy of the approximation and the computational time required to perform the calculations.

Another method to approximate the moment of inertia is deriving it experimentally using a bifilar pendulum; a two-suspension wire pendulum. One such bifilar pendulum is shown in the figure below.

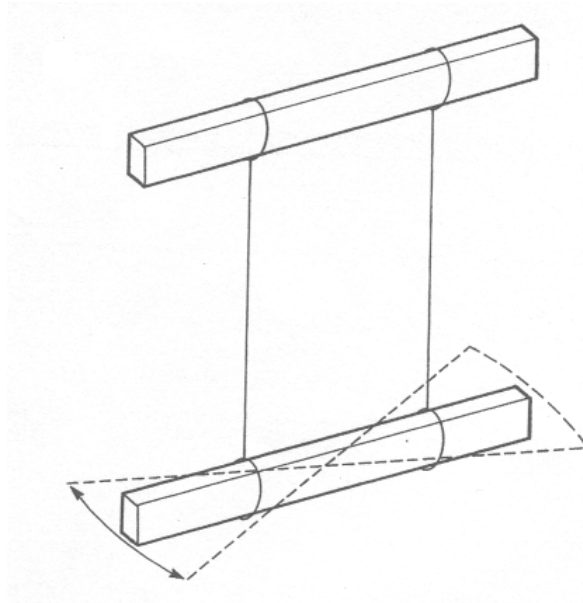


Figure 3.0.2: Bifilar Pendulum

For a given configuration of the pendulum, that is the mass of the object, the angles and length of the suspension wires, the period of rotational motion can be linked to the moment of inertia along that rotational axis. This relation can be retrieved from the equations of motion of the particular configuration of the bifilar pendulum. Performing the actual experiment is sometimes impractical due to the fact that there are no attachment points for the suspension wires on the object. In such case, a platform (with known moment of inertia) can be used to carry the object on it. Doing this results in the moment of inertia of the two object combined. Subtraction of the moment of inertia of the platform yields the desired moment of inertia of the object.

In this project, a numerical model will be made of the solar boat suspended by the bifilar pendulum. The equations of motion from this model will then be analyzed to attempt to obtain an optimal configuration for the bifilar pendulum such that the error in the estimation of the moment of inertia is smallest. To do this, the equations of motion of the solar boat suspended by a bifilar pendulum have to be determined. The suspension wires of the bifilar pendulum prevent the solar boat to move in certain directions. This makes the equations of motion special, in the sense that they contain these constraints. First, a less complex system will be considered to see which method is easiest in obtaining equations of motion with such constraints. The system which will be looked at is a pendulum which is not restricted to swing only in a plane, which will be referred to as a spherical pendulum (a second example of a 'planar' pendulum can be found in appendix A). The found method will then be applied to the bifilar

pendulum to obtain the equations of motion of the bifilar pendulum. It is important to note that these equations of motion are unique, and that every method which will be considered can result in a different formulation of a equation of motion, but describe the same unique solution.

4. Equations of motion with constraints

The equations of motion of a system are equations which describe the position and orientation of the system as a function of time. There are multiple ways of deriving the equations of motion of a system, some of these are:

- The classical Newtonian approach using Newton's second law of motion,
- A 'smart' Newtonian approach where in advance a preferable set of coordinates is known,
- The Lagrangian approach,
- Kane's Method.

The first three of these approaches will be elaborated on for point masses. Since a point mass has no dimension, orientation is not relevant and only the position will be considered. Kane's method will be described for objects with dimensions, since an explanation of Kane's method for point masses would not be sufficient for using this method for objects with dimensions. After these elaborations, each of the methods will be applied to the spherical pendulum to derive the equations of motion which contain constraints. From this examples, it will become evident that the certain approaches have advantages over others when dealing with these constraints.

4.1 Newtonian mechanics

Newton's second law of motion states that the rate of change of an object's momentum $\mathbf{p}(t) = m \cdot \mathbf{v}(t)$ equals the sum of the external forces. Now, consider a system of n connected particles each with mass m_i and acceleration \mathbf{a}_i ($i = 1, \dots, n$) and assume the mass does not change in time. The above equation can then be written as:

$$\sum_{i=1}^n \mathbf{F}_i = \left(\sum_{i=1}^n m_i \right) \mathbf{a}_o, \quad (4.1.1)$$

where \mathbf{F}_i is the force on particle i and \mathbf{a}_o is the acceleration of the center of mass of the system. Since all the internal forces between the particles cancel out, this can also be written as:

$$\mathbf{F}_{Ext} = \left(\sum_{i=1}^n m_i \right) \mathbf{a}_o, \quad (4.1.2)$$

here \mathbf{F}_{Ext} is the net external force on the system. Division of this equation by $\sum_{i=1}^n m_i$ yields a second-order differential equation which can be solved to get a expression for the position of the center of mass of the system as a function of time.

In some cases, the constraint force F_c is part of the given problem. However, when looking for example at a pendulum, the constraint force of the suspension wire is not known. In these cases, the constraint force can be calculated separately from the equation of motion by

decomposing the other forces along the extension of the constraint force and then using that $F_c + F_{net,other} = ma_c$, where a_c is the centripetal acceleration. This yields an extra equation for the constraint force which can be solved together with the equation of motion found using the above.

4.2 'Smart' Newtonian mechanics

For most systems, it is usually not evident which set of coordinates describes the system most efficiently. When using this approach, one tries to choose the coordinates in such a way that the constraints are more easily incorporated in the problem since they coincide with the coordinate planes in state-space. Examples of systems where this choice is obvious are a planar pendulum and a spherical pendulum. A planar pendulum is a pendulum which is restricted to move in a plane, whereas a spherical pendulum does not have this restriction and can move in three dimensions. In these systems, it is known that polar- and spherical-coordinates work most conveniently since the constraint coincides with the coordinate planes. The practical use of this approach is small, since usually this knowledge on the choice of coordinates follows from the actual equations of motion and is thus not applicable for systems of which the movement is not known in advance.

4.3 Lagrangian mechanics

In the Lagrangian approach, Lagrange's equation is used to derive the equations of motion of a system:

$$\frac{d}{dt} \frac{\partial L}{\partial \dot{q}} - \frac{\partial L}{\partial q} = 0. \quad (4.3.1)$$

In this equation, L is the so-called Lagrangian, a function of the kinetic- and potential energy of the system and q is a generalized coordinate. If the system requires n generalized coordinates q_i to be defined to capture the state of the system, there will also be a Lagrange's equation for each of the q_i .

Equation (4.3.1) can be derived from d'Alembert's principle. This principle states that for a system of n particles the sum over the difference between the external forces working on particle i and the change in momentum of that particle, multiplied by a virtual displacement is 0:

$$\sum_{i=1}^n (\mathbf{F}_i - \dot{\mathbf{p}}_i) \cdot \delta \mathbf{r}_i = 0. \quad (4.3.2)$$

The constraint forces are not taken into account here since there cannot be a virtual displacement $\delta \mathbf{r}_i$ in the direction of these forces, and thus including these forces in the equation above would only add 0 to the summation. A virtual displacement refers to a infinitesimal change in position at a given instance of time. The virtual displacement happens instantaneously without any time interval dt passing; hence why it is virtual, to distinguish it from an actual displacement where such a time interval does pass.

If it is assumed that the mass of any particle does not change with time the mass can be brought outside the time derivative and thus $\dot{\mathbf{p}}_i$ can be written as $m_i \mathbf{a}_i$. Substitution into equation (4.3.2) yields a more familiar form:

$$\sum_{i=1}^n (\mathbf{F}_i - m_i \mathbf{a}_i) \cdot \delta \mathbf{r}_i = 0.$$

In this form, with Newton's second law of motion it is immediately clear why this summation equals 0. In order to express d'Alembert's principle in Cartesian coordinates, 3 coordinates are needed for each particle; an x -, y - and z -coordinate. For a system of n particles, $3n$ coordinates would be needed to completely describe the system's position. Transforming this to generalized coordinates would also require $3n$ generalized coordinates. However, for each independent constraint the degrees of freedom of the system decrease by 1 and thus the number of required generalized coordinates. The transformation equations for the Cartesian coordinates assuming k independent constraints then becomes:

$$\begin{aligned} x_1 &= x_1(q_1, \dots, q_{3n-k}, t) \\ &\vdots \\ x_{3n} &= x_{3n}(q_1, \dots, q_{3n-k}, t) \end{aligned} \quad (4.3.3)$$

Another way of looking at this is by noting that the Cartesian coordinates form a dependent set of coordinates, where the dependencies result from the constraints. Assuming there are k constraints, k coordinates can be discarded to obtain a basis q_1, \dots, q_{3n-k} with which the system can be described.

Writing d'Alembert's principle in terms of Cartesian coordinates gives:

$$\sum_{i=1}^{3n} (F_i - m_i a_i) \cdot \delta x_i = 0. \quad (4.3.4)$$

Taking the derivative of the transformation equations from (4.3.3) leads to:

$$dx_i = \sum_{j=1}^{3n-k} \frac{\partial x_i}{\partial q_j} \delta q_j + \frac{\partial x_i}{\partial t} dt.$$

Since for a virtual displacement δx_i the time is assumed to be frozen, the last term vanishes in the expression for the virtual displacement:

$$\delta x_i = \sum_{j=1}^{3n-k} \frac{\partial x_i}{\partial q_j} \delta q_j. \quad (4.3.5)$$

With this expression, the summation over $F_i \delta x_i$ in the Cartesian version of d'Alembert (4.3.4) can be written as:

$$\sum_{i=1}^{3n} F_i \delta x_i = \sum_{i=1}^{3n} F_i \left(\sum_{j=1}^{3n-k} \frac{\partial x_i}{\partial q_j} \delta q_j \right) = \sum_{i=1}^{3n} \sum_{j=1}^{3n-k} \left(F_i \frac{\partial x_i}{\partial q_j} \right) \delta q_j = \sum_{j=1}^{3n-k} Q_j \delta q_j. \quad (4.3.6)$$

Here Q_j denotes the total virtual work done during the entire virtual displacement.

For the summation over the second part in the Cartesian version of d'Alembert (4.3.4) we have that:

$$\sum_{i=1}^{3n} m_i a_i \delta x_i = \sum_{i=1}^{3n} m_i a_i \sum_{j=1}^{3n-k} \frac{\partial x_i}{\partial q_j} \delta q_j = \sum_{i=1}^{3n} \sum_{j=1}^{3n-k} m_i \ddot{x}_i \frac{\partial x_i}{\partial q_j} \delta q_j. \quad (4.3.7)$$

This equation can be reformulated using:

$$\begin{aligned} \frac{d}{dt} \left(m_i \dot{x}_i \frac{\partial x_i}{\partial q_j} \right) &= m_i \ddot{x}_i \frac{\partial x_i}{\partial q_j} + m_i \dot{x}_i \frac{d}{dt} \frac{\partial x_i}{\partial q_j} \iff \\ m_i \ddot{x}_i \frac{\partial x_i}{\partial q_j} &= \frac{d}{dt} \left(m_i \dot{x}_i \frac{\partial x_i}{\partial q_j} \right) - m_i \dot{x}_i \frac{d}{dt} \frac{\partial x_i}{\partial q_j}, \end{aligned} \quad (4.3.8)$$

and noting that

$$\frac{\partial x_i}{\partial q_j} = \frac{\partial \dot{x}_i}{\partial \dot{q}_j}, \quad (4.3.9)$$

$$\frac{d}{dt} \frac{\partial x_i}{\partial q_j} = \frac{\partial v_i}{\partial q_j} = \frac{\partial \dot{x}_i}{\partial q_j}. \quad (4.3.10)$$

Equation (4.3.9) follows from the fact that, for a single particle, it holds that its Cartesian coordinates depend at most on all of the generalized coordinates; $x_i = x_i(q_1, q_2, q_3, t)$. The velocity of the particle in the x_i direction is the time derivative of this transformation, yielding:

$$v_i = \frac{dx_i}{dt} = \sum_{j=1}^3 \frac{\partial x_i}{\partial q_j} \frac{dq_j}{dt} + \frac{dx_i}{dt} = \sum_{j=1}^3 \frac{\partial x_i}{\partial q_j} \dot{q}_j + \frac{dx_i}{dt}.$$

This can be rewritten by using the fact that the order of taking partial derivatives does not influence the outcome. As a result it follows that:

$$\frac{\partial}{\partial \dot{q}_j} \frac{dx_i}{dt} = \frac{d}{dt} \frac{\partial x_i}{\partial \dot{q}_j} = 0,$$

and because the Cartesian coordinate x_i is independent of the generalized velocity \dot{q}_j , this quantity is equal to 0. Taking the partial derivative of v_i with respect to the generalized velocity \dot{q}_j and using twice that the above equation is equal to 0 leads to:

$$\begin{aligned} \frac{\partial v_i}{\partial \dot{q}_j} &= \frac{\partial}{\partial \dot{q}_j} \left(\sum_{h=1}^3 \frac{\partial x_i}{\partial q_h} \dot{q}_h + \frac{dx_i}{dt} \right) \\ &= \frac{\partial}{\partial \dot{q}_j} \sum_{h=1}^3 \frac{\partial x_i}{\partial q_h} \dot{q}_h + \frac{\partial}{\partial \dot{q}_j} \frac{dx_i}{dt} \\ &= \frac{\partial}{\partial \dot{q}_j} \sum_{h=1}^3 \frac{\partial x_i}{\partial q_h} \dot{q}_h + 0 \\ &= \sum_{h=1}^3 \left(\frac{\partial}{\partial \dot{q}_j} \frac{\partial x_i}{\partial q_h} \right) \dot{q}_h + \sum_{h=1}^3 \frac{\partial x_i}{\partial q_h} \frac{\partial \dot{q}_h}{\partial \dot{q}_j} \\ &= 0 + \sum_{h=1}^3 \frac{\partial x_i}{\partial q_h} \delta_{hj} \\ &= \frac{\partial x_i}{\partial q_j}, \end{aligned}$$

such that $\delta_{hj} = 1$ if and only if $h = j$, and $\delta_{hj} = 0$ for $h \neq j$. From this derivation equation (4.3.9) follows. Substitution of equations (4.3.8) and (4.3.9) into equation (4.3.7) then yields:

$$\begin{aligned} \sum_{i=1}^{3n} m_i a_i \delta x_i &= \sum_{i=1}^{3n} \sum_{j=1}^{3n-k} \left[\frac{d}{dt} \left(m_i \dot{x}_i \frac{\partial x_i}{\partial q_j} \right) - m_i \dot{x}_i \frac{\partial \dot{x}_i}{\partial q_j} \right] \delta q_j, \\ &= \sum_{i=1}^{3n} \sum_{j=1}^{3n-k} \left[\frac{d}{dt} \left(m_i \dot{x}_i \frac{\partial \dot{x}_i}{\partial \dot{q}_j} \right) - m_i \dot{x}_i \frac{\partial \dot{x}_i}{\partial q_j} \right] \delta q_j. \end{aligned} \quad (4.3.11)$$

For the kinetic energy of the entire system holds:

$$\begin{aligned} \frac{\partial T}{\partial q_j} &= \frac{\partial}{\partial q_j} \sum_{i=1}^{3n} \left(\frac{1}{2} m_i \dot{x}_i^2 \right) = \sum_{i=1}^{3n} \frac{1}{2} m_i \left(\frac{\partial}{\partial q_j} \dot{x}_i^2 \right) = \sum_{i=1}^{3n} m_i \dot{x}_i \frac{\partial \dot{x}_i}{\partial q_j}, \\ \frac{\partial T}{\partial \dot{q}_j} &= \frac{\partial}{\partial \dot{q}_j} \sum_{i=1}^{3n} \left(\frac{1}{2} m_i \dot{x}_i^2 \right) = \sum_{i=1}^{3n} \frac{1}{2} m_i \left(\frac{\partial}{\partial \dot{q}_j} \dot{x}_i^2 \right) = \sum_{i=1}^{3n} m_i \dot{x}_i \frac{\partial \dot{x}_i}{\partial \dot{q}_j}. \end{aligned} \quad (4.3.12)$$

Substitution of the above the above into equation (4.3.11) then gives:

$$\sum_{i=1}^{3n} m_i a_i \delta x_i = \sum_{j=1}^{3n-k} \left(\frac{d}{dt} \frac{\partial T}{\partial \dot{q}_j} - \frac{\partial T}{\partial q_j} \right) \delta q_j \quad (4.3.13)$$

Substitution of equations (4.3.6) and (4.3.13) back into d'Alemberts principle (4.3.4) gives:

$$\begin{aligned} \sum_{i=1}^{3n} (F_i - m_i a_i) \cdot \delta x_i &= \sum_{j=1}^{3n-k} Q_j \delta q_j - \sum_{j=1}^{3n-k} \left(\frac{d}{dt} \frac{\partial T}{\partial \dot{q}_j} - \frac{\partial T}{\partial q_j} \right) \delta q_j \iff \\ &= \sum_{j=1}^{3n-k} \left(Q_j - \frac{d}{dt} \frac{\partial T}{\partial \dot{q}_j} - \frac{\partial T}{\partial q_j} \right) \delta q_j = 0. \end{aligned} \quad (4.3.14)$$

The virtual displacements δq_j 's form a linear independent set and thus form a basis for \mathbb{R}^{3n-k} . Therefore, an arbitrary combination of δq_j 's has to result in the above summation equal to 0. As a consequence, each of the summation terms has to be 0:

$$Q_j - \frac{d}{dt} \frac{\partial T}{\partial \dot{q}_j} - \frac{\partial T}{\partial q_j} = 0, \quad \forall j \in \{1, \dots, 3n - k\}. \quad (4.3.15)$$

If the forces acting upon the system are conservative, it follows that the work done by a conservative force is equal to the change in potential energy due to that force. Therefore, the above equation can be rewritten by using:

$$Q_j = - \frac{\partial V}{\partial q_j}.$$

With this equality, equation (4.3.15) becomes:

$$\frac{d}{dt} \frac{\partial T}{\partial \dot{q}_j} - \frac{\partial T}{\partial q_j} + \frac{\partial V}{\partial q_j} = 0,$$

or after rewriting:

$$\frac{d}{dt} \frac{\partial T}{\partial \dot{q}_j} - \frac{\partial (T - V)}{\partial q_j} = 0.$$

Finally, because the potential energy V is not a function of velocity \dot{q}_j it holds that $\frac{\partial V}{\partial \dot{q}_j} = 0$. Adding this term to the equation and defining the Lagrangian to be the difference between the kinetic and potential energies, $L \equiv T - V$, Lagrange's equation for conservative forces becomes:

$$\frac{d}{dt} \frac{\partial L}{\partial \dot{q}_j} - \frac{\partial L}{\partial q_j} = 0, \quad j = 1, \dots, 3n - k. \quad (4.3.16)$$

Further on in this section, equation (4.3.16) will be used to illustrate how the equations of motion of a spherical pendulum follows from this equation.

4.4 Kane's Method [4]

Consider a multi-body system of n interconnected rigid bodies. Each body is subject to a external and constraint force. Each external force can be decomposed into their equivalent force \mathbf{F}_i through the center of mass of body i and equivalent torque \mathbf{T}_i ($i = 1, \dots, n$). In the

same way, each constraint force can be decomposed into its equivalent force through the center of mass of the object its working on and torque: $\mathbf{F}_i^c, \mathbf{T}_i^c$.

Using d'Alembert's principle for the force equilibrium of body i yields:

$$\mathbf{F}_i + \mathbf{F}_i^c = m_i \mathbf{a}_i ,$$

and defining the inertia force of body i as $\mathbf{F}_i^* = -m_i \mathbf{a}_i$ this equation becomes:

$$\mathbf{F}_i + \mathbf{F}_i^c + \mathbf{F}_i^* = 0 .$$

Applying the principle of virtual work to the system and considering only the work resulting from the forces on the system gives:

$$\delta W = (\mathbf{F}_i + \mathbf{F}_i^* + \mathbf{F}_i^c) \delta \mathbf{r}_i = 0 , \quad (i = 1, \dots, n) . \quad (4.4.1)$$

The constraints typically encountered in problems do not allow a displacement in the direction of the constraint force, and are thus workless (e.g. with the bifilar pendulum the constraint forces of the suspension wires do not result in displacement along these wires). In symbols: $\mathbf{F}_i^c \delta \mathbf{r}_i = 0$.

This simplifies the virtual work equation (4.4.1) to:

$$\delta W = (\mathbf{F}_i + \mathbf{F}_i^*) \delta \mathbf{r}_i = 0 , \quad (i = 1, \dots, n) , \quad (4.4.2)$$

or when using the alternate form of a virtual displacement from equation (4.3.5):

$$\begin{aligned} \delta W &= (\mathbf{F}_i + \mathbf{F}_i^*) \left(\sum_{j=1}^{3n} \frac{\partial \mathbf{r}_i}{\partial q_j} \delta q_j \right) = 0 \Rightarrow \\ \delta W &= (\mathbf{F}_i + \mathbf{F}_i^*) \frac{\partial \mathbf{r}_i}{\partial q_j} \delta q_j = 0 , \quad (j = 1, \dots, 3n) , \end{aligned} \quad (4.4.3)$$

where the implication holds since the virtual displacement is arbitrary and therefore equality must hold for each term. Define generalized active and generalized inertia force f_r and f_r^* as:

$$\begin{aligned} f_j &= \mathbf{F}_i \cdot \frac{\partial \mathbf{r}_i}{\partial q_j} \\ f_j^* &= \mathbf{F}_i^* \cdot \frac{\partial \mathbf{r}_i}{\partial q_j} \end{aligned}$$

Substitution of f_j and f_j^* into equation (4.4.3) gives:

$$(f_j + f_j^*) \delta q_j = 0 . \quad (4.4.4)$$

It has been shown in equation (4.3.9) that:

$$\frac{\partial \dot{\mathbf{r}}_i}{\partial \dot{q}_j} = \frac{\partial \mathbf{r}_i}{\partial q_j} .$$

This property can be substituted to find an alternate expression for f_j and f_j^* ¹:

$$\begin{aligned} f_j &= \mathbf{F}_i \cdot \frac{\partial \mathbf{r}_i}{\partial q_j} = \mathbf{F}_i \cdot \frac{\partial \dot{\mathbf{r}}_i}{\partial \dot{q}_j} = \mathbf{F}_i \cdot \frac{\partial \mathbf{v}_i}{\partial \dot{q}_j} \\ f_j^* &= \mathbf{F}_i^* \cdot \frac{\partial \mathbf{r}_i}{\partial q_j} = \mathbf{F}_i^* \cdot \frac{\partial \dot{\mathbf{r}}_i}{\partial \dot{q}_j} = \mathbf{F}_i^* \cdot \frac{\partial \mathbf{v}_i}{\partial \dot{q}_j} \end{aligned}$$

¹It is clear that these expressions are equivalent. However, why these substitutions are necessary for the further derivation of Kane's equations is not clear.

Since the virtual displacement δq_j in equation (4.4.4) is arbitrary, it follows that:

$$(f_j + f_j^*) = 0 .$$

In a similar way, using virtual work can be used to show that the sum of the moments equal 0. To this extend, one can use Euler's equation to obtain:

$$\mathbf{T}_i + \mathbf{T}_i^c = \boldsymbol{\alpha}_i \cdot \vec{I} + \boldsymbol{\omega}_i \times \vec{I} \cdot \boldsymbol{\omega}_i .$$

Defining $\mathbf{T}_i^* = - \left(\boldsymbol{\alpha}_i \cdot \vec{I} + \boldsymbol{\omega}_i \times \vec{I} \cdot \boldsymbol{\omega}_i \right)$ this can be written as:

$$\mathbf{T}_i + \mathbf{T}_i^c + \mathbf{T}_i^* = 0 .$$

Letting $\delta \boldsymbol{\phi}_i$ be a virtual rotation and using the principle of virtual work again obtains:

$$(\mathbf{T}_i + \mathbf{T}_i^c + \mathbf{T}_i^*) \delta \boldsymbol{\phi}_i = 0 .$$

Because the constraint force does not allow for a (virtual) displacement it does not do any work. As a result, it must hold that its equivalent torque T_i^c also does not do any work: $\mathbf{T}_i^c \delta \boldsymbol{\phi}_i = 0$. It then follows that:

$$\begin{aligned} (\mathbf{T}_i + \mathbf{T}_i^*) \delta \boldsymbol{\phi}_i &= 0 \iff \\ (\mathbf{T}_i + \mathbf{T}_i^*) \left(\sum_{j=1}^{3n} \frac{\partial \boldsymbol{\phi}_i}{\partial q_j} \delta q_j \right) &= 0 , \end{aligned}$$

and again because the virtual displacement is arbitrary, it must hold that:

$$(\mathbf{T}_i + \mathbf{T}_i^*) \frac{\partial \boldsymbol{\phi}_i}{\partial q_j} = 0 ,$$

which can be written as:

$$M_j + M_j^* = 0 ,$$

where M_j and M_j^* are respectively defined as the generalized active and generalized inertia moments (using equation (4.3.9)):

$$\begin{aligned} M_j &= \mathbf{T}_i \cdot \frac{\partial \boldsymbol{\omega}_i}{\partial \dot{q}_j} , \\ M_j^* &= - \left(\boldsymbol{\alpha}_i \cdot \vec{I} + \boldsymbol{\omega}_i \times \vec{I} \cdot \boldsymbol{\omega}_i \right) \cdot \frac{\partial \boldsymbol{\omega}_i}{\partial \dot{q}_j} . \end{aligned}$$

Since the dimension of both equations are the same, one can add the equalities:

$$\begin{aligned} f_j + f_j^* &= 0 , \\ M_j + M_j^* &= 0 , \end{aligned}$$

to yield:

$$f_j + f_j^* + M_j + M_j^* = 0 . \tag{4.4.5}$$

Defining the generalized active and generalized inertia forces F_j and F_j^* as follows:

$$\begin{aligned} F_j &= f_j + M_j , \\ F_j^* &= f_j^* + M_j^* , \end{aligned}$$

and substitution into equation (4.4.5) results in Kane's equation:

$$F_j + F_j^* = 0, \quad (4.4.6)$$

where:

$$\begin{aligned} F_j &= f_j + M_j = \mathbf{F}_i \cdot \frac{\partial \mathbf{v}_i}{\partial \dot{q}_j} + \mathbf{T}_i \frac{\partial \boldsymbol{\omega}_i}{\partial \dot{q}_j}, \\ F_j^* &= f_j^* + M_j^* = \mathbf{F}_i^* \cdot \frac{\partial \mathbf{v}_i}{\partial \dot{q}_j} - \left(\boldsymbol{\alpha}_i \cdot \vec{I} + \boldsymbol{\omega}_i \times \vec{I} \cdot \boldsymbol{\omega}_i \right) \cdot \frac{\partial \boldsymbol{\omega}_i}{\partial \dot{q}_j}, \quad (j = 1 \dots 3n). \end{aligned}$$

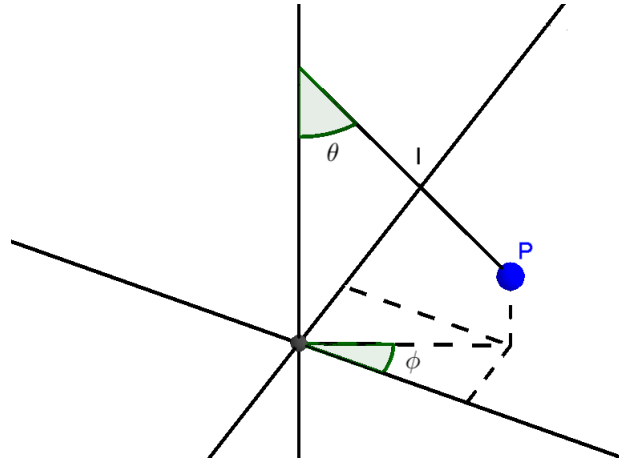
For a problem with n degrees of freedom, n generalized coordinates q_i have to be chosen. Typically, the time derivatives of these coordinates, u_i , are defined as the generalized velocities. Subsequently, for each of the j , expressions for $\frac{\partial \mathbf{v}_i}{\partial \dot{q}_j}$ and $\frac{\partial \boldsymbol{\omega}_i}{\partial \dot{q}_j}$ have to be found in terms of the generalized velocities u_i and its time derivatives \dot{u}_i with respect to a Cartesian reference system. Because these expressions are linear in \dot{u}_i this can be written in matrix form as:

$$M(\mathbf{q}, \mathbf{u})\dot{\mathbf{u}} = \mathbf{f}(\mathbf{q}, \mathbf{u}),$$

where M contains the coefficients of \dot{u}_i in equations (4.4.6). Multiplying with the inverse matrix M^{-1} yields the equations of motion of the system.

4.5 Example: Spherical pendulum

In this example, a regular pendulum is considered which, as discussed earlier, is not restricted to moving solely in a plane. In the figure below such a pendulum can be seen.



The equations of motion will be derived using the different methods. For this example, the Newtonian approach will not be used since an example with a planar pendulum (see appendix A) made it apparent that this method is not efficient in deriving equations of motion of a system with constraints. Furthermore, the 'smart' Newtonian approach will also not be used due to its lack of practicality, discussed in Section 4.2.

- **Lagrangian Mechanics**

The spherical pendulum is an extension to the planar pendulum, where the pendulum can only swing in a plane. The three degrees of freedom of this system require an additional parameter φ to describe the rotation along the z -axis relative to the x -axis. Again the kinetic- and potential energy of the system are determined to obtain the Lagrangian of the system. For the kinetic energy we have $T = \frac{1}{2}mv^2$. Similarly to the Euclidean distance,

the velocity v can be expressed as $v = \sqrt{\dot{x}^2 + \dot{y}^2 + \dot{z}^2}$, where from spherical coordinates one has that:

$$\begin{aligned}x &= l \sin(\theta) \cos(\varphi), \\y &= l \sin(\theta) \sin(\varphi), \\z &= l \cos(\theta).\end{aligned}$$

Taking the time derivative of x, y, z and substituting in the expression for the velocity yields an expression for the kinetic energy (using $\cos^2(\theta) = 1 - \sin^2(\theta)$):

$$T = \frac{1}{2}ml^2 \left(\dot{\theta}^2 + \dot{\varphi}^2 \sin^2(\theta) \right).$$

The potential energy is calculated as:

$$V = -mgh = -mgl \cos(\theta).$$

The Lagrangian then becomes:

$$L = \frac{1}{2}ml^2 \left(\dot{\theta}^2 + \dot{\varphi}^2 \sin^2(\theta) \right) + mgl \cos(\theta).$$

Lagrange's equation is used twice, with respect to θ and φ :

$$\begin{aligned}\frac{d}{dt} \left(\frac{dL}{d\dot{\theta}} \right) - \frac{dL}{d\theta} &= 0, \\ \frac{d}{dt} \left(\frac{dL}{d\dot{\varphi}} \right) - \frac{dL}{d\varphi} &= 0.\end{aligned}$$

Solving these two equations for $\ddot{\theta}$ and $\ddot{\varphi}$ respectively yields the two equations of motion which describe the movement of the spherical pendulum:

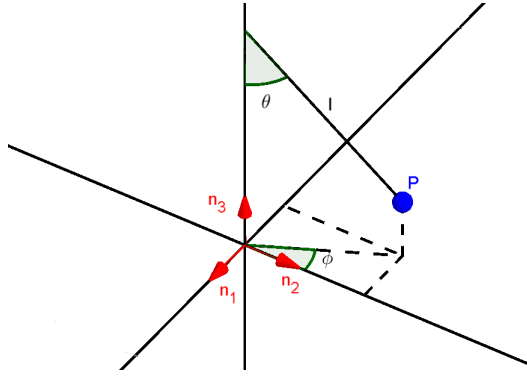
$$\begin{aligned}\ddot{\theta}(t) &= \frac{l\dot{\varphi}^2 \sin(\theta) \cos(\theta) - g \sin(\theta)}{l} \\ \ddot{\varphi}(t) &= -\frac{2\dot{\varphi} \cos(\theta)\dot{\theta}}{\sin(\theta)}\end{aligned}\tag{4.5.1}$$

Using Lagrangian mechanics the equations of motion can be determined with relative ease, only having to determine the kinetic- and potential energy and taking derivatives. Another advantage of this method is that the constraint of the pendulum wire is incorporated in the problem naturally, and does not have to be added to the system as a separate equation as seen in the approach using Newtonian mechanics (see appendix A).

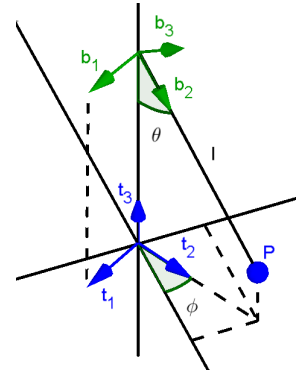
- **Kane's Method**

To describe the motion of the spherical pendulum three sets of orthonormal unit vectors will be defined. These sets are shown in the figures below.

The set $\{\mathbf{t}_1, \mathbf{t}_2, \mathbf{t}_3\}$ is obtained by rotating $\{\mathbf{n}_1, \mathbf{n}_2, \mathbf{n}_3\}$ counter-clockwise through an angle of ϕ around the origin in the horizontal plane. The origin is defined to be vertically below the beginning of the suspension wire. The set $\{\mathbf{b}_1, \mathbf{b}_2, \mathbf{b}_3\}$ is then obtained by rotating



(a) Cartesian unit vectors $\{\mathbf{n}_1, \mathbf{n}_2, \mathbf{n}_3\}$



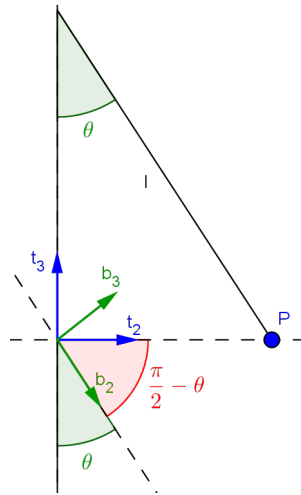
(b) Rotated unit vectors $\{\mathbf{t}_1, \mathbf{t}_2, \mathbf{t}_3\}, \{\mathbf{b}_1, \mathbf{b}_2, \mathbf{b}_3\}$

$\{\mathbf{t}_1, \mathbf{t}_2, \mathbf{t}_3\}$ clockwise through an angle of $\frac{\pi}{2} - \theta$ around the origin in the plane spanned by $(\mathbf{t}_2, \mathbf{t}_3)$. In the figure above, the set $\{\mathbf{b}_1, \mathbf{b}_2, \mathbf{b}_3\}$, which is obtained by these two consecutive rotations, is translated vertically as to show that the orientation of vector \mathbf{b}_2 coincides with the orientation of the suspension wire.

The transformation matrix between $\{\mathbf{n}_1, \mathbf{n}_2, \mathbf{n}_3\}$ and $\{\mathbf{t}_1, \mathbf{t}_2, \mathbf{t}_3\}$ is the trivial extension from a two-dimensional rotation matrix:

	\mathbf{t}_1	\mathbf{t}_2	\mathbf{t}_3
\mathbf{n}_1	$\cos(\phi)$	$-\sin(\phi)$	0
\mathbf{n}_2	$\sin(\phi)$	$\cos(\phi)$	0
\mathbf{n}_3	0	0	1

Before the transformation matrix is given which relates $\{\mathbf{t}_1, \mathbf{t}_2, \mathbf{t}_3\}$ and $\{\mathbf{b}_1, \mathbf{b}_2, \mathbf{b}_3\}$, a figure is provided as to motivate why these sets are related by a rotation through an angle of $\frac{\pi}{2} - \theta$.



This figure displays the plane spanned by $(\mathbf{t}_2, \mathbf{t}_3)$. Since $\mathbf{t}_1, \mathbf{b}_1$ are perpendicular to this plane, these vectors are invariant to the rotation in this plane and are left out of consideration. Translating vectors $\mathbf{t}_2, \mathbf{t}_3$ down vertically such that the center coincides with the center of $\{\mathbf{b}_2, \mathbf{b}_3\}$, it can be easily verified that $\{\mathbf{b}_2, \mathbf{b}_3\}$ is obtained by rotating $\{\mathbf{t}_2, \mathbf{t}_3\}$ clockwise through an angle of $\frac{\pi}{2} - \theta$. This results in the following transformation matrix.

$$\begin{array}{c|ccc} & \mathbf{b}_1 & \mathbf{b}_2 & \mathbf{b}_3 \\ \hline \mathbf{t}_1 & 1 & 0 & 0 \\ \mathbf{t}_2 & 0 & \cos(\frac{\pi}{2} - \theta) & \sin(\frac{\pi}{2} - \theta) \\ \mathbf{t}_3 & 0 & -\sin(\frac{\pi}{2} - \theta) & \cos(\frac{\pi}{2} - \theta) \end{array} = \begin{array}{c|ccc} & \mathbf{b}_1 & \mathbf{b}_2 & \mathbf{b}_3 \\ \hline \mathbf{t}_1 & 1 & 0 & 0 \\ \mathbf{t}_2 & 0 & \sin(\theta) & \cos(\theta) \\ \mathbf{t}_3 & 0 & -\cos(\theta) & \sin(\theta) \end{array}$$

Multiplying the two rotation matrices yields the relation between $\{\mathbf{n}_1, \mathbf{n}_2, \mathbf{n}_3\}$ and $\{\mathbf{b}_1, \mathbf{b}_2, \mathbf{b}_3\}$:

$$\begin{array}{c|ccc} & \mathbf{b}_1 & \mathbf{b}_2 & \mathbf{b}_3 \\ \hline \mathbf{n}_1 & \cos(\phi) & -\sin(\phi) \sin(\theta) & -\sin(\phi) \cos(\theta) \\ \mathbf{n}_2 & \sin(\phi) & \cos(\phi) \sin(\theta) & \cos(\phi) \cos(\theta) \\ \mathbf{n}_3 & 0 & -\cos(\theta) & \sin(\theta) \end{array}$$

Since the spherical pendulum has two degrees of freedom, two generalized coordinates q_1, q_2 have to be chosen. These are chosen as: $q_1 = \phi, q_2 = \theta$, where $\phi = \phi(t), \theta = \theta(t)$. The generalized velocities u_1, u_2 are then defined as the time derivatives of q_1, q_2 respectively; $u_1 = \dot{\phi}, u_2 = \dot{\theta}$.

Now the angular velocity $\boldsymbol{\omega}$ of P can be calculated by the sum of the angular velocities resulting from the rotations along angles ϕ and θ :

$$\begin{aligned} \boldsymbol{\omega} &= \boldsymbol{\omega}_\phi + \boldsymbol{\omega}_\theta = \dot{\phi} \mathbf{n}_3 + \dot{\theta} \mathbf{b}_1 \iff \\ &= \dot{\phi} \mathbf{n}_3 + \dot{\theta} (\cos(\phi) \mathbf{n}_1 + \sin(\phi) \mathbf{n}_2) \iff \\ &= \dot{\theta} \cos(\phi) \mathbf{n}_1 + \dot{\theta} \sin(\phi) \mathbf{n}_2 + \dot{\phi} \mathbf{n}_3. \end{aligned} \tag{4.5.2}$$

With the angular velocity, the velocity \mathbf{v} of P can be calculated by taking the cross-product of the angular velocity $\boldsymbol{\omega}$ and the vector from the origin to point P , \mathbf{r}^P :

$$\begin{aligned} \mathbf{v} &= \boldsymbol{\omega} \times \mathbf{r}^P \iff \\ &= \left(\dot{\theta} \cos(\phi) \mathbf{n}_1 + \dot{\theta} \sin(\phi) \mathbf{n}_2 + \dot{\phi} \mathbf{n}_3 \right) \times l \mathbf{b}_2 \iff \\ &= \left(\dot{\theta} \cos(\phi) \mathbf{n}_1 + \dot{\theta} \sin(\phi) \mathbf{n}_2 + \dot{\phi} \mathbf{n}_3 \right) \times \\ &\quad l \left(-\sin(\phi) \sin(\theta) \mathbf{n}_1 + \cos(\phi) \sin(\theta) \mathbf{n}_2 - \cos(\theta) \mathbf{n}_3 \right) \iff \\ &= -l \left(\dot{\theta} \sin(\phi) \cos(\theta) + \dot{\phi} \cos(\phi) \sin(\theta) \right) \mathbf{n}_1 \\ &\quad + l \left(\dot{\theta} \cos(\phi) \cos(\theta) - \dot{\phi} \sin(\phi) \sin(\theta) \right) \mathbf{n}_2 \\ &\quad + l \dot{\theta} \sin(\theta) \mathbf{n}_3. \end{aligned} \tag{4.5.3}$$

Taking the time derivate of \mathbf{v} results in the acceleration \mathbf{a} of P with respect to the Newtonian reference frame:

$$\begin{aligned} \mathbf{a} &= \frac{d}{dt} \mathbf{v} \iff \\ &= l \left(\sin(\phi) \sin(\theta) \dot{\phi}^2 - 2 \cos(\phi) \dot{\theta} \cos(\theta) \dot{\phi} + \sin(\theta) \dot{\theta}^2 \sin(\phi) - \cos(\phi) \sin(\theta) \ddot{\phi} \right. \\ &\quad \left. - \ddot{\theta} \cos(\theta) \sin(\phi) \right) \mathbf{n}_1 \\ &\quad + l \left(-\cos(\phi) \sin(\theta) \dot{\theta}^2 + \ddot{\theta} \cos(\phi) \cos(\theta) - 2 \dot{\theta} \cos(\theta) \sin(\phi) \dot{\phi} \right. \\ &\quad \left. - \sin(\theta) \sin(\phi) \ddot{\phi} - \cos(\phi) \sin(\theta) \dot{\phi}^2 \right) \mathbf{n}_2 \\ &\quad + l \left(\dot{\theta}^2 \cos(\theta) + \ddot{\theta} \sin(\theta) \right) \mathbf{n}_3 \end{aligned}$$

The partial velocities \mathbf{v}_r and partial angular velocities $\boldsymbol{\omega}_r$ follow from taking the partial derivatives of \mathbf{v} and $\boldsymbol{\omega}$ respectively with respect to $\dot{\phi}$ and $\dot{\theta}$:

$$\begin{aligned}\mathbf{v}_1 &= \frac{\partial \mathbf{v}}{\partial \dot{\phi}} = -l \cos(\phi) \sin(\theta) \mathbf{n}_1 - l \sin(\phi) \sin(\theta) \mathbf{n}_2, \\ \mathbf{v}_2 &= \frac{\partial \mathbf{v}}{\partial \dot{\theta}} = -l \cos(\theta) \sin(\phi) \mathbf{n}_1 + l \cos(\phi) \cos(\theta) \mathbf{n}_2 + l \sin(\theta) \mathbf{n}_3, \\ \boldsymbol{\omega}_1 &= \frac{\partial \boldsymbol{\omega}}{\partial \dot{\phi}} = \mathbf{n}_3, \\ \boldsymbol{\omega}_2 &= \frac{\partial \boldsymbol{\omega}}{\partial \dot{\theta}} = \cos(\phi) \mathbf{n}_1 + \sin(\phi) \mathbf{n}_2.\end{aligned}\tag{4.5.4}$$

Kane's equation can now be assembled by calculating the generalized active forces F_1, F_2 and the generalized inertia forces F_1^*, F_2^* . It follows that:

$$\begin{aligned}F_1 &= \mathbf{F}_z \cdot \mathbf{v}_1 + \mathbf{T} \cdot \boldsymbol{\omega}_1 = -mg \mathbf{n}_3 \cdot (-l \cos(\phi) \sin(\theta) \mathbf{n}_1 - l \sin(\phi) \sin(\theta) \mathbf{n}_2) + 0 \cdot \boldsymbol{\omega}_1 = 0, \\ F_2 &= \mathbf{F}_z \cdot \mathbf{v}_2 + \mathbf{T} \cdot \boldsymbol{\omega}_2 = -mg \mathbf{n}_3 \cdot (l \cos(\theta) \sin(\phi) \mathbf{n}_1 + l \cos(\phi) \cos(\theta) \mathbf{n}_2 + l \sin(\theta) \mathbf{n}_3) + 0 \cdot \boldsymbol{\omega}_2 \\ &= -mgl \sin(\theta), \\ F_1^* &= -m \mathbf{a} \cdot \mathbf{v}_1 - \left(\boldsymbol{\alpha}_1 \cdot \vec{I} + \boldsymbol{\omega}_1 \times \vec{I} \cdot \boldsymbol{\omega}_1 \right) \cdot \boldsymbol{\omega}_1 \iff \\ &= -ml^2 \sin(\theta) (2\dot{\phi}\dot{\theta} \cos(\theta) + \sin(\theta)\ddot{\phi}) - 0, \\ F_2^* &= -m \mathbf{a} \cdot \mathbf{v}_2 - \left(\boldsymbol{\alpha}_2 \cdot \vec{I} + \boldsymbol{\omega}_2 \times \vec{I} \cdot \boldsymbol{\omega}_2 \right) \cdot \boldsymbol{\omega}_2 \iff \\ &= ml^2 (\dot{\phi}^2 \sin(\theta) \cos(\theta) - \ddot{\theta}) - 0.\end{aligned}$$

The object suspended by the spherical pendulum is a point mass and thus has no moments of inertia, $\mathbf{I} = 0$. Since the external force F_z is already working on the center of mass of the object, there is no equivalent torque, $\mathbf{T} = 0$.

Assembling Kane's equations yields:

$$\begin{aligned}F_1 + F_1^* &= -ml^2 \sin(\theta) (2\dot{\phi}\dot{\theta} \cos(\theta) + \sin(\theta)\ddot{\phi}) = 0, \\ F_2 + F_2^* &= -mgl \sin(\theta) + ml^2 (\dot{\phi}^2 \sin(\theta) \cos(\theta) - \ddot{\theta}) = 0.\end{aligned}\tag{4.5.5}$$

Writing these equations in matrix form:

$$\begin{pmatrix} -ml^2 \sin^2(\theta) & 0 \\ 0 & -ml^2 \end{pmatrix} \begin{pmatrix} \ddot{\phi} \\ \ddot{\theta} \end{pmatrix} = \begin{pmatrix} 2ml^2 \dot{\phi}\dot{\theta} \sin(\theta) \cos(\theta) \\ mgl \sin(\theta) - ml^2 \dot{\phi}^2 \sin(\theta) \cos(\theta) \end{pmatrix}.\tag{4.5.6}$$

Solving this system for $\ddot{\phi}, \ddot{\theta}$ by inverting the matrix leads to the equations of motion for the spherical pendulum:

$$\boxed{\begin{aligned}\ddot{\theta}(t) &= \frac{l \dot{\phi}^2 \sin(\theta) \cos(\theta) - g \sin(\theta)}{l} \\ \ddot{\phi}(t) &= -\frac{2 \dot{\phi} \cos(\theta) \dot{\theta}}{\sin(\theta)}\end{aligned}}\tag{4.5.7}$$

This formulation of the equations of motion is the same as the one found using the Lagrangian approach. Similarly to Lagrangian mechanics, the constraint of the system is incorporated naturally into the formulation of the problem, which is an advantage of these methods over using Newtonian mechanics.

- **Numerical Solution**

In order to solve these equations of motion, the equations of motion from (4.5.7) are rewritten as a system of four first-order differential equations. Setting: $y_1 = \theta$, $y_2 = \dot{\theta}$, $y_3 = \phi$, $y_4 = \dot{\phi}$ the system becomes:

$$\begin{aligned} \dot{y}_1 &= y_2, \\ \dot{y}_2 &= \frac{ly_4^2 \sin(y_1) \cos(y_1) - g \sin(y_1)}{l}, \\ \dot{y}_3 &= y_4, \\ \dot{y}_4 &= -\frac{2y_4 \cos(y_1)y_2}{\sin(y_1)}. \end{aligned}$$

Solving this system with initial speeds $\dot{\theta}(0) = 1$ and $\dot{\phi}(0) = 2$ results in the following figure:

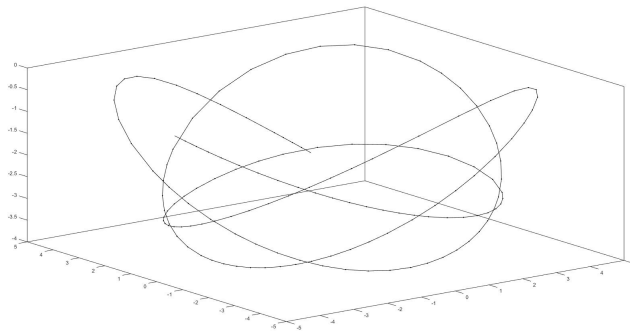


Figure 4.5.2: Pendulum with initial speeds $\dot{\theta}(0) = 1$, $\dot{\phi}(0) = 2$

The length of the suspension wire is $l = 5$. The spherical pendulum moves in three dimensions because it is given an angular speed in both directions. Setting either of these initial speeds to 0 results in a 2-dimensional movement:

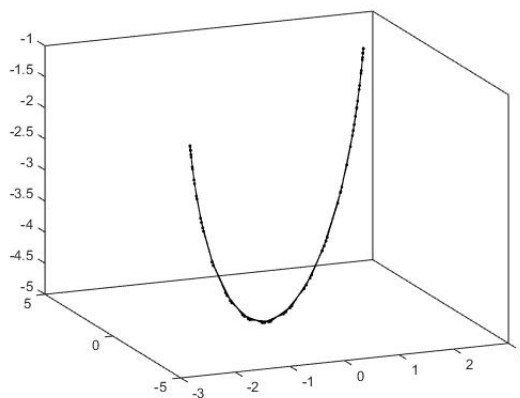


Figure 4.5.3: Pendulum with initial speeds $\dot{\theta}(0) = 1$, $\dot{\phi}(0) = 0$

From the above example it becomes clear that the Lagrangian approach and Kane's method are to be preferred over the approach using classical Newtonian mechanics for deriving the equations of motion with constraints. This results from the fact that in these two approaches the constraints are incorporated in the formulation of the problem in a natural way such that these constraints do not have to be added to the system as an extra equation.

5. Bifilar pendulum

The bifilar pendulum is a torsional pendulum where an object is suspended by two wires. Dynamic modeling of the equations of motion is used to relate the measurable parameters of the pendulum's configuration to the moment of inertia of the object [1]. In this section, Kane's method and the Lagrangian approach will be used to derive the equations of motion of the bifilar pendulum. The full non-linear model for the bifilar pendulum will be derived with Kane's model. The derivation using the Lagrangian approach will assume certain simplifications and will only be used as a verification of Kane's model for these assumptions.

5.1 Kane's method

This derivation follows a paper which derives the 'full nonlinear equations of motion of a bifilar pendulum ... without the aid of simplifying assumptions about the geometry of the suspension or the inertia properties of the suspended body' [3]. In this paper, the derivation of the equations of motion is presented in a rather unstructured way. The derivation below attempts to reformulate this unstructured derivation in such a way that it is more structured and as a result better readable and easier to comprehend. In order to describe the motion of the bifilar pendulum, geometric quantities have to be introduced with which the motion will be described. These quantities can be seen in the figure below. It is important to note that the figure intentionally displays a state of the bifilar pendulum while not at rest; the figure displays the bifilar pendulum while at a certain orientation and position during its movement. This is done to help the reader create an understanding how each angle influences the suspended objects' orientation and position.

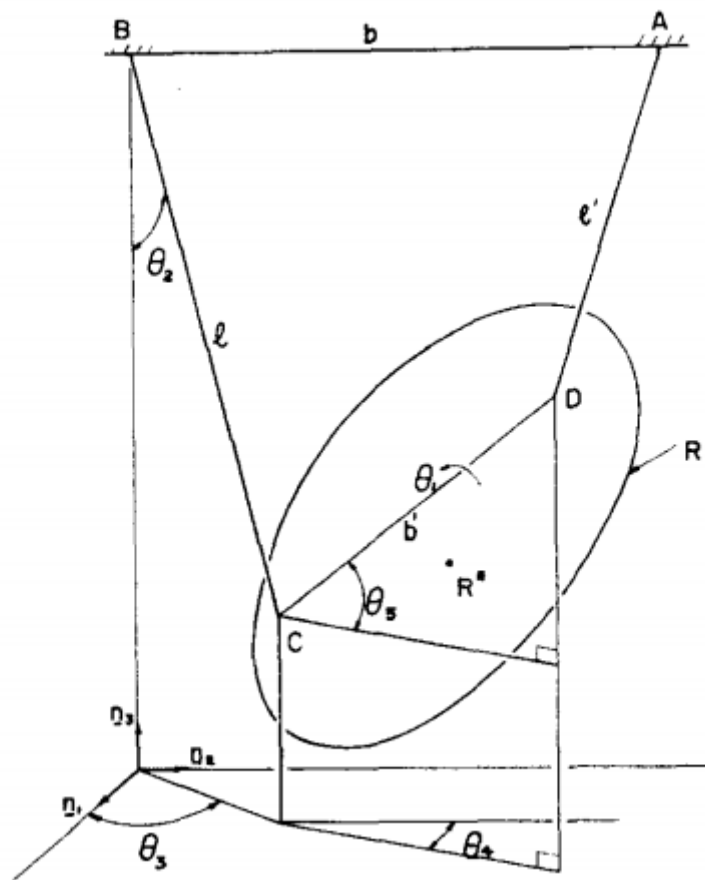


Figure 5.1.1: Geometric quantities used to describe the motion of the bifilar pendulum

A list of these basic quantities with descriptions is:

- A, B, C, D labels for the attachment points of suspension wires
- R label for suspended object
- R^* label for center of mass of object R
- b, b' distances between attachment points
- l, l' lengths of suspension wires
- \mathbf{n}_i unit vectors earth-fixed reference system
- θ_i orientation angles.

The angles $\theta_2, \dots, \theta_5$ are used to capture the orientation of lines BC and CD . From figure 5.1.1 it is clear that $\overrightarrow{AB} + \overrightarrow{BC} + \overrightarrow{CD} = \overrightarrow{AD}$, and thus that the angles corresponding to these lines, $\theta_2, \dots, \theta_5$, do not form an independent set. Decomposing \overrightarrow{AB} , \overrightarrow{BC} and \overrightarrow{CD} into their components along the earth-fixed reference system axes yields:

$$\begin{aligned}\overrightarrow{AB} &= -b\mathbf{n}_2, \\ \overrightarrow{BC} &= l \sin(\theta_2) \cos(\theta_3)\mathbf{n}_1 + l \sin(\theta_2) \sin(\theta_3)\mathbf{n}_2 - l \cos(\theta_2)\mathbf{n}_3, \\ \overrightarrow{CD} &= b' \sin(\theta_4) \cos(\theta_5)\mathbf{n}_1 + b' \cos(\theta_4) \cos(\theta_5)\mathbf{n}_2 + b' \sin(\theta_5)\mathbf{n}_3.\end{aligned}$$

Introducing the following notation to keep the expressions with cos and sin terms compact: $\cos(\theta_i) = c_i$, $\sin(\theta_i) = s_i$, $\overrightarrow{AB} + \overrightarrow{BC} + \overrightarrow{CD} = \overrightarrow{AD}$ can be written as:

$$-b\mathbf{n}_2 + l(s_2(c_3\mathbf{n}_1 + s_3\mathbf{n}_2) - c_2\mathbf{n}_3) + b'(c_5(s_4\mathbf{n}_1 + c_4\mathbf{n}_2) + s_5\mathbf{n}_3) = \overrightarrow{AD}. \quad (5.1.1)$$

The above constraint equation can be graphically verified by plotting the vectors \overrightarrow{AB} , \overrightarrow{BC} and \overrightarrow{CD} and checking whether the vector \overrightarrow{AD} closes the 'loop'.

To this extend, consider the pendulum at rest such that the angles are given by $\boldsymbol{\theta} = [0, \frac{\pi}{6}, \frac{\pi}{2}, 0, 0]^T$ and the cable lengths are 5 meters. This choice of values, $\theta_3 = \frac{\pi}{2}$ and $\theta_4 = 0$, results in all the vectors will lie in the plane spanned by $(\mathbf{n}_2, \mathbf{n}_3)$. Plotting the earlier mentioned constraint vectors yields the plot where vector \overrightarrow{AD} is shown red:

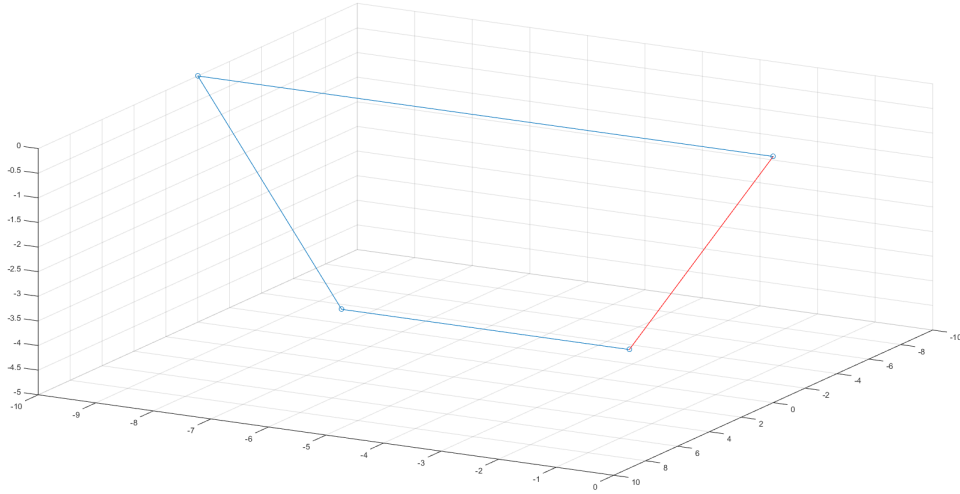


Figure 5.1.2: Graphical verification of constraint equation

Now consider the pendulum at a different initial, non-stationary, position with angles $\boldsymbol{\theta} = [0, \frac{\pi}{6}, \frac{\pi}{4}, \frac{\pi}{4}, 0]^T$ and cable lengths of 5 meters. Plotting vectors \overrightarrow{AB} , \overrightarrow{BC} , \overrightarrow{CD} and \overrightarrow{AD} again yields the plot:

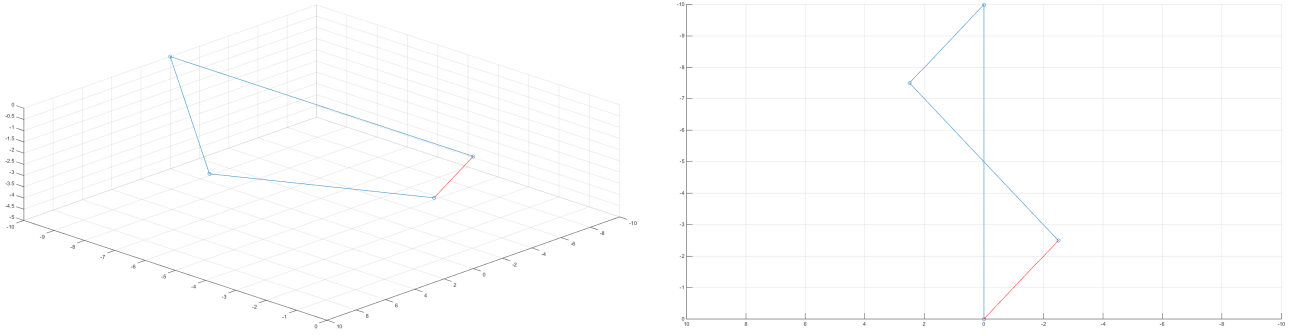


Figure 5.1.3: Graphical verification of constraint equation; diagonal and top view

Both of the above figures graphically verify that the vectors $\overrightarrow{AB} + \overrightarrow{BC} + \overrightarrow{CD}$ and \overrightarrow{AD} are equal, which verifies the constraint from equation (5.1.1).

Since both of these vectors are equal, it must hold that their lengths are equal (and their lengths squared). Therefore, scalar multiplication of each component of equation (5.1.1) with itself leads to the constraint of the system:

$$(ls_2c_3 + b's_4c_5)^2 + (-b + ls_2s_3 + b'c_4c_5)^2 + (-lc_2 + b's_5)^2 = (l')^2.$$

The left-hand side of this equation is only a function of $\theta_1, \dots, \theta_5$ and the right-hand side a constant. Therefore, the above equation can be compactly written as:

$$g(\boldsymbol{\theta}) = a. \quad (5.1.2)$$

The notation $g(\boldsymbol{\theta})$ is used to compactly denote that g is a function of $\boldsymbol{\theta} = (\theta_1, \dots, \theta_5)$. Further on in the derivation, the notation $\mathbf{f}(\boldsymbol{\theta})$ will also be used, which denotes that \mathbf{f} is a vector of which the components are functions of $\boldsymbol{\theta}$.

Five angles have been defined to capture the orientation of the entire system. However, these angles do not form an independent set since the constraint equation (5.1.2) above reduces the degrees of freedom by 1 and as a result, the system has 4 degrees of freedom. When $\theta_1 \dots \theta_5$ are seen as generalized coordinates of the system, θ_5 's is a function of the other four.

Equation (5.1.2) can be converted into a differential equation by differentiating it with respect to time yielding:

$$\frac{dg(\boldsymbol{\theta})}{dt} = \left(\frac{dg(\boldsymbol{\theta})}{d\boldsymbol{\theta}} \right)^T \frac{d\boldsymbol{\theta}}{dt} := \boldsymbol{\beta}(\boldsymbol{\theta})^T \cdot \dot{\boldsymbol{\theta}} = 0. \quad (5.1.3)$$

From equation (5.1.3), $\dot{\theta}_5$ can easily be written as a function of $\dot{\theta}_1, \dot{\theta}_2, \dot{\theta}_3, \dot{\theta}_4$:

$$\dot{\theta}_5 = \left(\frac{-I_{45}\boldsymbol{\beta}(\boldsymbol{\theta})}{\mathbf{e}_5^T\boldsymbol{\beta}(\boldsymbol{\theta})} \right)^T I_{45} \dot{\boldsymbol{\theta}} := \boldsymbol{\gamma}(\boldsymbol{\theta})^T I_{45} \dot{\boldsymbol{\theta}}. \quad (5.1.4)$$

The vector \mathbf{e}_i is the 5th unit vector of the standard basis for \mathbb{R}^5 . The matrix I_{45} is a (4×4) identity matrix with an added column of zeros forming a (4×5) -matrix. Therefore, the product $I_{45} \dot{\boldsymbol{\theta}}$ is a (4×1) -vector with entries $\dot{\theta}_1, \dots, \dot{\theta}_4$ such that this is an explicit function for $\dot{\theta}_5$.

Equations (5.1.2) and (5.1.4) can be used to find initial values for θ_5 and $\dot{\theta}_5$ for chosen values of θ_i and $\dot{\theta}_i$, ($i = 1 \dots 4$).

Certain quantities needed for Kane's method are most conveniently described in a body-fixed reference frame. Therefore, two extra sets of unit vectors are defined. One set of body-fixed unit vectors $\{\tilde{\mathbf{n}}_1, \tilde{\mathbf{n}}_2, \tilde{\mathbf{n}}_3\}$ is defined as shown in the figure (5.1.4) below.

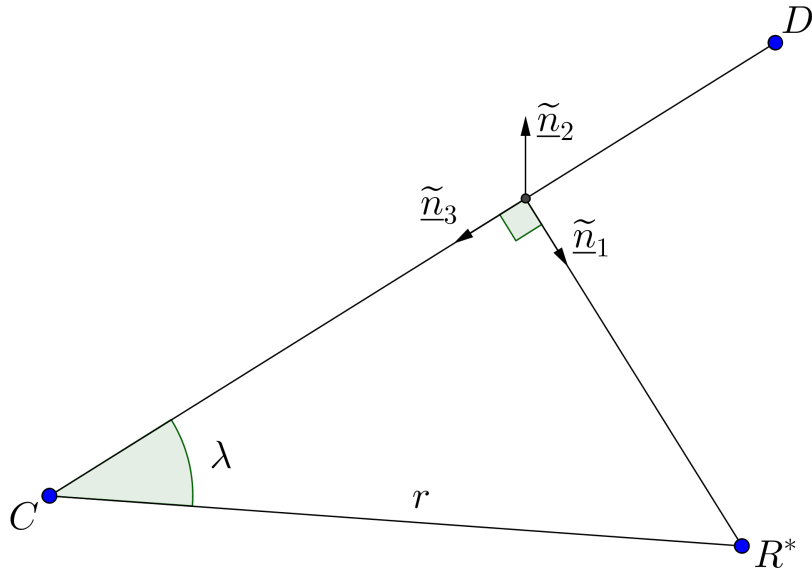


Figure 5.1.4: Unit vectors body-fixed reference system

The second set of body-fixed unit vectors $\{\mathbf{b}_1, \mathbf{b}_2, \mathbf{b}_3\}$ is defined as being parallel to the principal axes of inertia of R for R^* . That is, the unit vectors are parallel to a set of axes such that the moment of inertia tensor with respect to these axes is a diagonal matrix where the moments of inertia about these axes are on the diagonal, called the principal moments of inertia. Expressing quantities such as angular velocity or acceleration of body R with respect to this specific reference frame has the advantage that terms involving moment of inertia become less complex since they are only a function of the principle moments of inertia, as a result of the moment of inertia tensor being diagonal. If any other body-fixed reference frame was chosen, the moment of inertia tensor would have products of inertia on the off-diagonals, which would complicate the expressions.

Some notation will be introduced to compactly formulate the transformations between the unit bases sets. Suppose there are two unit vector sets: $\{\mathbf{a}_1, \mathbf{a}_2, \mathbf{a}_3\}$ and $\{\mathbf{b}_1, \mathbf{b}_2, \mathbf{b}_3\}$ and write: $A = [\mathbf{a}_1, \mathbf{a}_2, \mathbf{a}_3]$, $B = [\mathbf{b}_1, \mathbf{b}_2, \mathbf{b}_3]$. The transformation matrix from unit vectors A to B will be written as:

$$B = N_{\mathbf{a}}^{\mathbf{b}}(\boldsymbol{\theta}) A,$$

where $\boldsymbol{\theta}$ denotes the dependency of the transformation on angles $\theta_1, \dots, \theta_5$.

With this notation, the set $\{\tilde{\mathbf{n}}_1, \tilde{\mathbf{n}}_2, \tilde{\mathbf{n}}_3\}$ can be decomposed into components along the earth-fixed coordinate system. This gives a relation between $\{\tilde{\mathbf{n}}_1, \tilde{\mathbf{n}}_2, \tilde{\mathbf{n}}_3\}$ and $\{\mathbf{n}_1, \mathbf{n}_2, \mathbf{n}_3\}$:

$$\tilde{N} = N_{\mathbf{n}}^{\tilde{\mathbf{n}}}(\boldsymbol{\theta}) N, \tag{5.1.5}$$

where from figures 5.1.1 and 5.1.4 it follows that the transformation matrix $N_{\mathbf{n}}^{\tilde{\mathbf{n}}}(\boldsymbol{\theta})$ is given by:

$$N_{\mathbf{n}}^{\tilde{\mathbf{n}}}(\boldsymbol{\theta}) = \begin{pmatrix} s_1 c_4 + c_1 s_4 s_5 & c_1 c_4 - s_1 s_4 s_5 & -s_4 c_5 \\ -s_1 s_4 + c_1 c_4 s_5 & -c_1 s_4 - s_1 c_4 s_5 & -c_4 c_5 \\ -c_1 c_5 & s_1 c_5 & -s_5 \end{pmatrix} .$$

To see that \tilde{N} is in fact a orthonormal basis for \mathbb{R}^3 , one can verify that the inner products between each of the basis vectors is 0, and the inner products of the basis vectors with themselves is 1.

Both $\{\mathbf{b}_1, \mathbf{b}_2, \mathbf{b}_3\}$ and $\{\tilde{\mathbf{n}}_1, \tilde{\mathbf{n}}_2, \tilde{\mathbf{n}}_3\}$ are body-fixed reference frames and thus their orientation relative to each other does not change. Therefore, the relation between them is constant and can be written as:

$$B = N_{\tilde{\mathbf{n}}}^{\mathbf{b}} \tilde{N} , \quad (5.1.6)$$

where the coefficients of $N_{\tilde{\mathbf{n}}}^{\mathbf{b}}$ only depend on the choice of the attachment points C and D . Using equation (5.1.5), the relation between $(\mathbf{b}_1, \mathbf{b}_2, \mathbf{b}_3)$ and $(\mathbf{n}_1, \mathbf{n}_2, \mathbf{n}_3)$ can be given:

$$B = N_{\tilde{\mathbf{n}}}^{\mathbf{b}} \tilde{N} = N_{\tilde{\mathbf{n}}}^{\mathbf{b}} (N_{\mathbf{n}}^{\tilde{\mathbf{n}}}(\boldsymbol{\theta}) N) = N_{\mathbf{n}}^{\mathbf{b}}(\boldsymbol{\theta}) N . \quad (5.1.7)$$

From figures 5.1.1 and 5.1.4 the angular velocity $\boldsymbol{\omega}$ of R can be derived. Introducing a new basis Q :

$$Q = [\tilde{\mathbf{n}}_3, -\mathbf{n}_3, c_4 \mathbf{n}_1 - s_4 \mathbf{n}_2] ,$$

such that the angular velocity $\boldsymbol{\omega}$ with respect to this new basis can be expressed as:

$$[\boldsymbol{\omega}]_Q = \begin{pmatrix} \dot{\theta}_1 \\ \dot{\theta}_4 \\ \dot{\theta}_5 \end{pmatrix} = S_{145} \dot{\boldsymbol{\theta}} .$$

Here S_{145} is a (3×5) -matrix which selects the first, fourth and fifth components of a (5×1) -vector to obtain a (3×1) -vector.

The new basis Q can be written as (using $N = I_3$):

$$Q = N_{\mathbf{n}}^{\mathbf{q}}(\boldsymbol{\theta}) N = N_{\mathbf{n}}^{\mathbf{q}}(\boldsymbol{\theta}) ,$$

where $N_{\mathbf{n}}^{\mathbf{q}}(\boldsymbol{\theta})$ is given by:

$$N_{\mathbf{n}}^{\mathbf{q}}(\boldsymbol{\theta}) = \begin{pmatrix} -s_4 c_5 & 0 & c_4 \\ -c_4 c_5 & 0 & -s_4 \\ -s_5 & -1 & 0 \end{pmatrix} . \quad (5.1.8)$$

As a result, the angular velocity is given by:

$$\boldsymbol{\omega} = Q [\boldsymbol{\omega}]_Q = N_{\mathbf{n}}^{\mathbf{q}}(\boldsymbol{\theta}) [\boldsymbol{\omega}]_Q = N_{\mathbf{n}}^{\mathbf{q}}(\boldsymbol{\theta}) S_{145} \dot{\boldsymbol{\theta}} . \quad (5.1.9)$$

From equation (5.1.9) it follows that the angular velocity can be written as (using $N = I_3$):

$$\boldsymbol{\omega} = N N_{\mathbf{n}}^{\mathbf{q}}(\boldsymbol{\theta}) S_{145} \dot{\boldsymbol{\theta}} ,$$

which is of the form $\boldsymbol{\omega} = N[\boldsymbol{\omega}]_N$. From this it follows that $\boldsymbol{\omega}$ can be expressed with respect to the basis N as:

$$[\boldsymbol{\omega}]_N = N_{\mathbf{n}}^{\mathbf{q}}(\boldsymbol{\theta}) S_{145} \dot{\boldsymbol{\theta}} := G(\boldsymbol{\theta}) \dot{\boldsymbol{\theta}} . \quad (5.1.10)$$

Alternatively, $\boldsymbol{\omega}$ can be expressed with respect to the basis B . Using equation (5.1.10) and the transformation from equation (5.1.7) this gives:

$$[\boldsymbol{\omega}]_B = N_{\mathbf{b}}^{\mathbf{n}}(\boldsymbol{\theta}) G(\boldsymbol{\theta}) \dot{\boldsymbol{\theta}}, \quad (5.1.11)$$

where $N_{\mathbf{b}}^{\mathbf{n}}(\boldsymbol{\theta}) = N_{\mathbf{n}}^{\mathbf{b}}(\boldsymbol{\theta})^{-1}$. The inverse matrix of $N_{\mathbf{n}}^{\mathbf{b}}(\boldsymbol{\theta})$ has to be used here since all vectors expressed with respect to a basis are contravariant to a change of basis. To illustrate the concept of contravariance, consider a temperature scale with intervals of 1 °Celsius. For an object of 5 °Celsius, the quantitative vector on this scale has to have a length of 5. Now, if the scale is divided by a factor 10, the vector for displaying the temperature has to be multiplied by the inverse, multiplied by 10. The analogous happens when a basis is rotated where the quantitative vectors are rotated opposite to the basis such that their quantitative description of a physical entity remains equal.

The angular acceleration $\boldsymbol{\alpha}$ of R can also be expressed either with respect to the basis N or B . Since $\boldsymbol{\alpha} = \frac{d}{dt}\boldsymbol{\omega}$ it follows from equation (5.1.10) that:

$$\begin{aligned} [\boldsymbol{\alpha}]_N &= N [\boldsymbol{\alpha}]_N = \boldsymbol{\alpha} = \frac{d}{dt}\boldsymbol{\omega} = \frac{d}{dt}(N [\boldsymbol{\omega}]_N) = N \frac{d}{dt}([\boldsymbol{\omega}]_N) \iff \\ &= \frac{d}{dt}[\boldsymbol{\omega}]_N = \frac{d}{dt}(G(\boldsymbol{\theta}) \dot{\boldsymbol{\theta}}) = \frac{d}{dt}(N_{\mathbf{n}}^{\mathbf{q}}(\boldsymbol{\theta})) S_{145} \dot{\boldsymbol{\theta}} + N_{\mathbf{n}}^{\mathbf{q}}(\boldsymbol{\theta}) S_{145} \ddot{\boldsymbol{\theta}}, \end{aligned} \quad (5.1.12)$$

or, because B is a orthonormal basis, using the transformation matrix from equation (5.1.7):

$$[\boldsymbol{\alpha}]_B = N_{\mathbf{b}}^{\mathbf{n}}(\boldsymbol{\theta}) \left(\frac{d}{dt}(N_{\mathbf{n}}^{\mathbf{q}}(\boldsymbol{\theta})) S_{145} \dot{\boldsymbol{\theta}} + N_{\mathbf{n}}^{\mathbf{q}}(\boldsymbol{\theta}) S_{145} \ddot{\boldsymbol{\theta}} \right). \quad (5.1.13)$$

The position \mathbf{r} of the center of mass R^* relative to the attachment point C can be derived from figure 5.1.4. It is immediately clear that \mathbf{r} can be give in terms of the angle λ and the distance r . It holds that because the position of the center of mass is stationary relative to attachment point C , \mathbf{r} can be expressed with respect to the basis \tilde{N} as:

$$[\mathbf{r}]_{\tilde{N}} = \begin{pmatrix} r \sin(\lambda) \\ 0 \\ -r \cos(\lambda) \end{pmatrix}, \quad (5.1.14)$$

such that:

$$\mathbf{r} = \tilde{N} [\mathbf{r}]_{\tilde{N}}.$$

Using the transformation matrix of equation (5.1.5) yields an expression with respect to the basis N :

$$[\mathbf{r}]_N = N_{\mathbf{n}}^{\mathbf{n}}(\boldsymbol{\theta}) [\mathbf{r}]_{\tilde{N}}. \quad (5.1.15)$$

The velocity \mathbf{v}^{R^*} of the center of mass R^* can be derived using:

$${}^N \mathbf{v}^{R^*} = {}^N \mathbf{v}^C + {}^N \boldsymbol{\omega}^R \times \mathbf{r}^{CR^*},$$

which is in this example:

$$[\mathbf{v}^{R^*}]_N = [\mathbf{v}^C]_N + [\boldsymbol{\omega}]_N \times [\mathbf{r}]_N,$$

where \mathbf{v}^C is the tangential velocity of attachment point C , which can be derived from figure 5.1.1:

$$[\mathbf{v}^C]_N = \begin{pmatrix} lc_2c_3\dot{\theta}_2 - ls_2s_3\dot{\theta}_3 \\ lc_2s_3\dot{\theta}_2 + ls_2c_3\dot{\theta}_3 \\ ls_2\dot{\theta}_2 \end{pmatrix} = \begin{pmatrix} 0 & lc_2c_3 & -ls_2s_3 & 0 & 0 \\ 0 & lc_2s_3 & ls_2c_3 & 0 & 0 \\ 0 & ls_2 & 0 & 0 & 0 \end{pmatrix} \dot{\boldsymbol{\theta}} := C(\boldsymbol{\theta}) \dot{\boldsymbol{\theta}}. \quad (5.1.16)$$

Substitution of $[\boldsymbol{\omega}]_N$, $[\mathbf{r}]_N$ and $[\mathbf{v}^C]_N$ from equations (5.1.10), (5.1.15) and (5.1.16) gives that the angular velocity can be written as:

$$\begin{aligned} [\mathbf{v}^{R^*}]_N &= C(\boldsymbol{\theta}) \dot{\boldsymbol{\theta}} + G(\boldsymbol{\theta}) \dot{\boldsymbol{\theta}} \times [\mathbf{r}]_N \iff \\ &= C(\boldsymbol{\theta}) \dot{\boldsymbol{\theta}} + W(\boldsymbol{\theta}) \dot{\boldsymbol{\theta}} = (C(\boldsymbol{\theta}) + W(\boldsymbol{\theta})) \dot{\boldsymbol{\theta}} \iff \\ &:= V(\boldsymbol{\theta}) \dot{\boldsymbol{\theta}}, \end{aligned} \quad (5.1.17)$$

where $W(\boldsymbol{\theta})$ is a (3×5) -matrix with columns $\mathbf{w}_i = G(\boldsymbol{\theta}) \mathbf{e}_i \times [\mathbf{r}]_N$.

Taking the time derivative of equation (5.1.17) results in an expression for the acceleration \mathbf{a}^{R^*} of R^* with respect to the basis N :

$$[\mathbf{a}^{R^*}]_N = \dot{V}(\boldsymbol{\theta}) \dot{\boldsymbol{\theta}} + V(\boldsymbol{\theta}) \ddot{\boldsymbol{\theta}}. \quad (5.1.18)$$

To use Kane's equation, the partial rates of change of orientation $\boldsymbol{\omega}_{\dot{\theta}_r}$ of the body R , and four partial rates of change of position $\mathbf{v}_{\dot{\theta}_r}$ of the center of mass R^* have to be known in order to calculate F_r and F_r^* . Since the partial rates of change of orientation are the partial derivatives of $\boldsymbol{\omega}$ with respect to $\dot{\theta}_1, \dots, \dot{\theta}_4$, these partial rates are the coefficients of $\dot{\theta}_1, \dots, \dot{\theta}_4$ in equation (5.1.10), where $\dot{\theta}_5$ has first been substituted out using the constraint equation (5.1.4).

Eliminating $\dot{\theta}_5$ from equation (5.1.10) using the constraint equation (5.1.4) yields an alternate expression for $[\boldsymbol{\omega}]_N$:

$$\begin{aligned} [\boldsymbol{\omega}]_N &= G(\boldsymbol{\theta}) \dot{\boldsymbol{\theta}} = N_{\mathbf{n}}^{\mathbf{q}}(\boldsymbol{\theta}) S_{145} \dot{\boldsymbol{\theta}} = N_{\mathbf{n}}^{\mathbf{q}}(\boldsymbol{\theta}) \begin{pmatrix} 1 & 0 & 0 & 0 & 0 \\ 0 & 0 & 0 & 1 & 0 \\ 0 & 0 & 0 & 0 & 1 \end{pmatrix} \dot{\boldsymbol{\theta}} \\ &= N_{\mathbf{n}}^{\mathbf{q}}(\boldsymbol{\theta}) \begin{pmatrix} 1 & 0 & 0 & 0 \\ 0 & 0 & 0 & 1 \\ & & \gamma(\boldsymbol{\theta})^T & \end{pmatrix} I_{45} \dot{\boldsymbol{\theta}} \\ &:= G_{new}(\boldsymbol{\theta}) I_{45} \dot{\boldsymbol{\theta}}. \end{aligned} \quad (5.1.19)$$

Because $\boldsymbol{\omega} = N [\boldsymbol{\omega}]_N$ and $N = I_3$ it follows that:

$$\boldsymbol{\omega} = G_{new}(\boldsymbol{\theta}) I_{45} \dot{\boldsymbol{\theta}}. \quad (5.1.20)$$

Equation (5.1.20) is of the form:

$$\boldsymbol{\omega} = \boldsymbol{\omega}_{\dot{\theta}_1} \dot{\theta}_1 + \boldsymbol{\omega}_{\dot{\theta}_2} \dot{\theta}_2 + \boldsymbol{\omega}_{\dot{\theta}_3} \dot{\theta}_3 + \boldsymbol{\omega}_{\dot{\theta}_4} \dot{\theta}_4,$$

such that the partial rates of change of orientation $\boldsymbol{\omega}_{\dot{\theta}_r}$ are the columns of the matrix $G_{new}(\boldsymbol{\theta})$.

Equivalently, the constraint equation (5.1.4) can be used to rewrite equation (5.1.17) as:

$$\begin{aligned} [\mathbf{v}^{R^*}]_N &= V(\boldsymbol{\theta}) \dot{\boldsymbol{\theta}} = (V(\boldsymbol{\theta}) I_{54} + V(\boldsymbol{\theta}) \mathbf{e}_5 \gamma(\boldsymbol{\theta})^T) I_{45} \dot{\boldsymbol{\theta}} \iff \\ &:= V_{new}(\boldsymbol{\theta}) I_{45} \dot{\boldsymbol{\theta}}, \end{aligned} \quad (5.1.21)$$

here I_{54} is a (4×4) -identity matrix with an added row of zeros forming a (5×4) -matrix such that $V_{new}(\boldsymbol{\theta})$ is a (3×4) -matrix.

Again, because $\mathbf{v}^{R^*} = N [\mathbf{v}^{R^*}]_N$ and $N = I_3$ it follows that:

$$\mathbf{v}^{R^*} = V_{new}(\boldsymbol{\theta}) I_{45} \dot{\boldsymbol{\theta}}. \quad (5.1.22)$$

Equation (5.1.22) is of the form:

$$\mathbf{v}^{R^*} = \mathbf{v}_{\dot{\theta}_1} \dot{\theta}_1 + \mathbf{v}_{\dot{\theta}_2} \dot{\theta}_2 + \mathbf{v}_{\dot{\theta}_3} \dot{\theta}_3 + \mathbf{v}_{\dot{\theta}_4} \dot{\theta}_4,$$

from which it follows that the partial rates of change of position $\mathbf{v}_{\dot{\theta}_r}$ are the columns of the matrix $V_{new}(\boldsymbol{\theta})$.

The generalized active forces F_1, \dots, F_4 can now be determined by multiplying the partial rates of change of position with the gravitational force. Because the gravitational force is the only external force in the system (and it is already working on the center of mass of the suspended object R), the generalized active forces can then be expressed as:

$$F_r = \mathbf{v}_{\dot{\theta}_r} \cdot (-mg\mathbf{n}_3), \quad (5.1.23)$$

where g is the gravitational acceleration and m the mass of the suspended body R . This expression can be given explicitly in terms of the earlier found matrix $V_{new}(\boldsymbol{\theta})$.

$$\begin{aligned} F_r &= \mathbf{v}_{\dot{\theta}_r} \cdot (-mg\mathbf{n}_3) \iff \\ &= (V_{new}(\boldsymbol{\theta}) \mathbf{e}_r^*)^T (-mg\mathbf{n}_3). \end{aligned} \quad (5.1.24)$$

The notation \mathbf{e}_r^* for the r -th unit vector of \mathbb{R}^4 is used to emphasize the difference with earlier used unit vectors \mathbf{e}_r which have dimension 5, whereas the vector \mathbf{e}_r^* has dimension 4.

The generalized inertia forces F_r^* are calculated by adding the product of the inertia force and the partial rate of change of position with the product of the inertia torque and the partial rate of change of orientation:

$$\begin{aligned} F_r^* &= \mathbf{v}_{\dot{\theta}_r} \cdot (-m [\mathbf{a}^{\mathbf{R}^*}]_N) + \boldsymbol{\omega}_{\dot{\theta}_r} \cdot \mathbf{T} \iff \\ &= (\mathbf{v}_{\dot{\theta}_r})^T (-m [\mathbf{a}^{\mathbf{R}^*}]_N) + (\boldsymbol{\omega}_{\dot{\theta}_r})^T \mathbf{T}. \end{aligned} \quad (5.1.25)$$

Here $[\mathbf{a}^{\mathbf{R}^*}]_N$ is the expression for the acceleration of R^* without dependency on $\dot{\theta}_5$ or $\ddot{\theta}_5$ found by differentiating equation (5.1.21) with respect to time:

$$[\mathbf{a}^{\mathbf{R}^*}]_N = \dot{V}_{new}(\boldsymbol{\theta}) I_{45} \dot{\boldsymbol{\theta}} + V_{new}(\boldsymbol{\theta}) I_{45} \ddot{\boldsymbol{\theta}},$$

and \mathbf{T} denotes the vector containing the inertia torques about the principle axes $\mathbf{b}_1, \mathbf{b}_2, \mathbf{b}_3$:

$$\mathbf{T} = B [\mathbf{T}]_B, \quad (5.1.26)$$

where $[\mathbf{T}]_B$ can be calculated using Euler's Equations for rigid bodies:

$$[\mathbf{T}]_B = -(\mathbf{I} [\boldsymbol{\alpha}]_B + [\boldsymbol{\omega}]_B \times (\mathbf{I} [\boldsymbol{\omega}]_B)).$$

In this equation, $[\boldsymbol{\omega}]_B$ is derived from equation (5.1.20) by using $\boldsymbol{\omega} = N_{\mathbf{b}}^{\mathbf{n}}(\boldsymbol{\theta}) [\boldsymbol{\omega}]_B$:

$$[\boldsymbol{\omega}]_B = N_{\mathbf{b}}^{\mathbf{n}}(\boldsymbol{\theta}) G_{new}(\boldsymbol{\theta}) I_{45} \dot{\boldsymbol{\theta}},$$

and $[\boldsymbol{\alpha}]_B$ is also derived from equation (5.1.20) by first differentiating $\boldsymbol{\omega}$ with respect to time, and subsequently multiplying with the transformation matrix $N_{\mathbf{b}}^{\mathbf{n}}(\boldsymbol{\theta})$:

$$\begin{aligned} [\boldsymbol{\alpha}]_B &= N_{\mathbf{b}}^{\mathbf{n}}(\boldsymbol{\theta}) [\boldsymbol{\alpha}]_N = N_{\mathbf{b}}^{\mathbf{n}}(\boldsymbol{\theta}) \boldsymbol{\alpha} = N_{\mathbf{b}}^{\mathbf{n}}(\boldsymbol{\theta}) \frac{d\boldsymbol{\omega}}{dt} \\ &= N_{\mathbf{b}}^{\mathbf{n}}(\boldsymbol{\theta}) \left(\dot{G}_{new}(\boldsymbol{\theta}) I_{45} \dot{\boldsymbol{\theta}} + G_{new}(\boldsymbol{\theta}) I_{45} \ddot{\boldsymbol{\theta}} \right). \end{aligned}$$

Writing equation (5.1.25) in terms of earlier found expressions:

$$\begin{aligned} F_r^* &= (\mathbf{v}_{\dot{\theta}_r})^T (-m [\mathbf{a}^{\mathbf{R}^*}]_N) + (\boldsymbol{\omega}_{\dot{\theta}_r})^T \mathbf{T} \iff \\ &= -m (V_{new}(\boldsymbol{\theta}) \mathbf{e}_r^*)^T \left(\dot{V}_{new}(\boldsymbol{\theta}) I_{45} \dot{\boldsymbol{\theta}} + V_{new}(\boldsymbol{\theta}) I_{45} \ddot{\boldsymbol{\theta}} \right) + (G_{new}(\boldsymbol{\theta}) \mathbf{e}_r^*)^T \mathbf{T} \end{aligned} \quad (5.1.27)$$

Assembling Kane's equation yields four dynamical equations of motion:

$$F_r + F_r^* = 0, \quad (r = 1, \dots, 4). \quad (5.1.28)$$

These four equations together with constraint equation (5.1.2) govern all motions of the system.

The only quantities in Kane's equations which are functions of $\ddot{\theta}_1, \dots, \ddot{\theta}_5$ are $[\mathbf{a}^{\mathbf{R}^*}]_N$ and \mathbf{T} . Since these terms are linear in $\ddot{\theta}$ and are not multiplied with one another, the equations (5.1.28) are linear in $\ddot{\theta}$. Therefore, equations (5.1.28) can be written in matrix form as:

$$M_4(\boldsymbol{\theta}) \begin{pmatrix} \ddot{\theta}_1 \\ \ddot{\theta}_2 \\ \ddot{\theta}_3 \\ \ddot{\theta}_4 \end{pmatrix} = N_4(\boldsymbol{\theta}, \dot{\boldsymbol{\theta}}). \quad (5.1.29)$$

The constraint equation can be added to this system by differentiating the constraint equation (5.1.4) once with respect to time:

$$\ddot{\theta}_5 = \dot{\boldsymbol{\gamma}}(\boldsymbol{\theta})^T I_{45} \dot{\boldsymbol{\theta}} + \boldsymbol{\gamma}(\boldsymbol{\theta})^T I_{45} \ddot{\boldsymbol{\theta}}.$$

This expression is linear in $\ddot{\theta}$ and, as such, can be added to the matrix equation to obtain:

$$M_5(\boldsymbol{\theta}) \begin{pmatrix} \ddot{\theta}_1 \\ \ddot{\theta}_2 \\ \ddot{\theta}_3 \\ \ddot{\theta}_4 \\ \ddot{\theta}_5 \end{pmatrix} = N_5(\boldsymbol{\theta}, \dot{\boldsymbol{\theta}}). \quad (5.1.30)$$

The first four rows of matrix M_5 contain the coefficients of $\ddot{\theta}_1, \dots, \ddot{\theta}_5$ in equations (5.1.28) for respectively $r = 1, \dots, 4$. The fifth row contains the coefficients of $\ddot{\theta}_1, \dots, \ddot{\theta}_5$ in the time-differentiated constraint equation. The right-hand side vector N_5 contains all other terms which do not include any second-order time derivatives.

5.2 Lagrangian mechanics

In this section, the equations of motion are derived using a Lagrangian approach. As a guideline for this derivation a paper is used in which the suspension wires are assumed to be parallel [1]. The configuration of the bifilar pendulum is shown in the figure below.

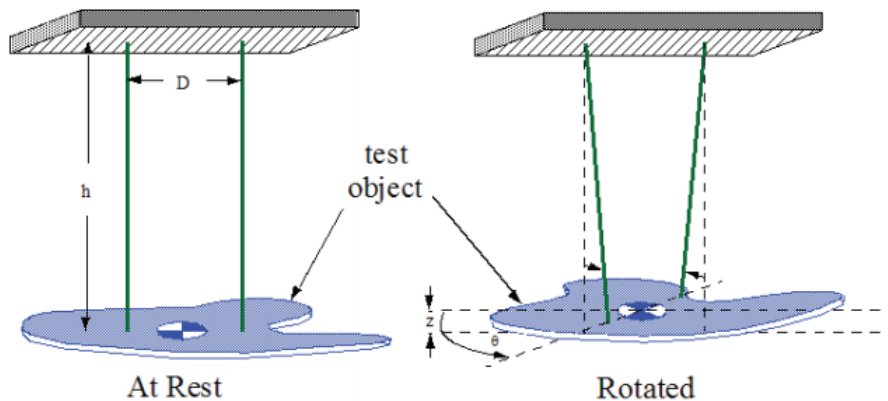


Figure 5.2.1: Configuration of the bifilar pendulum

The object is suspended by two parallel wires of length h separated by distance D . Once the object is rotated over angle θ along the vertical axes through the center of mass of the object, the object is slightly raised compared to the position at rest. This difference in height will be referred to as z .

Lagrange's equation (4.3.16) was derived in section 4.3:

$$\frac{d}{dt} \frac{\partial L}{\partial \dot{q}_j} - \frac{\partial L}{\partial q_j} = 0. \quad (5.2.1)$$

To determine the Lagrangian $L = T - V$, the kinetic energy T and potential energy V of the system are to be calculated.

Since the pendulum has rotational movement θ and a translational movement z the kinetic energy is the sum of these two components:

$$T = T_r + T_t = \frac{1}{2} I \dot{\theta}^2 + \frac{1}{2} m \dot{z}^2. \quad (5.2.2)$$

Now to determine z consider the figure below.

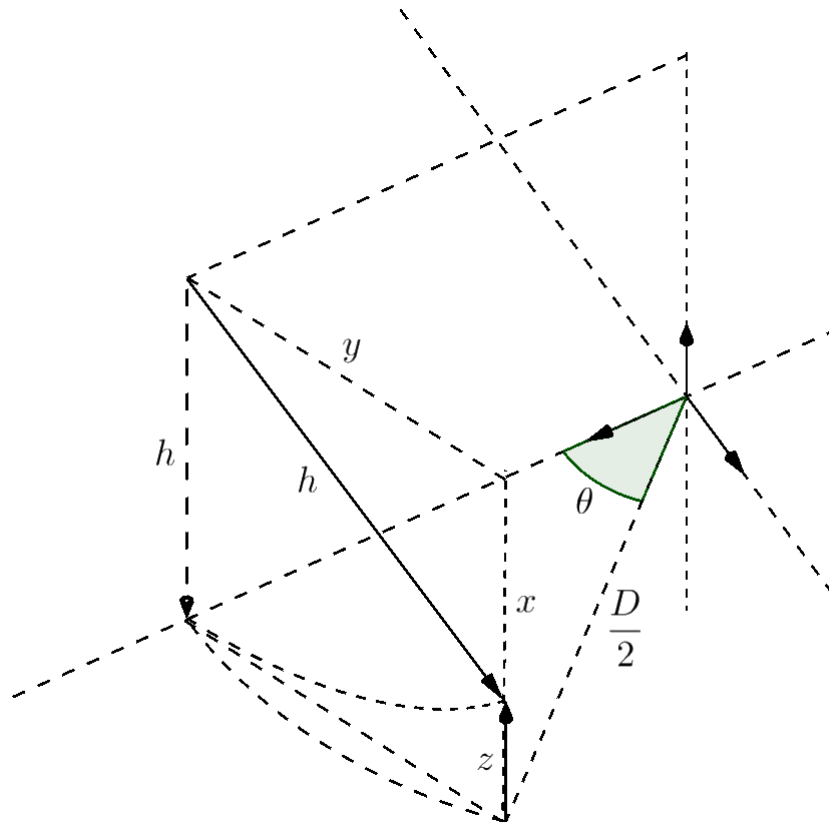


Figure 5.2.2: Schematic of bifilar pendulum rotation

This figure displays one half of the bifilar pendulum, since the other half is identical (except mirrored). It displays how one of the suspension wires changes position as the object rotates over an angle θ about the center of mass (the center of the three unit vectors). From this figure it immediately follows that:

$$z = h - x. \quad (5.2.3)$$

Because the triangle with sides (h, x, y) is right-angled, it follows with Pythagorean theorem that x can be expressed as:

$$x = \sqrt{h^2 - y^2}. \quad (5.2.4)$$

To determine y , note that y can be translated down vertically to form a triangle with sides $(\frac{D}{2}, \frac{D}{2})$ as shown in the figure below.

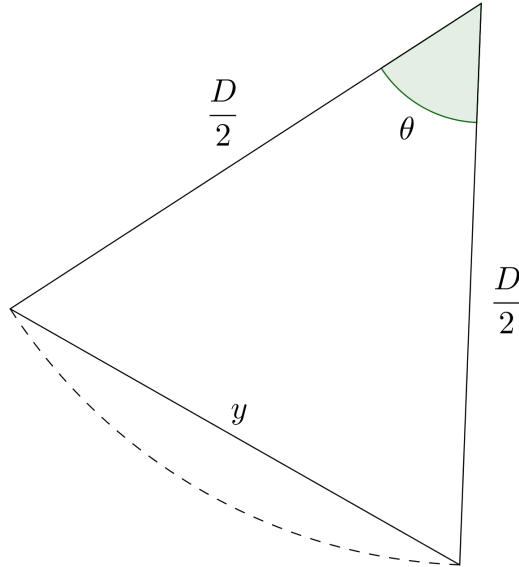


Figure 5.2.3: Projection of y on horizontal plane

Using the law of cosines gives an expression for y^2 :

$$y^2 = \left(\frac{D}{2}\right)^2 + \left(\frac{D}{2}\right)^2 - 2\frac{D}{2}\frac{D}{2}\cos(\theta) \iff \quad (5.2.5)$$

$$= \frac{D^2}{2}(1 - \cos(\theta)). \quad (5.2.6)$$

Combining equations (5.2.3), (5.2.4), (5.2.5) yields an expression for z in terms of θ :

$$\begin{aligned} z &= h - x \iff \\ &= h - \sqrt{h^2 - y^2} \iff \\ &= h - \sqrt{h^2 - \frac{D^2}{2}(1 - \cos(\theta))} \iff \\ &= h - h\sqrt{1 - \frac{1}{2}\left(\frac{D}{h}\right)^2(1 - \cos(\theta))} \iff \\ &= h\left(1 - \sqrt{1 - \frac{1}{2}\left(\frac{D}{h}\right)^2(1 - \cos(\theta))}\right). \end{aligned} \quad (5.2.7)$$

Note that h^2 can be taken out of the root without writing $|h|$ since the suspension wires per definition have a positive length and thus $|h| = h$.

Taking the time derivative of z from equation (5.2.5):

$$\begin{aligned}
\dot{z} &= \frac{d}{dt}z \iff \\
&= \frac{d}{dt} \left[h \left(1 - \sqrt{1 - \frac{1}{2} \left(\frac{D}{h} \right)^2 (1 - \cos(\theta))} \right) \right] \iff \\
&= -\frac{1}{2}h \left(1 - \frac{1}{2} \left(\frac{D}{h} \right)^2 (1 - \cos(\theta)) \right)^{-\frac{1}{2}} \left(-\frac{1}{2} \left(\frac{D}{h} \right)^2 \sin(\theta) \right) \dot{\theta} \iff \\
&= \frac{\frac{h}{4} \left(\frac{D}{h} \right)^2 \sin(\theta)}{\sqrt{1 - \frac{1}{2} \left(\frac{D}{h} \right)^2 (1 - \cos(\theta))}} \dot{\theta}. \tag{5.2.8}
\end{aligned}$$

With the above expression, the kinetic energy as in equation (5.2.2) is known. For the potential energy V it holds that:

$$V = mgz, \tag{5.2.9}$$

which is now also known. The Lagrangian thus becomes:

$$\begin{aligned}
L &= T - V \iff \\
&= \frac{1}{2}I\dot{\theta}^2 + \frac{1}{2}m \frac{\frac{h}{4} \left(\frac{D}{h} \right)^2 \sin(\theta)}{\sqrt{1 - \frac{1}{2} \left(\frac{D}{h} \right)^2 (1 - \cos(\theta))}} \dot{\theta} - mgz. \tag{5.2.10}
\end{aligned}$$

Assuming the bifilar pendulum will only be given small initial values for θ , the rotational kinetic energy $\frac{1}{2}I\dot{\theta}^2$ will be significantly greater than the translational kinetic energy $\frac{1}{2}m\dot{z}^2$. Neglecting the translation kinetic energy, the Lagrangian simplifies to:

$$L = \frac{1}{2}I\dot{\theta}^2 - mgz. \tag{5.2.11}$$

Using Lagrange's equation from (5.2.1) where $q_j = \theta, \dot{q}_j = \dot{\theta}$ the equation of motion for the bifilar pendulum follows:

$$I\ddot{\theta} + \frac{\frac{mgD^2}{4h} \sin(\theta)}{\sqrt{1 - \frac{1}{2} \left(\frac{D}{h} \right)^2 (1 - \cos(\theta))}} = 0, \tag{5.2.12}$$

which for convenience of solving can be rewritten as:

$$\ddot{\theta} + \frac{mgD^2}{4hI} \frac{\sin(\theta)}{\sqrt{1 - \frac{1}{2} \left(\frac{D}{h} \right)^2 (1 - \cos(\theta))}} = 0. \tag{5.2.13}$$

The second-order differential equation from (5.2.13) can be linearized using the assumption that the angle θ is small. As a result of this assumption, it follows from the series expansion of $\sin(\theta)$ and $\cos(\theta)$ that these can be approximated by:

$$\begin{aligned}
\sin(\theta) &= \theta + \mathcal{O}(\theta^3) \approx \theta, \\
\cos(\theta) &= 1 + \mathcal{O}(\theta^2) \approx 1. \tag{5.2.14}
\end{aligned}$$

Substitution of these approximations into (5.2.13) yields a linearized second-order differential equation:

$$\ddot{\theta} + \frac{mgD^2}{4hI}\theta = 0. \quad (5.2.15)$$

Solving this equation analytically, an approximating expression can be found for the moment of inertia I as a function of the period and the configuration parameters. The solution of equation (5.2.15) is of the form:

$$\theta(t) = c_1 \sin\left(\sqrt{\frac{mgD^2}{4hI}}t\right) + c_2 \cos\left(\sqrt{\frac{mgD^2}{4hI}}t\right), \quad (5.2.16)$$

where the constants c_1, c_2 can be determined from the initial conditions. These constants only have an influence on the amplitude of the solution, and are therefore intentionally left undetermined since only the period of the above solution will be of interest. The period of equation (5.2.16) follows directly from the coefficients inside the trigonometric functions:

$$T = \frac{2\pi}{\sqrt{\frac{mgD^2}{4hI}}}. \quad (5.2.17)$$

The above equation can be rewritten to an expression for I :

$$\begin{aligned} T &= \frac{2\pi}{\sqrt{\frac{mgD^2}{4hI}}} \iff \\ \sqrt{\frac{mgD^2}{4hI}} &= \frac{2\pi}{T} \iff \\ \frac{mgD^2}{4hI} &= \frac{4\pi^2}{T^2} \iff \\ I &= \frac{mgD^2}{4h} \frac{T^2}{4\pi^2} = \frac{mgD^2T^2}{16h\pi^2}. \end{aligned} \quad (5.2.18)$$

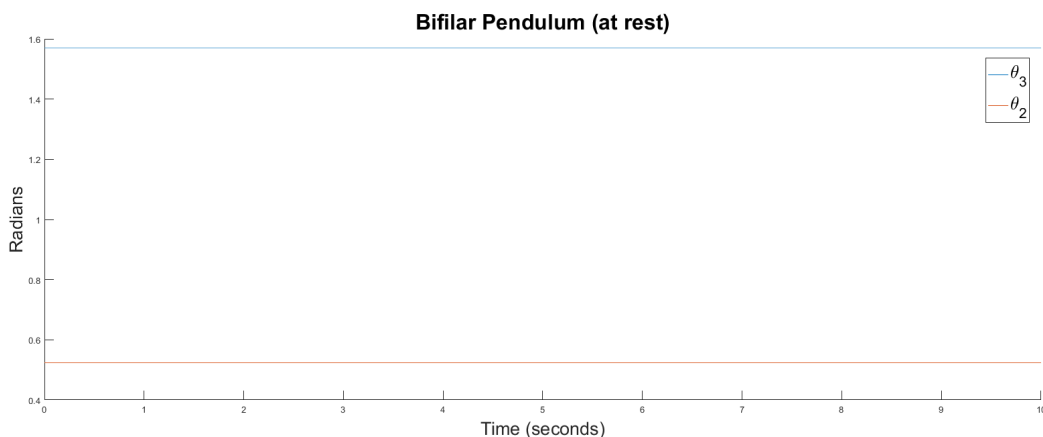
Having performed the actual measurement of the bifilar pendulum and measured the period of oscillation, this equation can then be used to determine the moment of inertia along the vertical axis of the suspended object.

6. Verification equations of motion

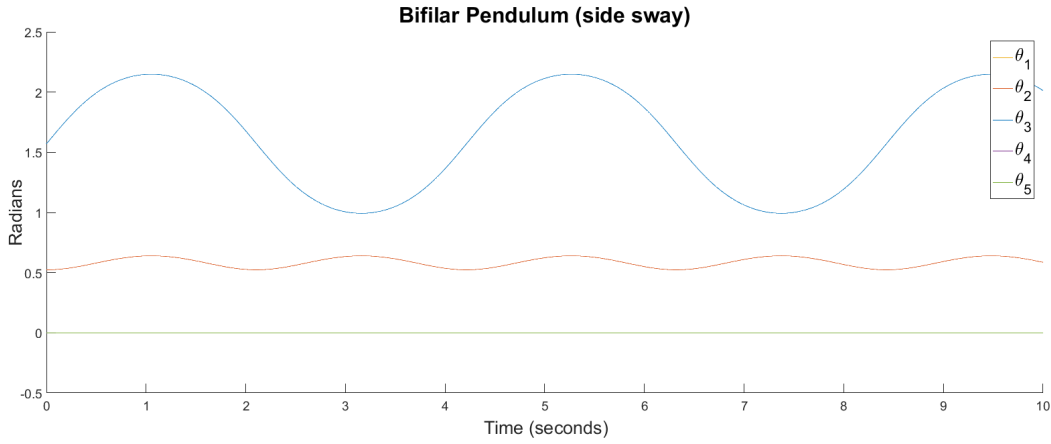
This section will numerically solve the equations of motion of the bifilar from equation (5.1.30) for a number of different configurations. These configurations have been chosen such that these can be verified by analogous models for which the solutions are known. Once the equations of motion have been sufficiently verified, the next section will look at several applications of the equations of motion.

6.1 Side-Sway

Recall the configuration used when graphically checking the constraint equation; figure 5.1.2. In this configuration, the pendulum is at rest since the center of mass is at its lowest point possible, and there are no initial velocities. As a result, one expects that the initial angles $\boldsymbol{\theta}(0) = [0, \frac{\pi}{6}, \frac{\pi}{2}, 0, 0]^T$ will remain constant. Numerically solving this configuration yields the following figure:



As expected all angles ($\theta_1, \theta_4, \theta_5$ are not shown) stay constant at their initial values. Now instead of having no initial velocities, $\dot{\theta}_3(0)$ will be set to 1 radial per second. The object will sway sideways parallel to the \mathbf{n}_2 -axis and from figure 5.1.1, one expects that in this case θ_3 will oscillate around its initial value $\frac{\pi}{2}$ and that θ_2 will oscillate around a value slightly larger than its initial value $\frac{\pi}{6}$ due to the fact that θ_2 is smallest when the attachment point C is above the \mathbf{n}_2 -axis. Numerically solving this configuration yields:



In the above figure, the expected behavior of the configuration is shown; θ_2 is smallest when the object goes through its stationary point, that is $\theta_3 = \frac{\pi}{2}$.

The above motion is in fact analogous to a planar pendulum with same mass and a suspension wire of length $5 \cos(\frac{\pi}{6})$. The period for such a pendulum is known to be

$$T = 2\pi\sqrt{\frac{l}{g}} = 2\pi\sqrt{\frac{5 \cos(\frac{\pi}{6})}{9.81}} = 4.1744 \text{ seconds} .$$

Deriving the period of θ_3 from the simulation yields $T = 4.2$ seconds, which is relatively similar to the theoretical value, where the difference can be caused due to the error made in the ODE-solver of Matlab.

Another way of validating this result is to verify the relation between angles θ_2 and θ_3 . To derive this relation, a schematic of this particular configuration of the bifilar pendulum is shown in the figure below. The top half displays a side-view of the configuration while at rest whereas the bottom half displays a top-view of the bifilar pendulum both at rest and while in oscillation.

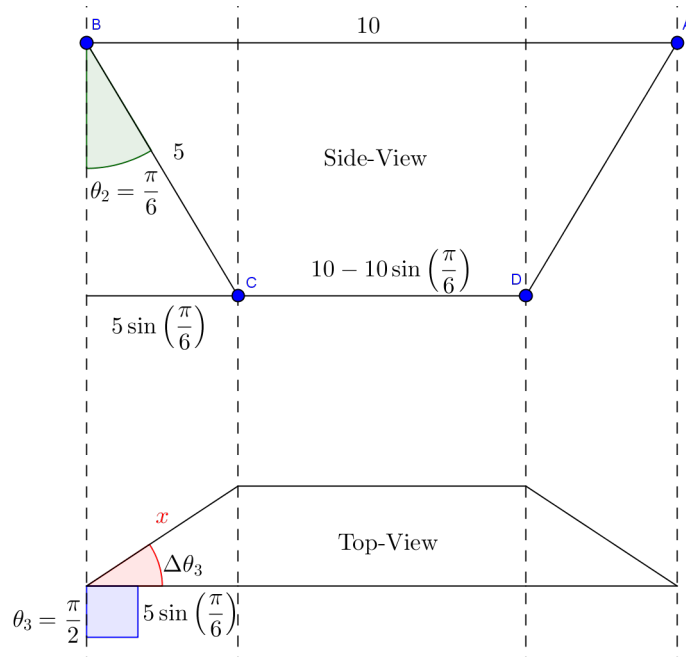


Figure 6.1.1: Side-view at rest & Top view at rest and during oscillation.

From this schematic, the length x can be derived:

$$x = \frac{5 \sin\left(\frac{\pi}{6}\right)}{\cos(\Delta\theta_3)},$$

where $\Delta\theta_3 = \theta_3 - \frac{\pi}{2}$.

Length x can also be expressed in terms of θ_2 by looking at the configuration in the plane spanned by $(\mathbf{n}_3, \overrightarrow{BC})$:

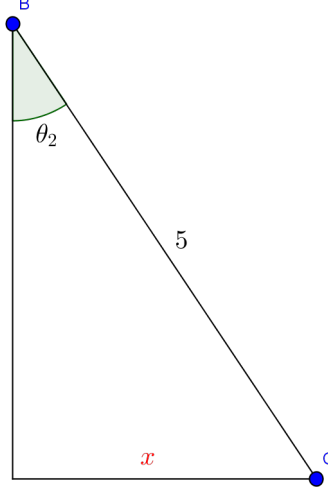


Figure 6.1.2: Bifilar pendulum in $(\mathbf{n}_3, \overrightarrow{BC})$ -plane.

From this view, it becomes immediately clear that x can be expressed as:

$$x = 5 \sin(\theta_2).$$

Both expressions for x should be equal resulting in the relation between θ_2 and θ_3 :

$$\frac{5 \sin\left(\frac{\pi}{6}\right)}{\cos(\Delta\theta_3)} = 5 \sin(\theta_2).$$

Seeing $\theta_2, \Delta\theta_3$ as random variables which are generated by the simulation, the mean and variance can be calculated of $\frac{5 \sin\left(\frac{\pi}{6}\right)}{\cos(\Delta\theta_3)} - 5 \sin(\theta_2)$. Doing so yields:

$$\begin{aligned} \mu &= -2.0496 \cdot 10^{-07}, \\ \sigma^2 &= 2.0200 \cdot 10^{-13}. \end{aligned}$$

Since the mean of $\frac{5 \sin\left(\frac{\pi}{6}\right)}{\cos(\Delta\theta_3)} - 5 \sin(\theta_2)$ is so close to 0 with such little variance, this verifies that the simulation complies with the theoretical relation between θ_2, θ_3 .

6.2 Torsional movement

To draw the parallel between the derivation using Kane's method and the lagrangian method, the suspension wires in Kane's model have to be parallel to one another, in other words $\theta_2 = 0$ and the bifilar pendulum should rotate along the vertical axis through the center of mass. However, setting θ_2 at 0 yields the situation in which θ_3 is not uniquely defined. As a result, there

is no unique solution. This can also be seen in the matrix $M_5(\boldsymbol{\theta})$ from equation (5.1.30) which is singular for $\theta_2 = 0$ for arbitrary values of $\theta_1, \theta_3, \theta_4, \theta_5$ as a result of having a column (third) and a row (third) of zeros.

In order for Matlab to be able to solve this problem, in which it will encounter a singular mass matrix each time the object goes through the stationary point, it has to be told that it will encounter such matrix. Because the matrix $M_5(\boldsymbol{\theta})$ is so large, the equations of motion are for computational reasons left in the form $M_5(\boldsymbol{\theta}) \dot{\boldsymbol{\theta}} = N_5(\boldsymbol{\theta}, \dot{\boldsymbol{\theta}})$. In the situation that M_5 is singular, the problem is a system of differential-algebraic equations (DAE). These systems only have a consistent solution $\boldsymbol{\theta}(0)$ when there is a initial slope $\dot{\boldsymbol{\theta}}(0)$ such that $M_5(\boldsymbol{\theta}(0)) \dot{\boldsymbol{\theta}}(0) = N_5(\boldsymbol{\theta}(0), \dot{\boldsymbol{\theta}}(0))$. One can give the ode-solver in Matlab a initial guess for the slope, or it can be entirely left to Matlab to calculate an initial slope.

Letting Matlab solve this system with initial angle $\theta_4 = \frac{\pi}{80}$ yields:

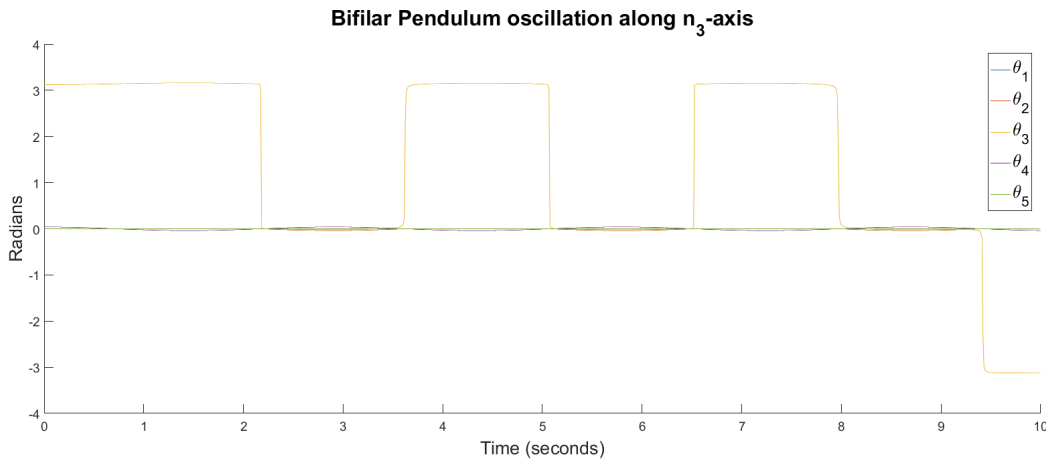


Figure 6.2.1: Numerical solution: rotation along vertical-axis through the center of mass

The jumps in the solution of θ_3 are the result of the mentioned singularity. To check whether this solution satisfies the constraint, for each time step of the numerical solution, one can substitute the values into equation (5.1.2). The obtained vector \mathbf{C} contains a value which should equal the theoretical value $a = l^2 = 25$ for each time step i . Looking at the maximum absolute error:

$$mae = \max_i |c_i - 25| ,$$

yields a absolute maximum error of $mae = 3.9453 \cdot 10^{-05}$. From the small error it can be concluded that the solution satisfies the constraint equation.

Since in this example, both models describe the same motion (both parallel suspension wires), one can compare their solutions. Comparing the solution of θ_3 of Kane's solution to the numerical solution of the Lagrangian approach from equation (5.2.13) for an initial angle $\theta_4(0) = \frac{\pi}{80}$ yields:

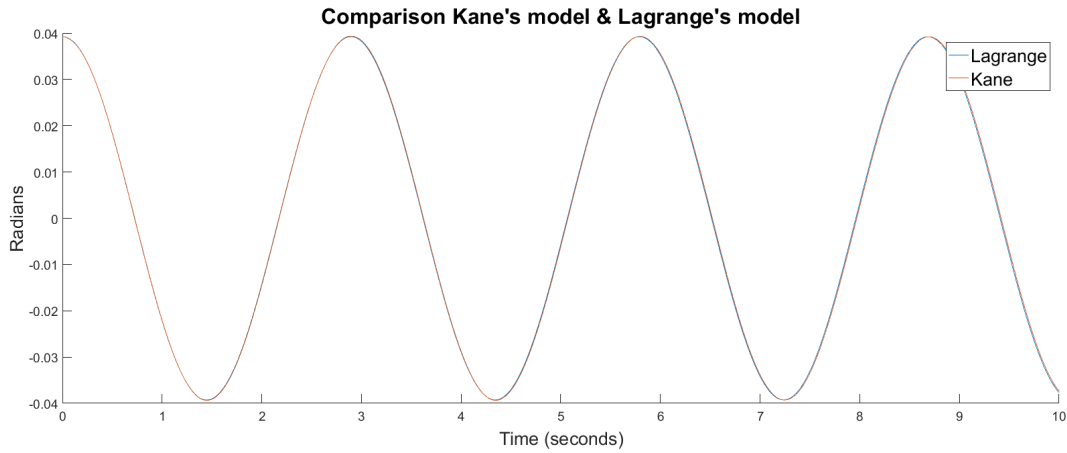


Figure 6.2.2: Comparison numerical solutions Kane's model & Lagrange's model

Both models describe the same motion and as a result their solutions should be equal. In the above figure it can be seen that this in fact holds for the numerical solutions for small initial angles θ_4 . This is in line with the expectations, since Lagrange's model considers a linearized model in which the angles are assumed to be small. For large initial angles this linearization is not accurate anymore and thus explains the different periods for these initial angles. Numerically solving the above example again but now for a significantly larger initial angle $\theta_4(0) = \frac{\pi}{8}$:

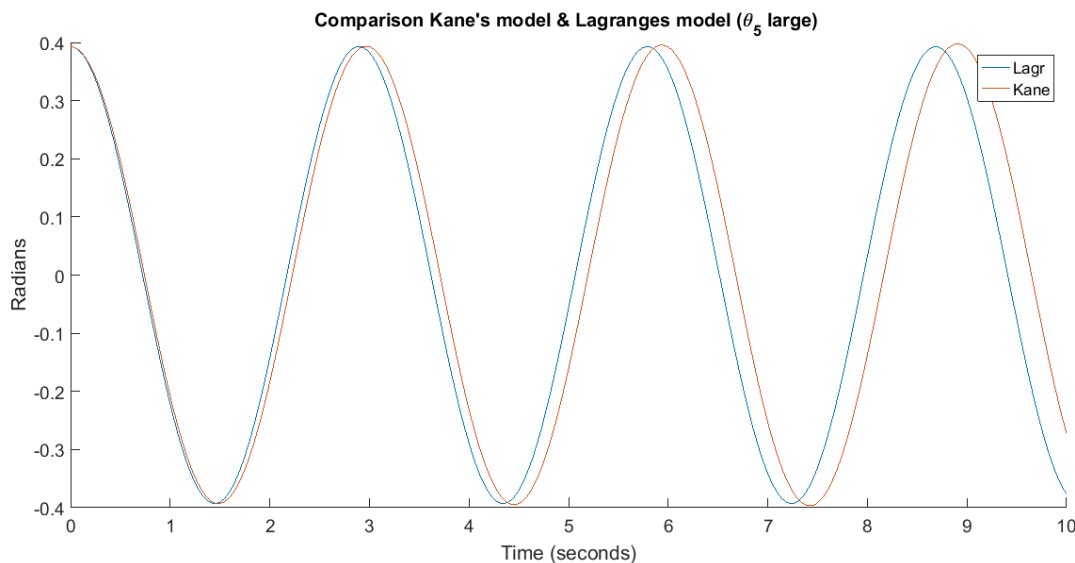


Figure 6.2.3: Comparison numerical solutions Kane's model & Lagrange's model

from which the difference in numerical solutions can be clearly seen as a result of the mentioned assumption in Lagrange's model.

Another method for validating Kane's model is by modifying Lagrange's model such that it no longer assumes parallel suspension wires. To do this, an extra angle ϕ has to be introduced which describes the angle the suspension wires makes with the vertical, similar to θ_2 in Kane's model. The angle ϕ is not independent of θ and this relation can be found by looking at the projection of the configuration on the horizontal plane:

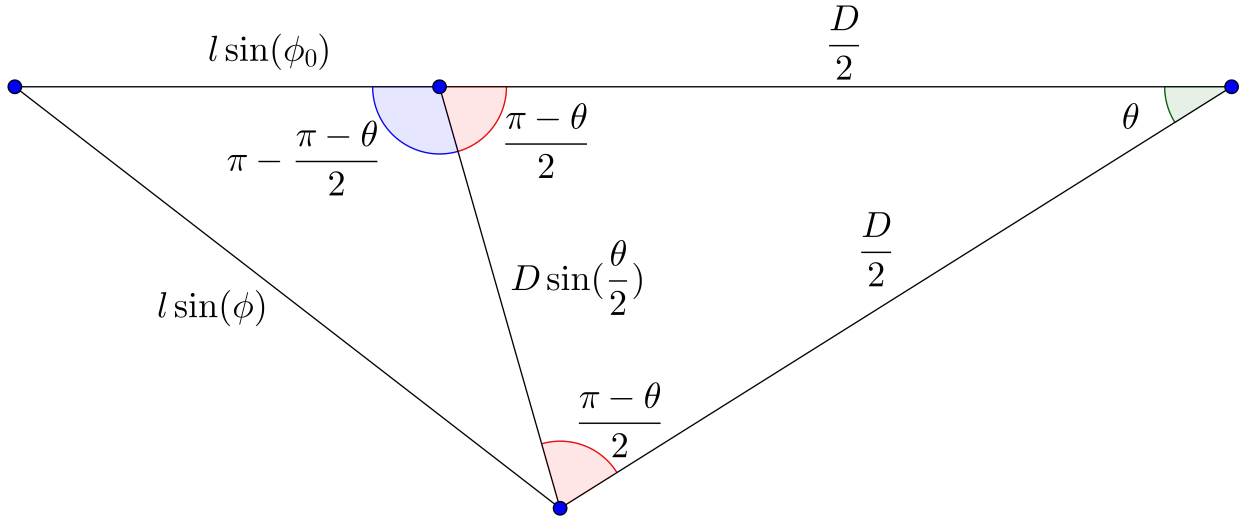


Figure 6.2.4: Adjusted Lagrange's model projection on horizontal plane

In this horizontal projection, θ is the angle over which the object rotates about its vertical axis, ϕ_0 is the angle ϕ while the object is in its stationary position. From this projection, the projection $l \sin(\phi)$ can also be expressed in terms of the other 2 sides and the enclosed angle:

$$l \sin(\phi) = \sqrt{D^2 \sin^2\left(\frac{\theta}{2}\right) + l^2 \sin^2(\phi_0) - 2\left(D \sin\left(\frac{\theta}{2}\right)\right) (l \sin(\phi_0)) \cos\left(\pi - \frac{\pi - \theta}{2}\right)},$$

from which it follows that:

$$\phi = \arcsin\left(\frac{\sqrt{D^2 \sin^2\left(\frac{\theta}{2}\right) + l^2 \sin^2(\phi_0) - 2\left(D \sin\left(\frac{\theta}{2}\right)\right) (l \sin(\phi_0)) \cos\left(\pi - \frac{\pi - \theta}{2}\right)}}{l}\right).$$

The translational height z can then be expressed as:

$$\begin{aligned} z &= l \cos(\phi_0) - l \cos(\phi) \iff \\ &= l \cos(\phi_0) \\ &\quad - l \cos\left(\arcsin\left(\frac{\sqrt{D^2 \sin^2\left(\frac{\theta}{2}\right) + l^2 \sin^2(\phi_0) - 2\left(D \sin\left(\frac{\theta}{2}\right)\right) (l \sin(\phi_0)) \cos\left(\pi - \frac{\pi - \theta}{2}\right)}}{l}\right)\right). \end{aligned}$$

Because ϕ_0 is a constant, z is now a function of θ . The Lagrangian then, as in section 5.2:

$$L = \frac{1}{2}I\dot{\theta}^2 - mgz.$$

Using Lagrange's equation again yields the equation of motion for Lagrange's model, without the assumption of parallel suspension wires. If now ϕ_0 is chosen such that it is equal to the value of θ_2 while at the stationary position, both models describe the exact same configuration. Comparing the solutions of both models results in the following figure.

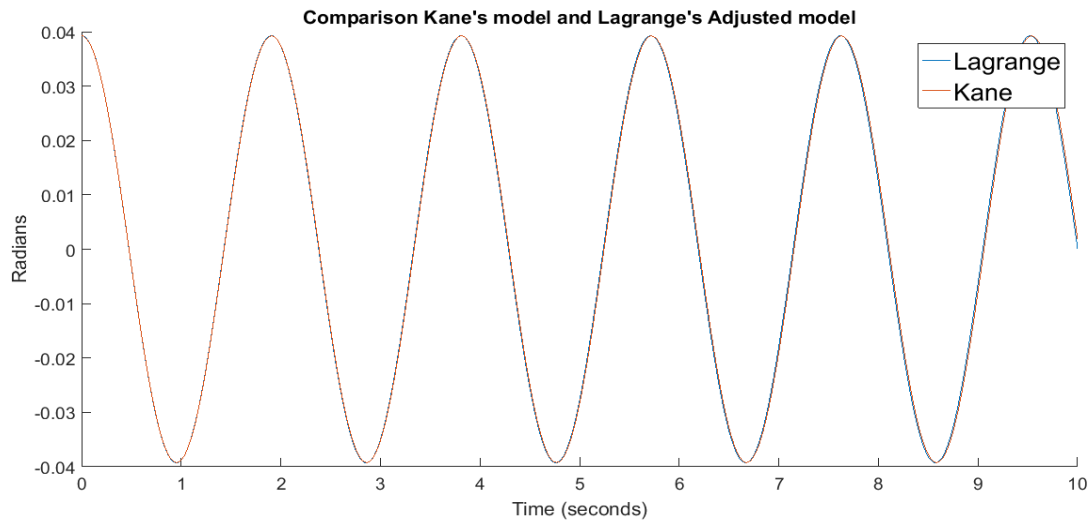


Figure 6.2.5: Comparison numerical solution Kane's model & Lagrange's adjusted model

It can be seen that both solutions do not display any differences, which is another verification that Kane's model has been properly modelled.

6.3 Suspended object with dimensions

In all of the previous examples above, the object was assumed to be infinitely thin and as a result of this the center of mass was located on the line CD . A final validation step for the model can be done for a configuration for which this is not the case: $\lambda > 0$. To do so, consider the first configuration again in which the bifilar pendulum only experienced side-sway, only now the center of mass is not on the line CD . Such configuration is analogous to a double-pendulum; a pendulum attached to another pendulum, as shown below.

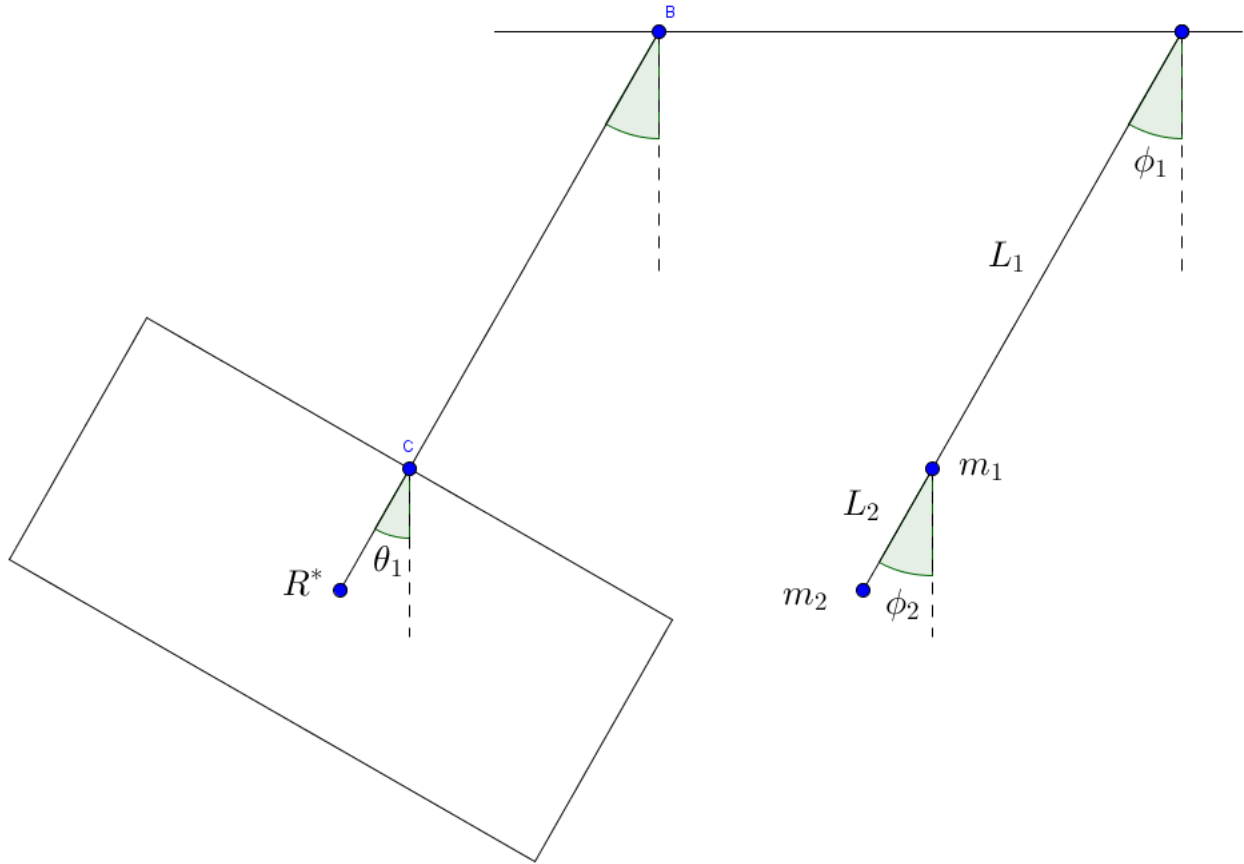


Figure 6.3.1: Analogy of bifilar pendulum (side-view) and double pendulum

The double pendulum's movement is entirely defined by the two lengths of the suspension wires L_1, L_2 and the angles ϕ_1, ϕ_2 , where $\phi_2 = \theta_1$ (and ϕ_1 is the projection of θ_2 on the plane spanned by $(\mathbf{n}_1, \mathbf{n}_3)$).

Solving the models with parameters $m_1 = m_2 = 5$, $L_1 = 5 \cos(\theta_2)$, $L_2 = \frac{1}{2}$ and $I = m_2 L_2^2$ and only giving $\theta_1 = \phi_2$ an initial angle not corresponding to a stationary angle, both solutions become:

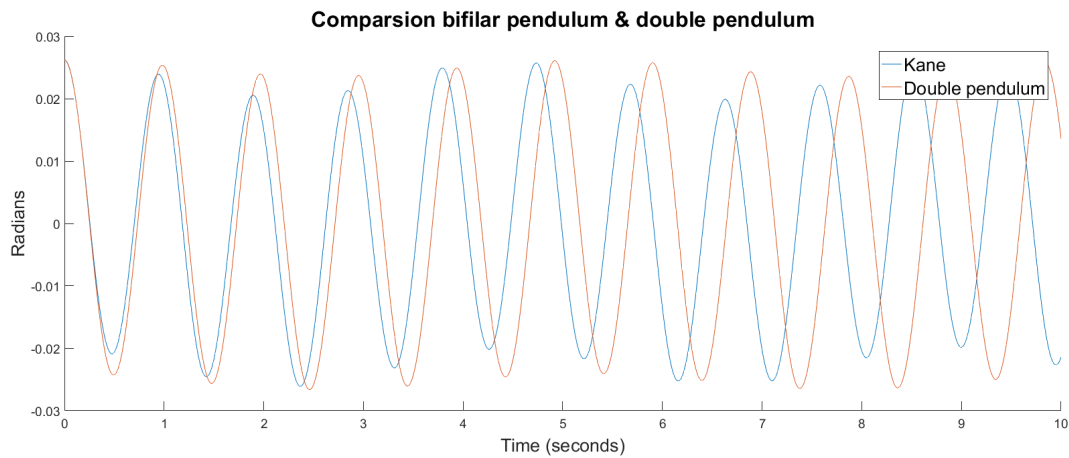


Figure 6.3.2: Numerical solutions of bifilar pendulum and double pendulum

Note that the solutions are only equal for the very first part. This is most likely caused by the

inherent chaotic property of the chaotic pendulum. As a result of this, any small error in the numeric solution could result to large difference in its further movement. As a motivation for this, two solutions of the chaotic pendulum's equations of motion will be calculated, one for initial conditions $\theta(0) = [0, \frac{\pi}{6}]$ and one for $\theta(0) = [0.05, \frac{\pi}{6}]$. The solutions for θ_2 are plotted in the following figure:

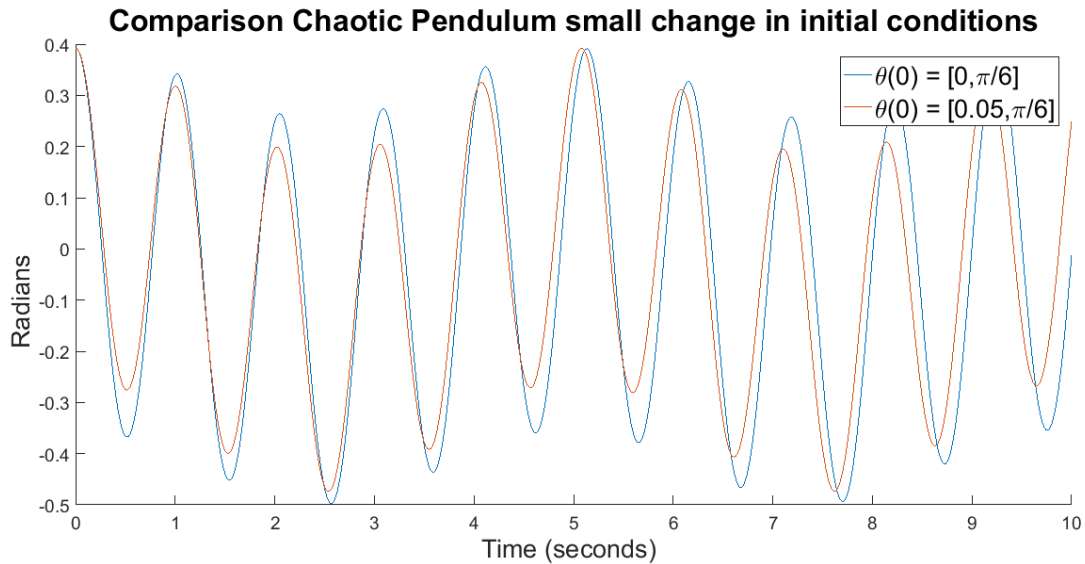


Figure 6.3.3: Numerical solutions of θ_2 for the chaotic pendulum

This figure displays the same kind of differences between the two solutions: a different period between the solutions and different values for the maximums and minimums.

6.4 Comparison paper: cylinder

In Kane's paper [3], the authors present a test case for a suspended solid cylinder with the corresponding solutions for given initial conditions. A solid cylinder, whose height and diameter are equal to the distance between the suspension wires on the overhead, is suspended by two suspension wires of unequal length, as shown in the figure below.

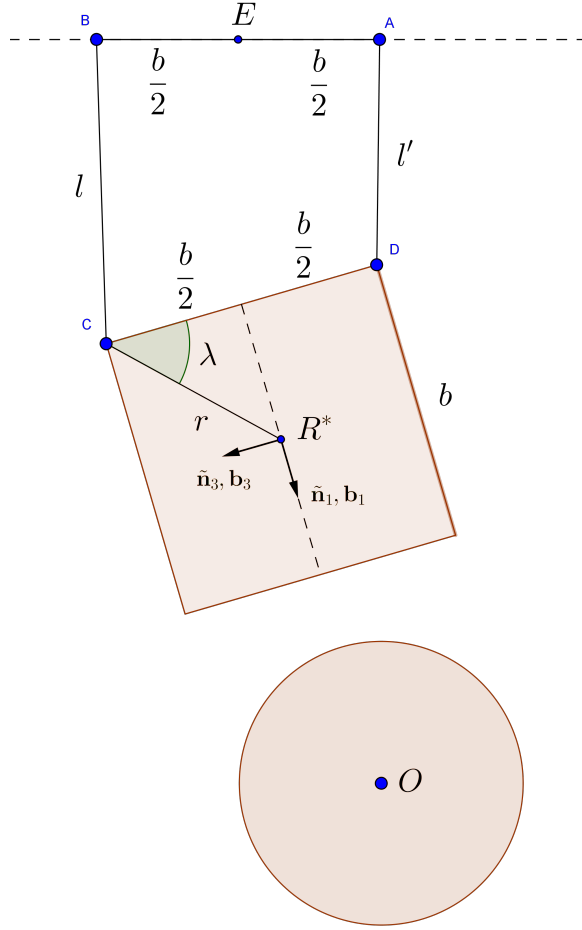


Figure 6.4.1: Solid cylinder attached to unequal suspension wires

From this side-view of the bifilar pendulum, it can be derived that:

$$r = \frac{b}{\sqrt{2}}, \quad \lambda = \frac{\pi}{4},$$

$$I_1 = \frac{1}{2}m \left(\frac{b}{2}\right)^2 = \frac{mb^2}{8}, \quad I_2 = I_3 = \frac{1}{12}m \left(3 \left(\frac{b}{2}\right)^2 + b^2\right) = \frac{7}{48}mb^2.$$

A set of initial conditions is obtained by imagining a situation in which the angles $\theta_1, \dots, \theta_4$ would have the value as if both suspension wires have equal length and the cylinder were raised vertically by rotating it about its axis of symmetry through an angle $\frac{\pi}{4}$. The initial angles then become:

$$\begin{aligned} \theta_1(0) &= 0, & \dot{\theta}_1(0) &= 0, \\ \theta_2(0) &= \arcsin\left(\frac{1}{2} \sin\left(\frac{\pi}{8}\right)\right), & \dot{\theta}_2(0) &= 0, \\ \theta_3(0) &= \frac{7}{8}\pi, & \dot{\theta}_3(0) &= 0, \\ \theta_4(0) &= \frac{\pi}{4}, & \dot{\theta}_4(0) &= 0, \end{aligned}$$

and the initial conditions of $\theta_5, \dot{\theta}_5$ can be found by substituting the above into the constraint equations (5.1.2) and (5.1.4) and solving for $\theta_5(0)$ and $\dot{\theta}_5(0)$. In Kane's paper, the results are presented on a dimensionless x -axis by scaling the time t with $\sqrt{\frac{g}{b}}$. By choosing $b = g$, time is scaled with 1 and thus the numerical solutions found in this report can be compared to those of Kane's paper without making any changes to the axes. Solving the equations of motion with the initial conditions from above, the time-development of θ_1 and θ_4 is:

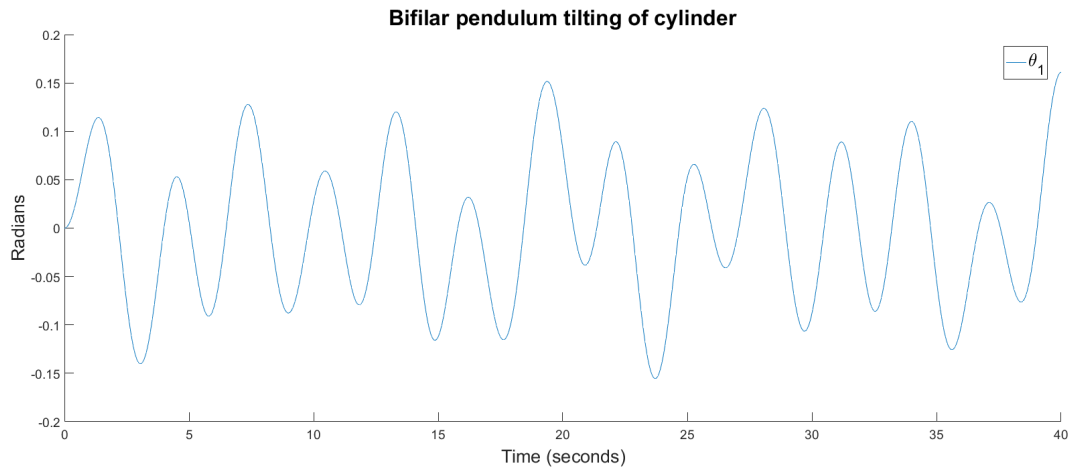


Figure 6.4.2: Tilting of the bifilar pendulum with a solid cylinder ($l = 2b, l' = 1.8b$)

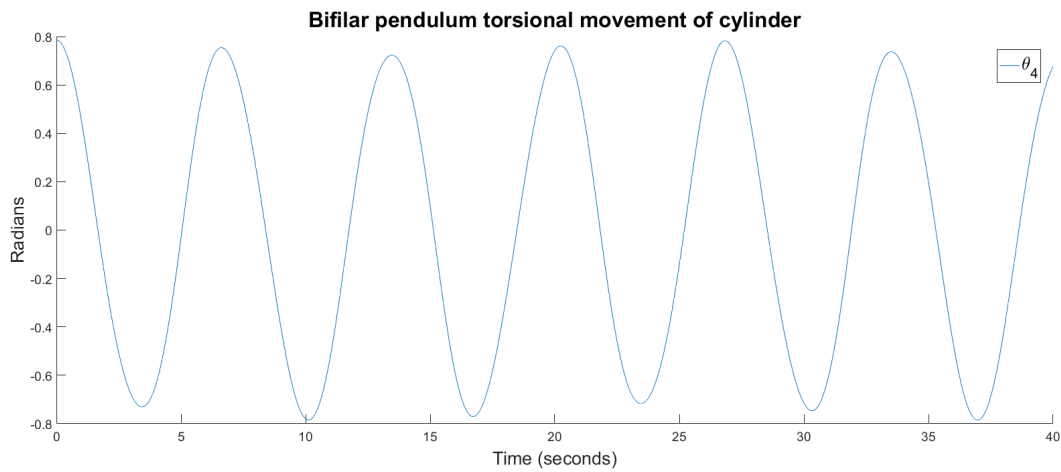


Figure 6.4.3: Torsion of the bifilar pendulum with a solid cylinder ($l = 2b, l' = 1.8b$)

These results are exactly the same as those presented in Kane's paper. Furthermore, the amount of side-sway can be quantified by looking at the projection of the line OE on the horizontal plane (see figure 6.4.1). Plotting the absolute value of this projection yields:

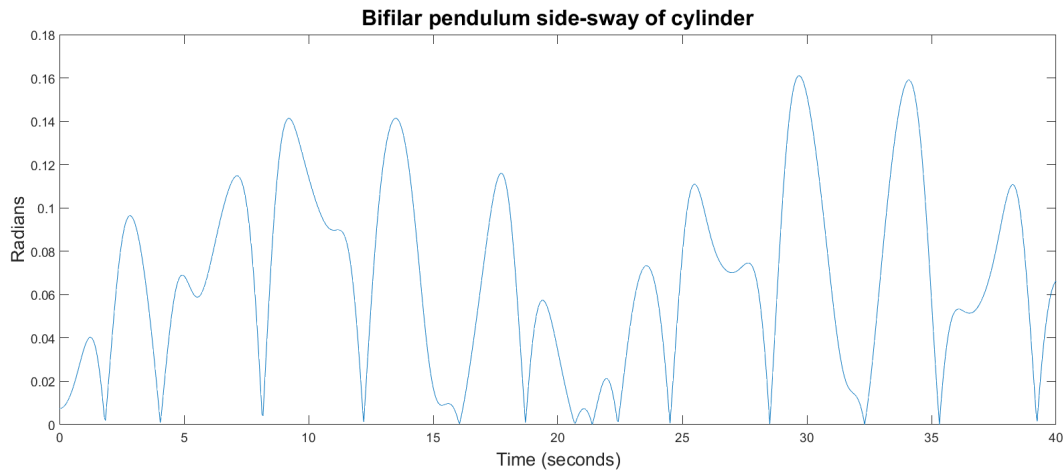


Figure 6.4.4: Side-sway of the bifilar pendulum with a solid cylinder ($l = 2b, l' = 1.8b$)

This result is in accordance with the results presented in Kane's paper [4].

In this section, several different configurations of the bifilar pendulum have been considered and compared to analogous models. In all these examples, the numerical solutions to Kane's model behaved the same as its comparable model, and thus indicate that the equations of motion have been properly modeled. It is therefore concluded that the equations of motion of the bifilar pendulum have been correctly modeled.

7. Applications equations of motion

This section will look two applications of the equations of motion of the bifilar pendulum. First, the equations of motion will be linearized around a stationary position, which can be used in calculating the moments of inertia when performing the experiment of the bifilar pendulum. Secondly, the tensional forces in the suspension wires will be derived which can be used to predict the strains the attachment points on either the ceiling or the object will have to undergo when performing the experiment.

7.1 Linearization

To reconstruct the moments of inertia I_1, I_2, I_3 from the numerical solutions, the equations of motion will be linearized around a stationary point. The eigenvalues of the system can then be expressed as a function of the configuration parameters and the moment of inertia along the corresponding axis. Using these eigenvalues, the experimentally determined period of oscillation can be directly linked to the configuration parameters and moment of inertia along the respective axis. After substitution of all configuration parameters and the experimentally determined period the only remaining unknown is the moment of inertia about that axis.

To linearize around a stationary point, define:

$$\boldsymbol{\theta} = \boldsymbol{\theta}_0 + \Delta\boldsymbol{\theta},$$

where $\boldsymbol{\theta}_0$ is the stationary point around which will be linearized and $\Delta\boldsymbol{\theta}$ the variations the angles have, which are assumed to be small. It then follows that:

$$\begin{aligned}\dot{\boldsymbol{\theta}} &= \Delta\dot{\boldsymbol{\theta}}, \\ \ddot{\boldsymbol{\theta}} &= \Delta\ddot{\boldsymbol{\theta}}.\end{aligned}$$

When the system is at rest, it holds that:

$$A(\boldsymbol{\theta}_0)\ddot{\boldsymbol{\theta}}_0 = 0 = B(\boldsymbol{\theta}_0).$$

It then follows that:

$$\begin{aligned}A(\boldsymbol{\theta}_0 + \Delta\boldsymbol{\theta})\Delta\ddot{\boldsymbol{\theta}} &= B(\boldsymbol{\theta}_0 + \Delta\boldsymbol{\theta}) \iff \\ \left(A(\boldsymbol{\theta}_0) + \frac{\partial}{\partial\boldsymbol{\theta}}A\Big|_{\boldsymbol{\theta}_0}\Delta\boldsymbol{\theta}\right)\Delta\ddot{\boldsymbol{\theta}} &= B(\boldsymbol{\theta}_0) + \frac{\partial}{\partial\boldsymbol{\theta}}B\Big|_{\boldsymbol{\theta}_0}\Delta\boldsymbol{\theta}.\end{aligned}$$

This can be further simplified by noting that:

$$\frac{\partial}{\partial\boldsymbol{\theta}}A\Big|_{\boldsymbol{\theta}_0}\Delta\boldsymbol{\theta}\Delta\ddot{\boldsymbol{\theta}} = \mathcal{O}(\Delta\boldsymbol{\theta}^2),$$

and thus because this is a higher-order term, what remains is:

$$A(\boldsymbol{\theta}_0)\Delta\ddot{\boldsymbol{\theta}} = \left. \frac{\partial}{\partial \boldsymbol{\theta}} B \right|_{\boldsymbol{\theta}_0} \Delta\boldsymbol{\theta},$$

which can then be rewritten to the desired form:

$$\begin{aligned} \Delta\ddot{\boldsymbol{\theta}} &= \left(A(\boldsymbol{\theta}_0)^{-1} \left. \frac{\partial}{\partial \boldsymbol{\theta}} B \right|_{\boldsymbol{\theta}_0} \right) \Delta\boldsymbol{\theta} \\ &:= L(\boldsymbol{\theta}_0)\Delta\boldsymbol{\theta}. \end{aligned}$$

The stationary position $\boldsymbol{\theta}_0$ which will be used for reconstructing all three moments of inertia is: $\boldsymbol{\theta}_0 = [0, \frac{\pi}{6}, \frac{\pi}{2}, 0, 0]^T$, and the body-fixed axes around which the moments of inertia will be determined are shown in the figure below.

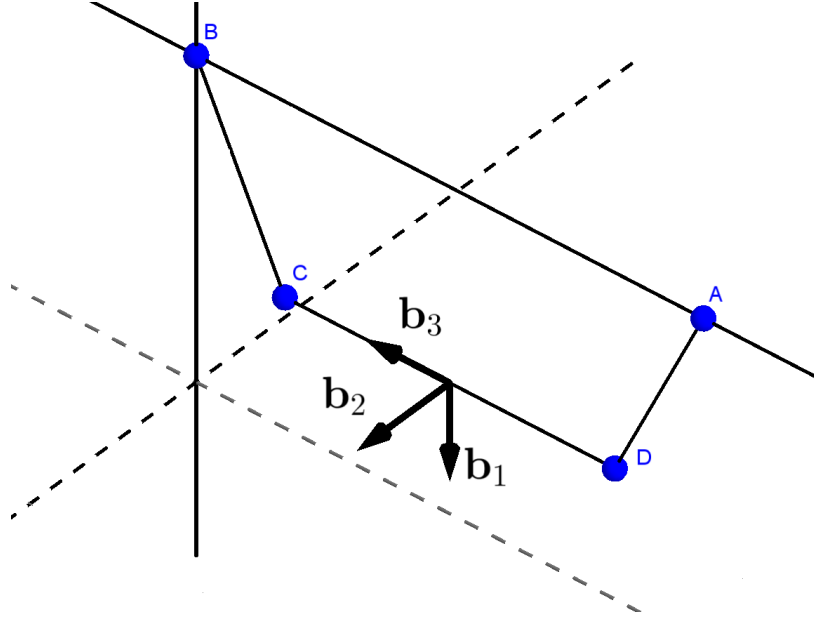


Figure 7.1.1: Body-fixed axes along which the moments of inertia will be calculated (while object is at stationary position).

Linearization 1

To reconstruct the moment of inertia along the \mathbf{b}_1 -axis, the bifilar pendulum will given an initial condition such that it will only rotate along this axis, in other words:

$$\begin{aligned} \theta_1 &= 0, \\ \theta_2 &= \frac{\pi}{6} + \Delta\theta_2, \\ \theta_3 &= \frac{\pi}{2} + \Delta\theta_3, \\ \theta_4 &= 0 + \Delta\theta_4, \\ \theta_5 &= 0. \end{aligned}$$

Assuming that the length of the suspension wire l is very large, $\Delta\theta_2$ can be taken constant¹ as a result of:

$$\Delta\theta_2 \ll \Delta\theta_3, \Delta\theta_4 \quad \text{for } l \gg 0.$$

¹This assumption only holds for very long suspension wires, that is $l \gg 0$. However, in practice it is impossible to use suspension wires of such length. Therefore, when performing the experiment, one should use the longest possible suspension wires to justify this assumption as good as possible.

Since $\theta_1, \theta_2, \theta_5$ are stationary, only the third and fourth rows/columns of L are of interest. Discarding the other rows and columns yields:

$$\Delta \ddot{\theta}_{3,4} = L_{3,4}(\theta_0) \Delta \theta_{3,4} .$$

This system can now be rewritten to its corresponding first-order system. After substitution of the configuration parameters;

$$\begin{aligned} l = l' &= 500 & \lambda &= 0 \\ b &= 505 & r &= \frac{b'}{2} \\ b' &= 5 & g &= 9.81 \\ m &= 100 , \end{aligned}$$

into the matrix L , its eigenvalues can be determined. The eigenvalues are then only a function of the respective moment of inertia. Since these eigenvalues are purely imaginary, the solution to $\theta_4(t)$ is:

$$\theta_4(t) = c_1 e^{\lambda_1 t} + c_2 e^{\lambda_2 t} ,$$

but since the two eigenvalues λ_1, λ_2 are the complex conjugates of each other ($\lambda_1 = xi, \lambda_2 = -xi$), only one of them is needed to obtain:

$$\begin{aligned} \theta_4(t) &= c_1 e^{\lambda_1 t} && \iff \\ &= c_1 e^{xit} && \iff \\ &= c_1 (\cos(xt) + i \sin(xt)) . \end{aligned}$$

Now, from linearity it follows that both the real and imaginary part of this solution, are again solutions for $\theta_4(t)$. Therefore:

$$\theta_4(t) = c_3 \cos(xt) + c_4 \sin(xt) .$$

The period of this solution is:

$$T = \frac{2\pi}{x} ,$$

and because the eigenvalue λ_1 is a function of the moment of inertia I_1 , this equation can be used to calculate the moment of inertia where the period T is the experimentally determined period of oscillation. Since this experiment has not been performed, the numerical periods of oscillation will be used to calculate the moments of inertia using this linearization.

Performing the simulation for an object of which the moment of inertia $I_{1_{analytical}}$ can be calculated analytically and comparing it to the moment of inertia $I_{1_{lin}}$ found using this linearization results in:

$$\begin{aligned} I_{1_{analytical}} &= 260.4167 , \\ I_{1_{lin}} &= 259.2135 . \end{aligned}$$

Linearization 2

To reconstruct the moment of inertia along the \mathbf{b}_2 -axis, the bifilar pendulum will be given an initial condition such that the pendulum will rotate only along that axis:

$$\begin{aligned} \theta_1 &= 0 , \\ \theta_2 &= \frac{\pi}{6} + \Delta\theta_2 , \\ \theta_3 &= \frac{\pi}{2} , \\ \theta_4 &= 0 , \\ \theta_5 &= 0 + \Delta\theta_5 . \end{aligned}$$

Again, after discarding the non-relevant rows/columns, substituting the configuration parameters;

$$\begin{aligned} l = l' = 5 \quad \lambda &= \arccos\left(\frac{b'}{r}\right) \\ b = 10 \quad r &= \sqrt{\left(\frac{b'}{2}\right)^2 + \left(\frac{1}{2}\right)^2} \\ b' = 5 \quad g &= 9.81 \\ m &= 100, \end{aligned}$$

and rewriting the system to its corresponding first-order system the eigenvalues can be calculated as a function of I_2 . From these eigenvalues, the analytical value for the moment of inertia I_3 can be compared to the one found using the above linearization (again using the period of oscillation from the numerical solution):

$$\begin{aligned} I_{3_{analytical}} &= 208.333, \\ I_{3_{lin}} &= 201.8223. \end{aligned}$$

Linearization 3

For reconstructing the moment of inertia along the \mathbf{b}_3 -axis, the bifilar pendulum will be given an initial condition such that the pendulum will rotate only along that axis:

$$\begin{aligned} \theta_1 &= 0 + \Delta\theta_1, \\ \theta_2 &= \frac{\pi}{6} + \Delta\theta_2, \\ \theta_3 &= \frac{\pi}{2} + \Delta\theta_3, \\ \theta_4 &= 0, \\ \theta_5 &= 0. \end{aligned}$$

Assuming again that the suspension wires are very long, θ_2 will change insignificantly, as mentioned in the first case. Therefore, $\Delta\theta_2 = 0$. The columns and rows which are of interest in this situation are the first and third. Again, after discarding the other rows/columns, substituting the configuration parameters;

$$\begin{aligned} l = l' = 500 \quad \lambda &= \arccos\left(\frac{b'}{r}\right) \\ b = 10 \quad r &= \sqrt{\left(\frac{b'}{2}\right)^2 + \left(\frac{1}{2}\right)^2} \\ b' = 5 \quad g &= 9.81 \\ m &= 100, \end{aligned}$$

and rewriting the system to its corresponding first-order system the eigenvalues can be calculated as a function of I_3 . From these eigenvalues, the analytical value for the moment of inertia I_3 can be compared to the one found using the above linearization (again using the period of oscillation from the numerical solution):

$$\begin{aligned} I_{3_{analytical}} &= 52.0833, \\ I_{3_{lin}} &= 52.1033. \end{aligned}$$

Summarizing all of the three results from the linearizations:

	I_1	I_2	I_3
Analytical	260.4167	208.333	52.0833
Linearization	259.2135	201.8223	52.1033

Table 7.1.1: Comparison analytical and approximated values for moments of inertia

Having all approximations side-by-side, it is clear that the approximations for I_1, I_3 are more accurate than the one for I_2 . This is caused by the fact that the movement along the \mathbf{b}_2 -axis is significantly influenced by the mass of the object. Therefore, the effect of the moment of inertia along this axis is less compared to the other axis, and as a result the approximation of the moment of inertia is less accurate.

7.2 Tensional forces

For practical reasons of conducting experiments with a bifilar pendulum, one can be interested in the tensional forces in the suspension wires. First, a derivation for the tensional forces will be derived for a situation in which the suspension wires are symmetric along the vertical line through the center of mass of the object. For some torsional motions of the bifilar pendulum this derivation suffices. However, to be able to calculate the tensional forces in an arbitrary configuration, a derivation will also be presented which does not assume symmetric suspension wires.

To calculate the tensional forces when assuming symmetry, equation (5.1.18) for the acceleration of the center of mass in the earth-fixed reference frame can be used:

$$2F_3 = -m a_3 - m g ,$$

where F_3 is the vertical component of the tensional force along the earth-fixed axis \mathbf{n}_3 and a_3 is the third component of $[\mathbf{a}^{R^*}]_N$. The factor 2 results from the assumption of symmetry. From the constraint function of the bifilar pendulum it follows that:

$$[\overrightarrow{BC}]_N = \begin{pmatrix} l \sin(\theta_2) \cos(\theta_3) \\ l \sin(\theta_2) \sin(\theta_3) \\ -l \cos(\theta_2) \end{pmatrix} .$$

However, the tensional force works in the opposite direction \overrightarrow{CB} :

$$[\overrightarrow{CB}]_N = \begin{pmatrix} -l \sin(\theta_2) \cos(\theta_3) \\ -l \sin(\theta_2) \sin(\theta_3) \\ l \cos(\theta_2) \end{pmatrix} .$$

As a result, the tensional force F_t can be decomposed into its vertical component only using angle θ_2 :

$$2 \cos(\theta_2) F_t = -m a_3 - m g .$$

When calculating the tensional forces, it is assumed that the movement of the bifilar pendulum is symmetric along the vertical line through the center of mass of the suspended object. As a result, the two tensional forces are of same magnitude. From this the tensional force in one suspension wire follows as:

$$F_t = \frac{-m a_3 - m g}{2 \cos(\theta_2)} .$$

For an object with mass of 100 kilograms, the gravitational force is 981 Newton. This same force, only with opposite direction, should hold in the vertical component of the suspension wires while at rest. Calculating the tensional force in one of the suspension wires while the bifilar pendulum is at rest, $\boldsymbol{\theta} = [0, \frac{\pi}{6}, \frac{\pi}{2}, 0, 0]^T$, yields:

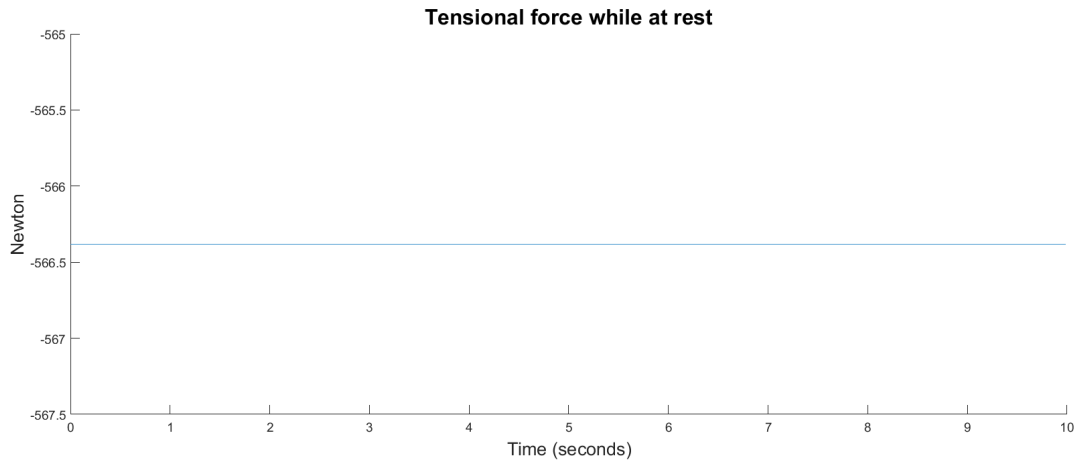


Figure 7.2.1: The tensional force in one suspension wire while at rest for a mass of 100 kilograms

In the above figure it can be seen that the tensional force remains constant at a little over -566 Newton, where the minus sign originates from it being in opposite direction of gravity. Calculating the vertical component of this force by multiplying it with $\cos(\theta_2)$ yields -490.5 Newton, which is exactly half of the gravitational force, as expected ($\theta_2 = \frac{\pi}{6}$).

To illustrate what happens with the tensional forces when the bifilar pendulum is in movement, θ_4 will be given an initial angle of $\frac{\pi}{12}$ after which torsional rotation along the vertical line through the center of mass ensues. The figure below displays the time development of the tensional force F_t as well as the angles θ_2, θ_4 . Note that the the angles θ_2, θ_4 have been added to the figure to illustrate how the tensional force behaves compared to these angles. The units on the vertical axis only apply to the tensional force, θ_2, θ_4 have been scaled and translated since only their shape is of interest in this figure.

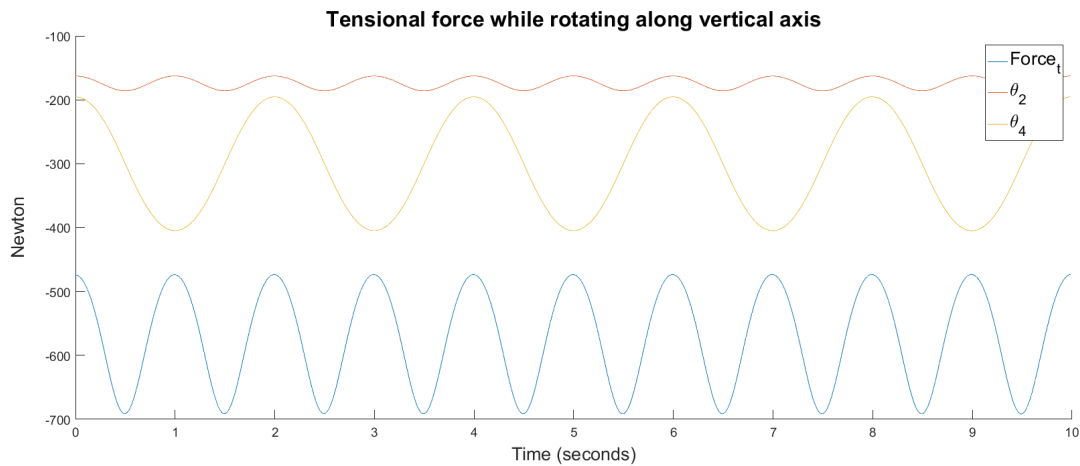


Figure 7.2.2: The tensional force in one suspension wire while rotating along the vertical axis through the center of mass

One can expect that the tensional forces are greatest when the object goes through its stationary point where the objects velocity will be greatest, and smallest at the extremes of the movement. This follows from the figure, as F_t is greatest (in absolute sense) when θ_2 is smallest and the force is smallest for the extremes of θ_4 . Furthermore, it is also important to notice that the tensional force never reaches 0, which means that the suspension wires stay taut.

Knowing the tensional force F_t makes it possible to reconstruct the moments of inertia by using Euler's equation for rigid bodies:

$$\mathbf{I} \cdot [\boldsymbol{\alpha}]_B + [\boldsymbol{\omega}]_B \times (\mathbf{I} \cdot [\boldsymbol{\omega}]_B) = [\mathbf{M}]_B, \quad (7.2.1)$$

where again \mathbf{I} is a diagonal matrix containing the moments of inertia I_1, I_2, I_3 and $[\boldsymbol{\alpha}]_B, [\boldsymbol{\omega}]_B$ are the angular velocity and -acceleration with respect to the body-fixed axes $\mathbf{b}_1, \mathbf{b}_2, \mathbf{b}_3$.

Since the tensional force F_t is known, the torque vector \mathbf{M} can be determined by using:

$$\begin{aligned} \mathbf{M} &= \mathbf{r} \times \mathbf{F}_t \iff \\ &= N_n^b(\boldsymbol{\theta})[\mathbf{r}]_B \times \mathbf{F}_t, \end{aligned}$$

where \mathbf{F}_t is a tensional force $[\mathbf{r}]_B$ is the vector connecting the point of force application and the center of the axes of rotation, which is the center of mass R^* . It then follows from $\mathbf{M} = N_n^b(\boldsymbol{\theta})[\mathbf{M}]_B$ that Euler's equations becomes:

$$\mathbf{I} \cdot [\boldsymbol{\alpha}]_B + [\boldsymbol{\omega}]_B \times (\mathbf{I} \cdot [\boldsymbol{\omega}]_B) = N_n^b(\boldsymbol{\theta}) (N_n^b(\boldsymbol{\theta})[\mathbf{r}]_B \times \mathbf{F}_t). \quad (7.2.2)$$

The only unknowns remaining in Euler's equation are the moments of inertia I_1, I_2, I_3 , and because there are 3 equations with equal unknowns, it can be solved for I_1, I_2, I_3 . Evaluating the left-hand side for the analytical values of the moments of inertia I_1, I_2, I_3 of a solid plate and calculating the right-hand side of the equation from the numerical solution in which the 1 meter thick plate was given an initial angle θ_4 of $\frac{\pi}{12}$ for numerical timestep $i = 5$:

LHS	RHS
610.55	611.97
$-3.5003 \cdot 10^{-4}$	$-1.4786 \cdot 10^{-6}$
$-1.064 \cdot 10^{-4}$	$1.0291 \cdot 10^{-6}$

and for timestep $i = 900$:

LHS	RHS
-612.10	-612.33
$4.30 \cdot 10^{-2}$	1.1257
$-5.1774 \cdot 10^{-2}$	$3.4258 \cdot 10^{-2}$

At the beginning of the numerical solution, the two sides of equation (7.2.2) are almost equal. However, after 900 timesteps, especially the torque around the \mathbf{b}_2 -axis is inaccurate. This can be explained by considering the movement from which these torques were derived. An initial angle was given to θ_4 which mainly ensues a torsional motion of the pendulum along its vertical axis, \mathbf{b}_1 . As a result of the center of mass not being on the line between the attachment points the pendulum will have some rotation along the axis along the length of the object, \mathbf{b}_3 . However, the object will have nearly no rotation along its last axis, \mathbf{b}_2 . Because of this dominance of the rotation along \mathbf{b}_1 the moment of inertia about this axis will have the highest accuracy, and the axes along which the rotation is less significant will result in moments of inertia with a lower accuracy.

Equation (7.2.2) can also be used the other-way around as to which is mentioned above; for known moments of inertia I_1, I_2, I_3 it can be used to find the components of the tensional force F_t .

Now, instead of considering a case in which the suspension wires are symmetric along the vertical line, a derivation for the tensional forces will be given for arbitrary positions of the

suspension wires. To this extend, let F^1, F^2 be the tensional forces in the suspension wires BC, DA respectively. The force-vectors then are:

$$\begin{aligned} F_t^1 &= F^1 \hat{\mathbf{C}}\mathbf{B}, \\ F_t^2 &= F^2 \hat{\mathbf{D}}\mathbf{A}. \end{aligned}$$

Here $\hat{\mathbf{C}}\mathbf{B}, \hat{\mathbf{D}}\mathbf{A}$ are the normalized vectors $\overrightarrow{\mathbf{C}}\mathbf{B}, \overrightarrow{\mathbf{D}}\mathbf{A}$ from section 5.1. Using Newton's second law of motion then obtains:

$$F^1 \hat{\mathbf{C}}\mathbf{B} + F^2 \hat{\mathbf{D}}\mathbf{A} + F_z \mathbf{n}_3 = -m [\mathbf{a}^{R*}]_N.$$

This is a system of three equations with only two unknowns: F^1, F^2 . Because the system is overdetermined, it is sufficient to use two of the three equations to calculate F^1, F^2 . To demonstrate the above procedure, consider a configuration with unequal suspension wire lengths as shown in the figure below:

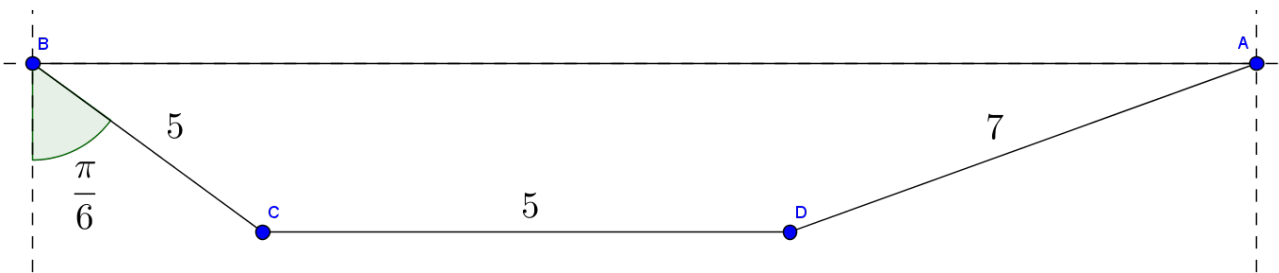


Figure 7.2.3: Non-symmetric configuration for tensional force calculation

Since, the configuration is not symmetric, the bifilar pendulum will ensue moving. The time-development of this movement can be seen in the figure below.

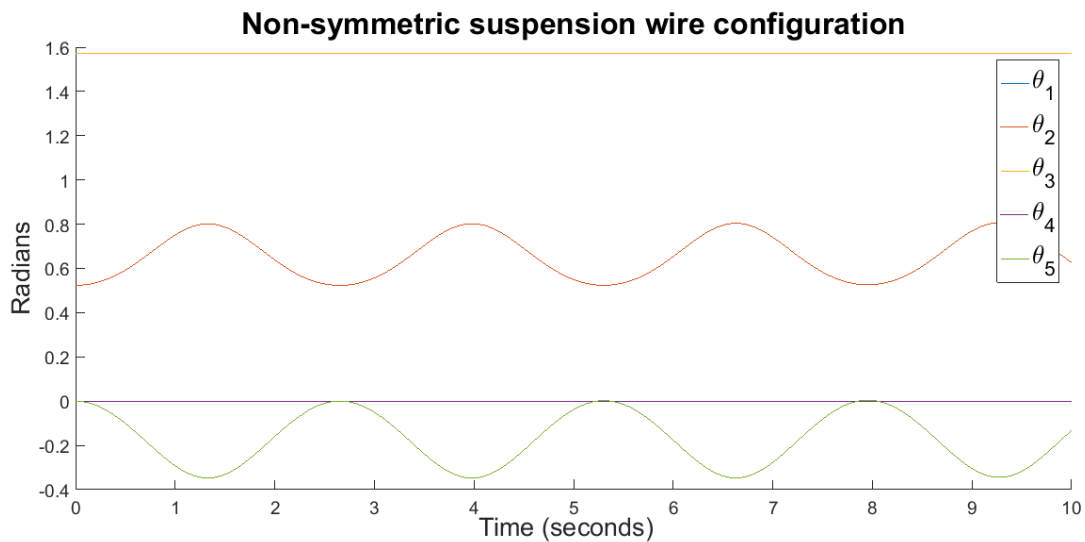


Figure 7.2.4: Time-development of non-symmetric configuration (100 kilogram object)

This movement is similar to the one seen when linearizing the movement of the bifilar pendulum along the \mathbf{b}_2 -axis. For this numerical solution, the tensional forces can be calculated using the above described method. Doing so yields the tensional forces F^1, F^2 :

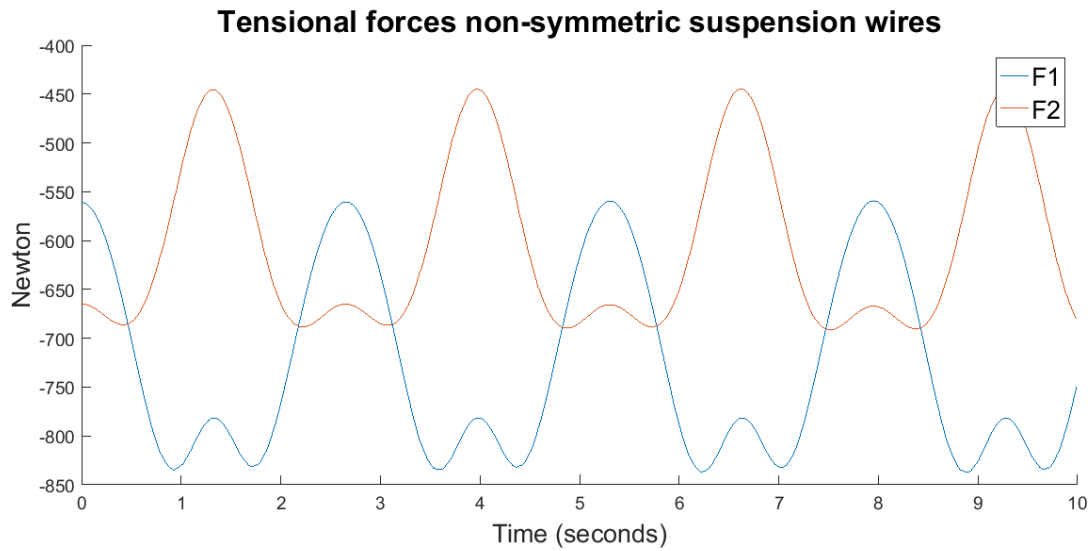


Figure 7.2.5: Tensional forces for non-symmetric configuration

The fact that these two tensional forces have alternating peaks is in correspondence with expectations. Since the object is tilting about the axis perpendicular to CD , in the extreme positions the tensional force will be greatest in the wire which has the lowest attachment point. Since this alternates between the two wires, so do their peaks, which also follows from the figure.

8. Solar Boat

In this section, all of the knowledge gathered concerning the bifilar pendulum will be applied to the Solar Boat. For practical reasons when wanting to conduct the actual experiment with the Solar Boat, several points are of interest before starting the experiment. These are:

- How much height is needed such that the Solar Boat will not hit the floor.
- What are the tensional forces the Solar Boat will undergo during its motion?
- How does the suspension of the Solar Boat influence the movement?
- How does one determine the period of oscillation during the experiment?

This section will try to answer these questions, as well as calculate approximations for moments of inertia of the Solar Boat using the numerical solutions and by using a geometric approximation of the boat.

8.1 Geometric model

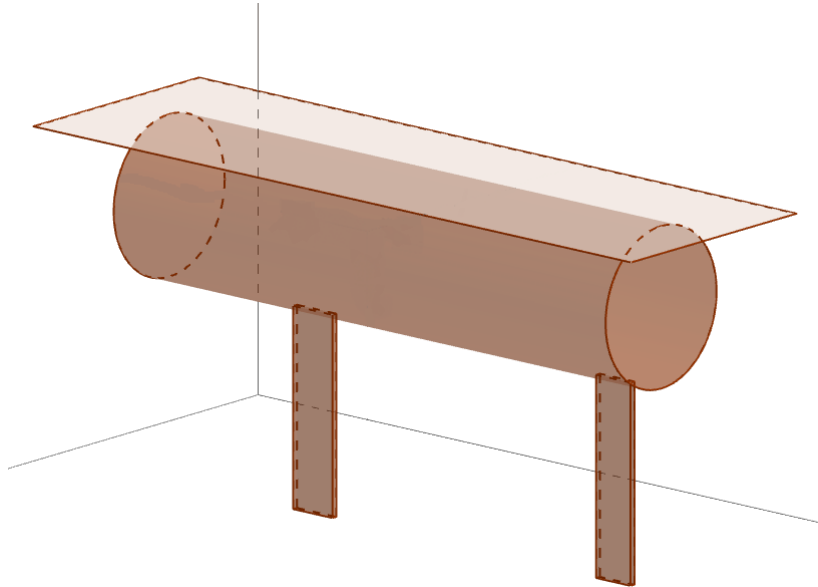
As mentioned earlier, to determinate the moments of inertia of an object one can approximate the objects' shape with basic geometries. From this approximation, an estimate for the moments of inertia can be calculated. In an earlier bachelor project, this approximation was done for the Solar Boat. A list of the boat's components and the corresponding approximating geometry is found below.

Part of boat	Approximation geometry
Hull	Hollow cylinder
Solar deck	Plate
Battery	Sphere
Cockpit	Hollow sphere
Additional electric	Sphere
Front & rear wing	Beam
Pilot	Cylinder

Table 8.1.1: Geometric approximation of the Solar Boat

Note that the pilot is also taken into account in this approximation.

The exterior of what this approximation looks like is shown in the figure below. Note that some of the electrical components and the pilot, which are mainly located inside the hull (cylinder) are not shown.



To compare the approximation with the actual design, a picture is added of the Solar Boat.



Comparing both figures, it is easy to see that the boat is very coarsely approximated, which will have as a consequence that the calculated moments of inertia of the boat have a low accuracy. In order to calculate the moments of inertia of the model, the moments of inertia of each of the individual components have to be calculated. For each of the basic geometries the moments of inertia are known analytically. After determining the center of mass of all these components by using:

$$r_{CM} = \frac{\sum_i m_i r_i}{M},$$

these moments of inertia were then used with the Parallel Axis Theorem to calculate the three moments of inertia of each geometry along the principle axis of the boat. The sum of all these moments of inertia then yields the desired moments of inertia of the model:

$$\begin{aligned} I_1 &= 317.278, \\ I_2 &= 317.154, \\ I_3 &= 83.143. \end{aligned}$$

It is important to note that the center of mass of this model lies only 20.5 centimeters below the solar deck. This is the result of the pilots weight being nearly 44% of the total weight and it being close to the solar deck. Since the vertical distance between the attachment points (solar deck) and the center of mass is relatively small, torsional movements of the boat will be accompanied with little tilting due to small lever arm of the forces causing tilting.

8.2 Suspension

There are numerous ways in which the solar boat can be attached to the bifilar pendulum, when not considering the constraint of the solar deck of the boat which prevents suspension on arbitrary positions. Three configurations of the suspended boat will be considered in this section. For each configuration, the suspension wires are attached to line CD , see figure 5.1.1. The difference between the configurations is distance from the attachment points to the edges of the deck:

- Configuration 1: Attachment points at either ends of line CD
- Configuration 2: Attachment points 0.5 meter from either ends of line CD
- Configuration 3: Attachment points 1 meter from either ends of line CD

Table 8.2.1: Suspension of the Solar Boat

Since the attachment points A and B on the ceiling are most likely fixed in practical applications, it is assumed that this distance b between these points is equal in all three configurations. Furthermore, it is assumed that when performing the actual measurements, only one length of suspension wires is available, and thus equal in each configuration. A side-view of the stationary positions of all three configurations is shown in the figure below (only the deck of the solar boat is shown).

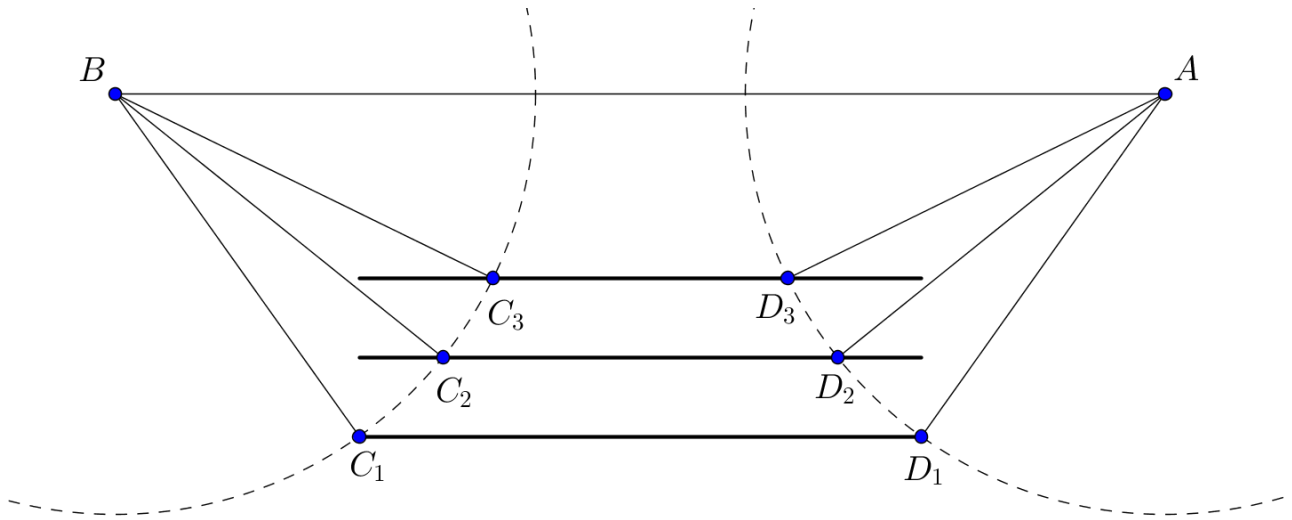


Figure 8.2.1: Side-view of the stationary positions of the Solar Boat (only deck is shown)

Each of these configurations will be used for each linearization from section 7.1. From the numerical solutions of each case, a comparison can be made as to which configuration yields a most accurate estimate for the moment of inertia about the respective axis.

8.3 Motion of configurations

First, all three configurations will be looked at for the torsional motion to determine an estimate for I_1 . The three configurations will be given an equal initial angle in θ_4 of $\frac{\pi}{80}$ such that a torsional movement ensues. The numerical solution for configuration 2 for this configurations is shown in the figure below.

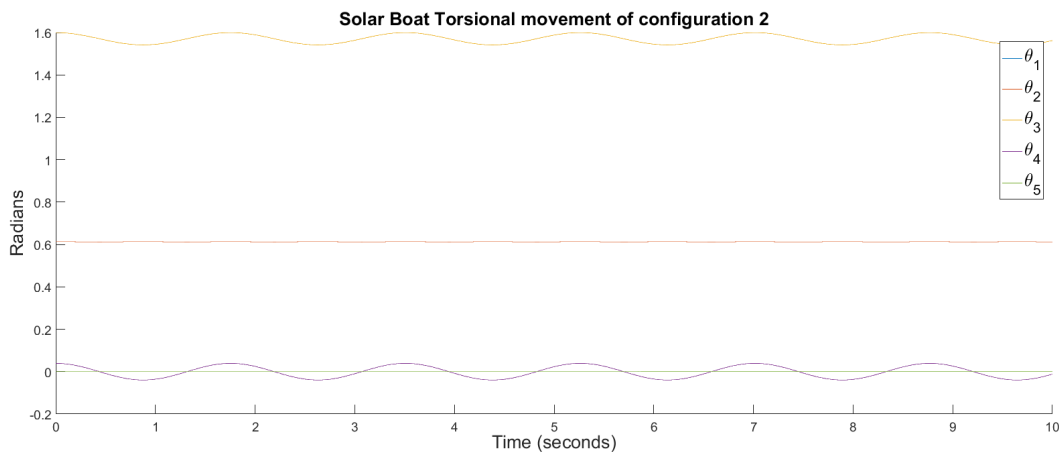


Figure 8.3.1: Rotation of the Solar boat along the \mathbf{b}_1 -axis for configuration 2

The results for the other two configurations are similar, only the periods of the solutions are different. From each of these numerical solutions, an estimate can be found for the moment of inertia I_1 , where from the geometric approximation it holds that $I_1 = 317.278$. The estimates for the three configurations are:

	Estimate
Configuration 1	$I_1 - 11.49$
Configuration 2	$I_1 + 25.05$
Configuration 3	$I_1 + 34.68$

Table 8.3.1: Estimates for I_1 for the different configurations

As mentioned earlier, the torsional motion will be accompanied with little tilting of the object due to the location of the center of mass. To motivate this, the time-development of this tilting, θ_1 , is plotted for all three configurations with initial angle $\theta_4 = \frac{\pi}{12}$. This yields the following figure:

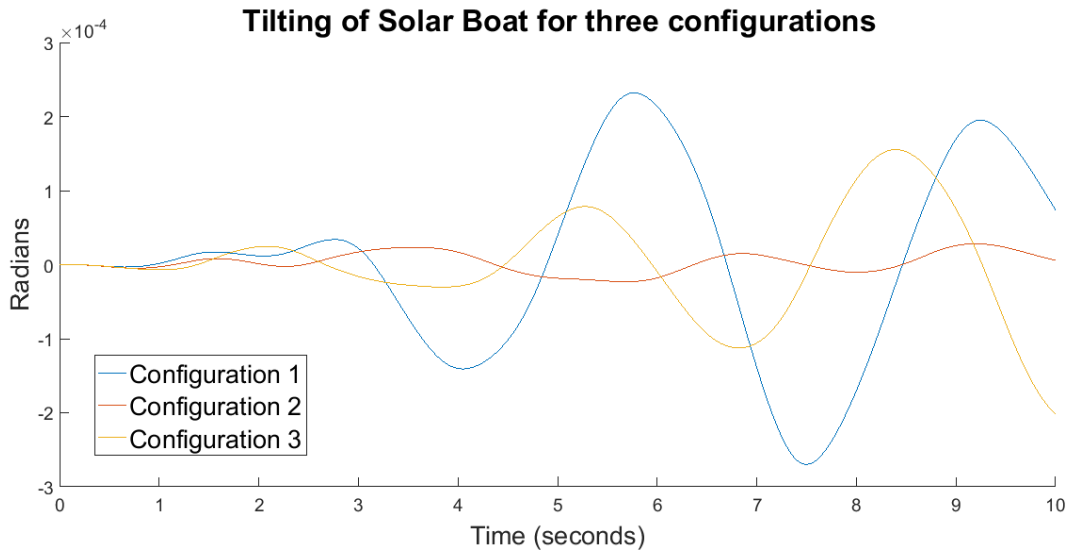


Figure 8.3.2: Tilting of the Solar Boat for each configuration

From this figure it can be concluded that, even though the tilting occurs for all three configurations, it remains insignificant compared to the torsional movement of θ_4 , which oscillates between its initial value and its negative value: $\frac{\pi}{12}$, $-\frac{\pi}{12}$. Because there is almost no tilting for either of the configurations, the height required for the actual experiment is fractionally larger than the height required to suspend the boat in stationary position: $l \cos(\theta_2(0)) + h_{boat}$. The minimal height should be taken slightly larger than this to allow for the, even though insignificant, tilting.

Secondly, all three configurations will be looked at for the second linearization from section 7.1. Again, θ_2 will be given an initial angle of $\theta_2(0) + \frac{\pi}{80}$, where $\theta_2(0)$ is θ_2 's stationary angle (which can be derived from figure 8.1). The numerical solution of this motion is shown below for configuration 1:

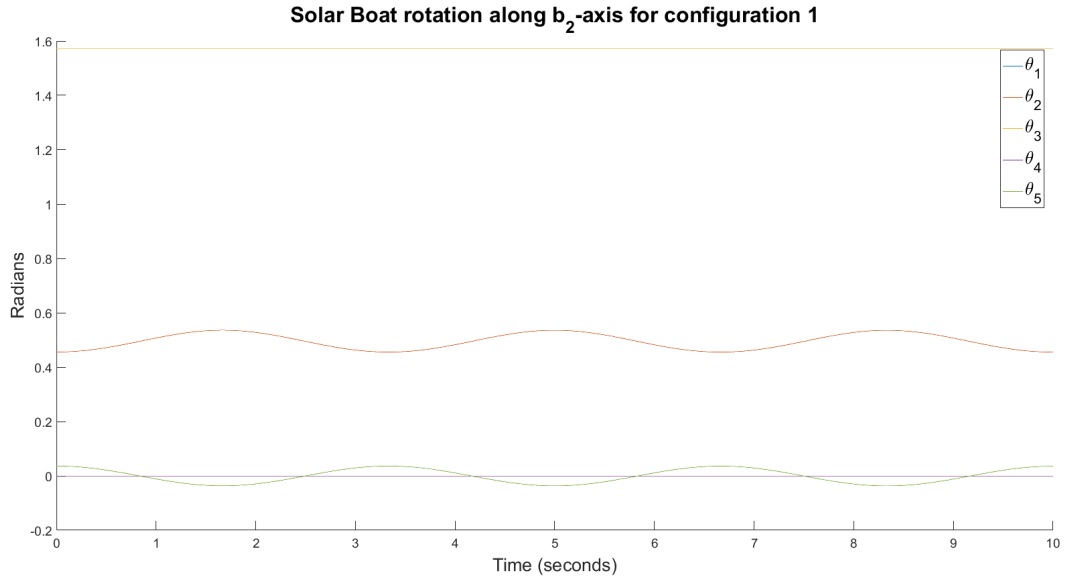


Figure 8.3.3: Rotation of the Solar boat along the \mathbf{b}_2 -axis for configuration 1

The estimates for the moment of inertia I_2 which can be derived from these numerical solutions for all three configurations are shown below:

	Estimate
Configuration 1	$I_2 + 11.95$
Configuration 2	$I_2 - 86.39$
Configuration 3	$I_2 - 132.80$

Table 8.3.2: Estimates for I_2 for the different configurations

Lastly, the three configurations will be looked at for the third linearization from section 7.1. To ensue rotation along the \mathbf{b}_1 -axis, θ_1 will be given an initial angle of $\frac{\pi}{80}$. The numerical solution for configuration 3 is shown below.

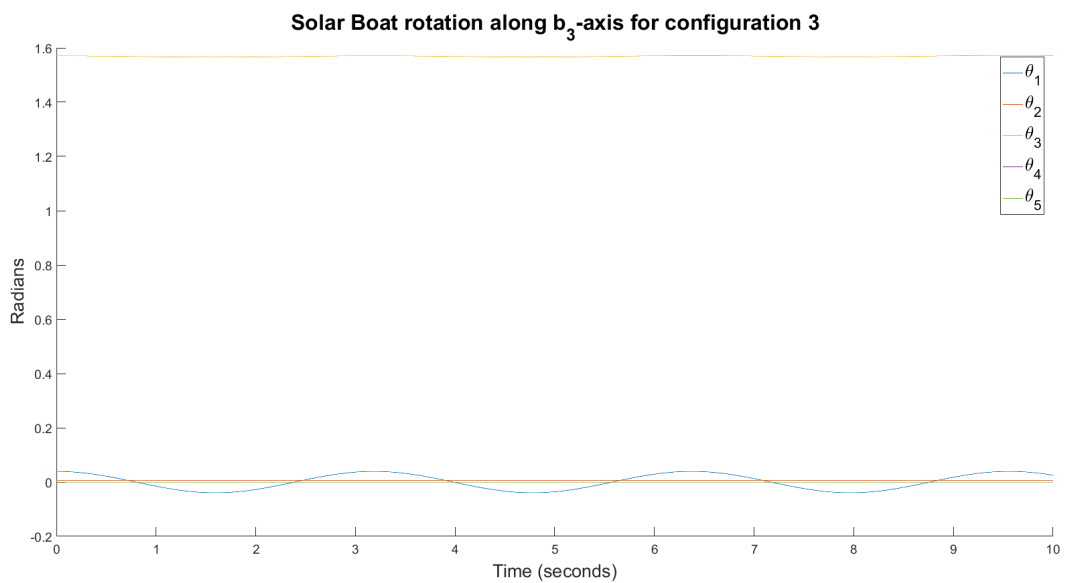


Figure 8.3.4: Rotation of the Solar boat along the \mathbf{b}_3 -axis for configuration 3

The estimates for the moment of inertia I_2 which can be derived from these numerical solutions for all three configurations are shown below:

	Estimate
Configuration 1	$I_3 - 0.162$
Configuration 2	$I_3 - 0.162$
Configuration 3	$I_3 - 0.162$

Table 8.3.3: Estimates for I_3 for the different configurations

The fact that each configuration yields the exact same estimate for I_3 is not surprising, since the suspension wires have no influence on this rotation of the boat along the \mathbf{b}_3 -axis as long as the attachment points remain on the line CD .

For each linearization, the estimates for the moments of inertia are determined for all three configurations of the suspended solar boat. Summarizing these results in table results in:

Estimate	I_1	I_2	I_3
Configuration 1	$I_1 - 11.49$	$I_2 + 11.95$	$I_3 - 0.162$
Configuration 2	$I_1 + 25.05$	$I_2 - 86.39$	$I_3 - 0.162$
Configuration 3	$I_1 + 34.68$	$I_2 - 132.80$	$I_3 - 0.162$

Table 8.3.4: The estimates for all moments of inertia for all three configurations

From this table, it is immediately clear that configuration 1 results in the best estimates for all three moments of inertia. Therefore, it is recommended to use this configuration when performing measurements with the Solar boat.

To use the period of oscillation of the actual experiment instead of the one from the numerical solution in the calculations for the moments of inertia in the linearizations, a methodology is needed to measure these periods. To measure the period of the bifilar pendulum, one can mark a single point on the surface of the boat with some high visibility tape. Examples of these points could be: attachment point C for measuring the periods of $\theta_2, \theta_4, \theta_5$ or a point on one of the edges of the solar deck to measure the period of θ_1 . The length of several periods could then be measured starting and ending when the point goes through its stationary position. Measuring several periods in one measurement decreases the influence of human error in the measurement. The obtained periods of oscillation with this method could then be used in the linearizations to approximate the moments of inertia.

8.4 Tensional forces

For the torsional motion, all three of the configurations are given the same initial angle $\theta_4(0) = \frac{\pi}{12}$ and the difference in tilting has been observed in the previous section. In order to be able to perform the actual experiment, it is mandatory to know how much force will be applied to the attachment points on the ceiling, but more importantly on the fragile solar panels of the Solar Boat. The derivations presented in section 7.2 can be used to calculate these tensional forces. Since the considered configurations of the Solar Boat are symmetric, either of the two derivations for the tensional forces can be used: the one considering symmetry or the one without this assumption (since symmetry is a special situation of this general case). Using the general case to calculate the tensional forces in all three configurations yields:

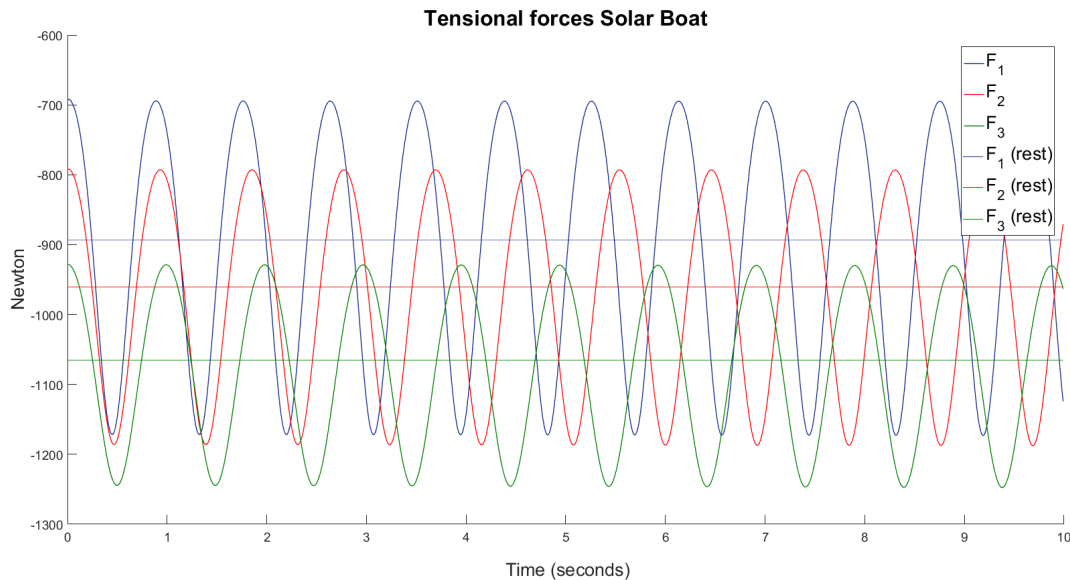


Figure 8.4.1: Tensional forces for three configurations of the Solar Boat

The horizontal lines are the tensional forces in the configuration while the Solar boat is stationary. From the figure above it follows that the tensional forces increase as the attachment points of the solar boat come closer to each other. This results from the fact that the suspension wires become increasingly horizontal as the attachment points on the Solar boat come closer to each other. As a result, the tensional force in these directions has to become larger such that the vertical component of these forces remain equal. The same holds in the other two linearized cases, where the tensional forces will be largest for the configurations with attachment points close together as a result of this. Therefore, if the strength of the solar deck is a limiting factor and the strains on it want to be kept at a minimum, the attachment points have to be kept as far apart as possible. It can therefore be concluded that configuration 1 is to be preferred over the other two, since it results in the most accurate estimates for the moments of inertia and causes the least amount of strain on the solar deck.

Now, to summarize all of the above and answer the questions posed at the beginning of this section:

- The height needed for the experiment is almost solely determined by the stationary position of the configuration. Since there is virtually no tilting and only small angles are considered in the linearizations, only a minimal extra clearance is needed for the boat not to hit the floor.
- The tensional forces depend on the configuration, and increase as the attachment points are closer together. Therefore, if the strain on the deck is wanted to be kept at a minimum, the attachment points have to be as far apart as possible. Furthermore, a configuration which has its attachment points far apart results in the most accurate estimates for the moments of inertia.
- The suspension of the boat has almost no influence on the motion of the boat. The tilting increases as the attachment points are further apart, however they remain insignificant compared to other oscillations due to the location of the center of mass (which is almost located on the line CD between the attachment points). In the two other motions which were considered in the linearization, only the period of the solution changed with the configuration and not its general behaviour.

- A methodology was presented to measure the periods of oscillation. This involves marking points on exterior of the boat and measuring several periods at once, to eliminate the human error as much as possible. The measured periods of oscillation could then be used in the linearizations of the equations of motion to calculate approximations of the moments of inertia.

9. Conclusion & Discussion

The full non-linear model for the bifilar pendulum has been derived and is presented in a structured way. The correctness of the model has been verified by comparing the numerical solutions of certain modes of oscillation to analogous models for which the solutions are known. These modes include: side-sway which could be compared to a planar pendulum and the torsional movement which was compared to the adjusted Lagrange's model. Another indication used to verify the model was by evaluating the constraint equation of the bifilar pendulum for the numerical solutions. Lastly, an example case presented in Kane's paper involving a suspended solid cylinder was evaluated, and the results obtained were the same as those presented in Kane's paper. All these verifications imply that the structured derivation of the non-linear model has been correctly modelled.

The project did not succeed in quantitatively predicting the accuracy of the moments of inertia. The system of equations which was obtained was too large to analytically work with. It was even impossible to invert the mass matrix M_5 to obtain the differential equations in their usual form $y' = Ay$ because of its size. However, three different configurations of the suspended Solar Boat have been considered. From the comparison of the estimates for the moments of inertia, it was concluded that a configuration which has its attachment points as far apart as possible results in the most accurate approximations for the moments of inertia.

Furthermore, it was concluded that the suspension of the solar boat has little influence on its movement. This results from the fact that the center of mass of the boat (including pilot) lies very close under the line connecting the attachment points. As a result, very little parasitic tilting occurs which could disturb the purely rotational motions of the bifilar pendulum. It turned out, that the tilting is of such a low order that it is of almost no significance to the motion of the Solar Boat.

To use the bifilar pendulum to obtain approximations for the moments of inertia, the equations of motion have been linearized around a stationary position. By each time considering movements of the bifilar pendulum along only one of the principle axes, the system could be reduced to a system of two linear second-order differential equations. Rewriting this system to a system of four first-order differential equations, the eigenvalues for the problem could be determined, which were a function of the configuration parameters and the moment of inertia along the corresponding axis. These eigenvalues could then be used in combination with the period of the numerical solution to obtain estimates for the moment of inertia. From this it was concluded that the estimate for the moment of inertia I_2 was significantly less accurate than those along the other two axes. This procedure was then applied to geometric approximation of the solar boat to obtain estimates for the moments of inertia of this approximation. Furthermore, a methodology was presented to measure the periods of oscillations for an actual experiment with the bifilar pendulum. This involves marking specific points on the exterior of the boat, and tracking these for several periods at a time to minimize human error in the time measurements. The periods found using this method can be used in the linearizations to

calculate approximations of the moments of inertia along the principle axis of the Solar Boat. These experiments have, unfortunately, not been performed in this project.

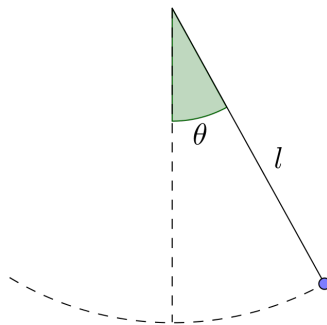
While working on the linearization, a limitation of this particular choice of coordinates to describe the system was encountered. With the current choice of coordinates it is impossible to analyze the behaviour of a single coordinate, since every movement of the object involves at least change in two coordinates (with the exception of θ_1 for an infinitely thin object). As a result, the eigenvalues in the linearization for the torsional movement did not simplify to the point that the expressions found for the moment of inertia along that vertical axis was equal to the one found in Lagrange's model. With a choice of coordinates in which it is possible to evaluate configurations in which only one coordinate plays a role, this might have been possible.

Finally, for practical reasons, the tensional forces in the suspension wires have been determined. First these were calculated for configurations which are symmetric, such that the suspension wires are line symmetric along the vertical line through the center of mass. It was found that the tensional forces show expected behaviour: the forces are smallest when the bifilar pendulum is at its extreme positions and largest when going through its stationary position. Once the tensional forces are known, Euler's equation was used to find estimates for the moments of inertia. From the example considered it was concluded that the axis along which the movement was dominant provided the best estimate for the respective moment of inertia, and the axis along which rotation was insignificant resulted in less accurate approximations of the moments of inertia. The assumption of symmetry was then discarded, and using Newton's second law of motion, a over-determined system of equations was obtained which could be used to calculate the tensional forces. Using these derivations, the tensional forces could be calculated for several different configurations of the Solar Boat. It turned out that if the strain on the solar deck is required to be kept at a minimum, the attachment points on the solar deck should be as far apart as possible.

10. Appendix A

Example 1: Monofilar pendulum

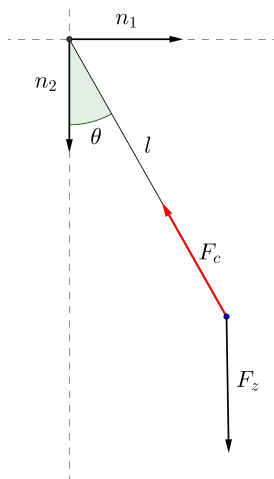
For the first example, a planar pendulum is considered which moves in a plane as shown in the figure below.



Each of the methods (with the exception of the 'smart' Newtonian approach due to its impracticality discussed earlier) will be used to derive the equations of motion.

- **Newtonian Mechanics**

Consider the pendulum with unit vectors \mathbf{n}_1 in the horizontal- and \mathbf{n}_2 in the vertical direction (which is chosen to be downwards for convenience):



From this choice of unit vectors, the position of the object can be easily expressed as:

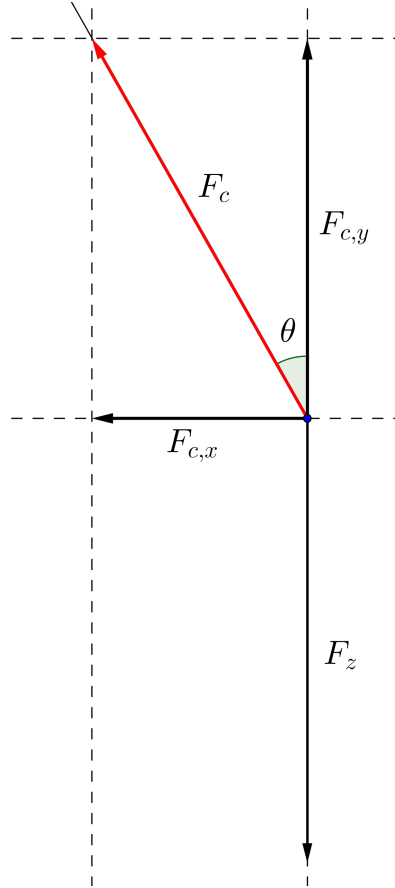
$$\mathbf{s} = x \mathbf{n}_1 + y \mathbf{n}_2 ,$$

where $\mathbf{s} = \mathbf{s}(t)$, $x = x(t)$, $y = y(t)$.

The variables x and y are not independent of each other: the constraint imposed by the suspension wire $x^2 + y^2 = l^2$ relates them. Taking the time derivative twice yields an expression for the acceleration:

$$\mathbf{a} = \ddot{x} \mathbf{n}_1 + \ddot{y} \mathbf{n}_2 .$$

In order to use Newton's second law of motion, the tensional force from the suspension wire is decomposed in components along the two predefined axes.



From this simple geometry it immediately follows that the tensional force F_c can be decomposed in $F_{c,x}$ and $F_{c,y}$ as follows:

$$\begin{aligned} F_{c,x} &= -F_c \sin(\theta) \mathbf{n}_1 , \\ F_{c,y} &= -F_c \cos(\theta) \mathbf{n}_2 . \end{aligned}$$

Filling in the above in Newton's second law of motion yields:

$$\begin{aligned} m \mathbf{a} &= \sum_i F_i \iff \\ m(\ddot{x} \mathbf{n}_1 + \ddot{y} \mathbf{n}_2) &= mg \mathbf{n}_2 - F_c \cos(\theta) \mathbf{n}_2 - F_c \sin(\theta) \mathbf{n}_1 \iff \\ &= (mg - F_c \cos(\theta)) \mathbf{n}_2 - F_c \sin(\theta) \mathbf{n}_1 . \end{aligned}$$

For both \mathbf{n}_1 - and \mathbf{n}_2 -components of this equation equality should hold. Therefore, it follows that:

$$\begin{aligned} \ddot{x} &= -\frac{1}{m} F_c \sin(\theta) , \\ \ddot{y} &= g - \frac{1}{m} F_c \cos(\theta) . \end{aligned} \tag{10.0.1}$$

Equations (10.0.1) are the equations of motion for a planar pendulum. These equations still have a dependency on θ in them. It follows immediately from the figure above that $\tan(\theta) = \frac{x}{y}$. Because $\theta \in (-\frac{\pi}{2}, \frac{\pi}{2})$ it follows that θ can be expressed in the Cartesian coordinates x and y as: $\theta = \arctan \frac{x}{y}$.

To solve these equations, an additional expression for the tensional force F_c has to be found. In order to find this expression, the gravitational force is decomposed into its component along the line of the constraint force F_c . From the simple geometry of the example it follows this component is equal to $F_z \cos(\theta)$. Using Newton's second law of motion in this centripetal direction, where pointing towards the rotational center of the pendulum is defined to be positive, yields the following expression:

$$F_c + F_{z,x} = ma_c,$$

where $F_{z,x} = -F_z \cos(\theta)$ and a_c is the centripetal acceleration which is known to be:

$$a_c = \frac{v^2}{l} = \frac{(\omega l)^2}{l} = \omega^2 l = \dot{\theta}^2 l.$$

Substitution and rearrangement of terms leads to:

$$F_c = mg \cos(\theta) + m\dot{\theta}^2 l. \quad (10.0.2)$$

To substitute $\dot{\theta}$ out, the expression $\tan(\theta) = \frac{x}{y}$ is differentiated once with respect to time to yield:

$$\begin{aligned} \frac{d}{dt} \tan(\theta) &= \frac{d}{dt} \left(\frac{x}{y} \right) \iff \\ \frac{\cos^2(\theta)\dot{\theta} + \sin^2(\theta)\dot{\theta}}{\cos^2(\theta)} &= \frac{y\dot{x} - x\dot{y}}{y^2} \iff \\ \dot{\theta} &= \frac{(y\dot{x} - x\dot{y})}{y^2} \cos^2(\theta) = \frac{(y\dot{x} - x\dot{y})}{y^2} \cos^2 \left(\arctan \frac{x}{y} \right) \end{aligned}$$

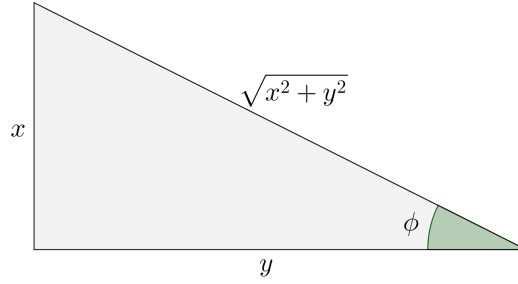
Substituting this equality into the constraint force equation (10.0.2) leads to:

$$F_c = mg \cos \left(\arctan \frac{x}{y} \right) + m \left(\frac{(y\dot{x} - x\dot{y})}{y^2} \cos^2 \left(\arctan \frac{x}{y} \right) \right)^2 l$$

This constraint equation together with the two equations from equation (10.0.1) form the equations of motion for a planar pendulum:

$$\begin{aligned} \ddot{x} &= -\frac{1}{m} F_c \sin \left(\arctan \frac{x}{y} \right), \\ \ddot{y} &= g - \frac{1}{m} F_c \cos \left(\arctan \frac{x}{y} \right), \\ F_c &= mg \cos \left(\arctan \frac{x}{y} \right) + m \left(\frac{(y\dot{x} - x\dot{y})}{y^2} \cos^2 \left(\arctan \frac{x}{y} \right) \right)^2 l. \end{aligned} \quad (10.0.3)$$

These equations can be further simplified by defining $\phi = \arctan \frac{x}{y}$. Taking the tangent on both sides of the equation obtains $\tan(\phi) = \frac{x}{y}$. This equation represents a right-angled triangle with angle ϕ , opposite side of length x and adjacent side of length y as shown in the figure below.



From this figure it is immediately obvious that:

$$\begin{aligned}\sin(\phi) &= \sin\left(\arctan\frac{x}{y}\right) = \frac{x}{\sqrt{x^2 + y^2}}, \\ \cos(\phi) &= \cos\left(\arctan\frac{x}{y}\right) = \frac{y}{\sqrt{x^2 + y^2}}.\end{aligned}$$

Substitution of these simplifications into equations (10.0.3) yields:

$$\begin{aligned}\ddot{x} &= -\frac{1}{m}F_c\frac{x}{\sqrt{x^2 + y^2}}, \\ \ddot{y} &= g - \frac{1}{m}F_c\frac{y}{\sqrt{x^2 + y^2}}, \\ F_c &= mg\frac{y}{\sqrt{x^2 + y^2}} + m\left(\frac{y\dot{x} - x\dot{y}}{x^2 + y^2}\right)^2 l.\end{aligned}\tag{10.0.4}$$

Now, the equation for the constraint force F_c can be substituted into the second-order differential equations for \ddot{x}, \ddot{y} to obtain the equations of motion for the planar pendulum:

$$\begin{aligned}\ddot{x} &= -\left(g\frac{y}{\sqrt{x^2 + y^2}} + \left(\frac{y\dot{x} - x\dot{y}}{x^2 + y^2}\right)^2 l\right)\frac{x}{\sqrt{x^2 + y^2}} \\ \ddot{y} &= g - \left(g\frac{y}{\sqrt{x^2 + y^2}} + \left(\frac{y\dot{x} - x\dot{y}}{x^2 + y^2}\right)^2 l\right)\frac{y}{\sqrt{x^2 + y^2}}\end{aligned}\tag{10.0.5}$$

The advantage of using Newtonian mechanics is that the formulation of the equations of motion remains very close to the geometric nature of the problem by only using Newton's second law of motion. As a result, it is easier to understand what is happening in the derivation of the equations of motion. However, from the above derivation of the equations of motion it is clear that, with this method, the constraint does not conveniently reduce the complexity of the problem, and as a result the equations of motion form a complex system for a relatively easy problem. Since the geometry of the bifilar pendulum and its constraints will be significantly more difficult than the planar pendulum, this method will not be used in the example with the spherical pendulum or used for the bifilar pendulum.

- **Lagrangian Mechanics**

To determine the Lagrangian for this system the kinetic energy T and the potential energy V of the system have to be determined.

Since this system involves rotational movement, it is convenient to use polar coordinates:

$$\begin{aligned}x &= l \cos(\theta), \\y &= l \sin(\theta).\end{aligned}$$

In Cartesian coordinates kinetic energy is defined by $T = \frac{1}{2}mv^2$. Since the size of the tangential velocity v can be written as the product of the radius and angular velocity, $l\dot{\theta}$, an alternate expression for the kinetic energy is:

$$T = \frac{1}{2}m(l\dot{\theta})^2.$$

For the potential energy the Cartesian expression is $V = mgh$. Choosing the rotational axis of the pendulum as reference point, it follows that the height h can be written as $-l \cos(\theta)$. The potential energy therefore becomes:

$$V = -mgl \cos(\theta).$$

Therefore, the Lagrangian of the 2-dimensional pendulum is given by:

$$L = \frac{1}{2}ml^2\dot{\theta}^2 + mgl \cos(\theta).$$

Lagrange's equation (4.3.16) is now used to derive the equation of motion using the expression of the Lagrangian above. Substitution of the Lagrangian into Lagrange's equation and rearrangement of the terms yields:

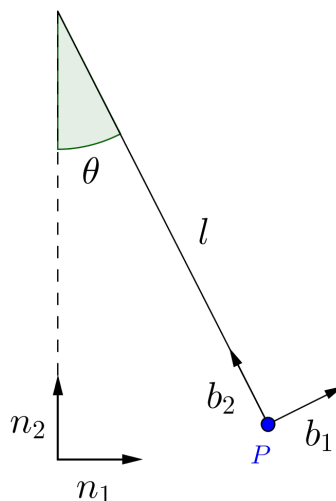
$$\ddot{\theta}(t) = -\frac{g}{l} \sin(\theta(t)) \tag{10.0.6}$$

the equation of motion for a planar pendulum.

It is immediately clear that this formulation of the equation of motion is significantly less complex than those obtained when using classical Newtonian mechanics as described previously. This formulation is also easier to obtain, since the only thing remaining once the kinetic- and potential energy are known, is taking derivatives. Furthermore, the constraint forces of the system do not have to be taken into consideration, except for the choice of coordinates (which have to be consistent with the constraints).

- **Kane's Method**

Consider the monofilar pendulum with point mass P as shown below.



Since the velocity and acceleration of point P are most conveniently expressed with respect to body-fixed unit vectors two sets of axes are defined: a earth-fixed set $\{\mathbf{n}_1, \mathbf{n}_2, \mathbf{n}_3\}$ and a body-fixed set $\{\mathbf{b}_1, \mathbf{b}_2, \mathbf{b}_3\}$. The vectors $\mathbf{n}_3, \mathbf{b}_3$ are also defined because the vector for angular velocity is perpendicular to the plane of rotation. These vectors are not displayed in the figure above since they point out of the paper. The set $\{\mathbf{b}_1, \mathbf{b}_2, \mathbf{b}_3\}$ is obtained by rotating the set $\{\mathbf{n}_1, \mathbf{n}_2, \mathbf{n}_3\}$ counter-clockwise through an angle θ about the rotational point. The corresponding rotation matrix can be used to express the vectors $\{\mathbf{b}_1, \mathbf{b}_2, \mathbf{b}_3\}$ in terms of the vectors $\{\mathbf{n}_1, \mathbf{n}_2, \mathbf{n}_3\}$:

	\mathbf{b}_1	\mathbf{b}_2	\mathbf{b}_3
\mathbf{n}_1	$\cos(\theta)$	$-\sin(\theta)$	0
\mathbf{n}_2	$\sin(\theta)$	$\cos(\theta)$	0
\mathbf{n}_3	0	0	1

Since there is only one degree of freedom for particle P , only one generalized coordinate has to be chosen. This generalized coordinate q_1 is chosen as the angle the pendulum makes with the stationary position, and the generalized velocity u_1 is its time derivative. It holds that $q_1 = \theta(t), u_1 = \dot{\theta}(t)$.

In order to use Kane's equation as in equation (4.4.6), expressions for $\frac{\partial \mathbf{v}}{\partial \dot{\theta}}$ and $\frac{\partial \boldsymbol{\omega}}{\partial \dot{\theta}}$ have to be found. Per definition it holds that $\dot{q}_1 = \dot{\theta}$. Therefore it is sufficient to find expressions for \mathbf{v} and $\boldsymbol{\omega}$. These expressions can then be differentiated with respect to $\dot{\theta}$ to find expressions for $\frac{\partial \mathbf{v}}{\partial \dot{\theta}}$ and $\frac{\partial \boldsymbol{\omega}}{\partial \dot{\theta}}$.

The size of the tangential velocity \mathbf{v} of P is given by the product of the angular velocity $\boldsymbol{\omega}$ and the radial distance \mathbf{r} . With the choice of unit vectors $\{\mathbf{b}_1, \mathbf{b}_2, \mathbf{b}_3\}$ it follows that:

$$\begin{aligned} \mathbf{v} &= \boldsymbol{\omega} \times \mathbf{r} \\ &= (\dot{\theta} \mathbf{b}_3) \times (-l \mathbf{b}_2) \\ &= \dot{\theta} l \mathbf{b}_1. \end{aligned}$$

Taking the time derivative of \mathbf{v} results in the acceleration \mathbf{a} of P:

$$\begin{aligned} \mathbf{a} &= \frac{d}{dt} \mathbf{v} \iff \\ &= \frac{d}{dt} (\dot{\theta} l \mathbf{b}_1) \iff \\ &= \frac{d}{dt} (\dot{\theta} l (\cos(\theta) \mathbf{n}_1 + \sin(\theta) \mathbf{n}_2)) \iff \\ &= \ddot{\theta} l (\cos(\theta) \mathbf{n}_1 + \sin(\theta) \mathbf{n}_2) + \dot{\theta}^2 l (-\sin(\theta) \mathbf{n}_1 + \cos(\theta) \mathbf{n}_2) \iff \\ &= \ddot{\theta} l \mathbf{b}_1 + \dot{\theta}^2 l \mathbf{b}_2. \end{aligned}$$

Taking the partial derivative with respect to $\dot{\theta}$ yields the partial velocities \mathbf{v}_1 and $\boldsymbol{\omega}_1$:

$$\begin{aligned} \mathbf{v}_1 &= \frac{\partial \mathbf{v}}{\partial \dot{\theta}} = l \mathbf{b}_1 = l (\cos(\theta) \mathbf{n}_1 + \sin(\theta) \mathbf{n}_2), \\ \boldsymbol{\omega}_1 &= \frac{\partial \boldsymbol{\omega}}{\partial \dot{\theta}} = \mathbf{b}_3 = \mathbf{n}_3. \end{aligned}$$

Kane's equation can be assembled by calculating the generalized active force F_1 and the generalized inertia force F_1^* ($r = 1$, since there is only one generalized coordinate). It

follows that:

$$\begin{aligned}
F_1 &= \mathbf{F}_z \cdot \mathbf{v}_1 + \mathbf{T} \cdot \boldsymbol{\omega}_1 = -mg\mathbf{n}_2 \cdot l\mathbf{b}_1 \iff \\
&= -mg\mathbf{n}_2 \cdot l(\cos(\theta)\mathbf{n}_1 + \sin(\theta)\mathbf{n}_2) = -mgl\sin(\theta), \\
F_1^* &= -m\mathbf{a} \cdot \mathbf{v}_1 - \left(\boldsymbol{\alpha}_1 \cdot \vec{I} + \boldsymbol{\omega}_1 \times \vec{I} \cdot \boldsymbol{\omega}_1 \right) \cdot \boldsymbol{\omega}_1 \iff \\
&= -m \left(\ddot{\theta}l\mathbf{b}_1 + \dot{\theta}^2l\mathbf{b}_2 \right) \cdot l\mathbf{b}_1 = -ml^2\ddot{\theta}.
\end{aligned}$$

Both the second terms in the equations for F_1, F_1^* disappear since this example considers a point mass which has a moment of inertia of 0 along all principle axes, $\mathbf{I} = 0$, and the torque $\mathbf{T} = 0$ since all forces work along a line through the center of mass of P .

Assembling Kane's equation, $F_1 + F_1^* = 0$ thus yields:

$$-mgl\sin(\theta) - mL^2\ddot{\theta} = 0,$$

from which the equation of motion follows directly:

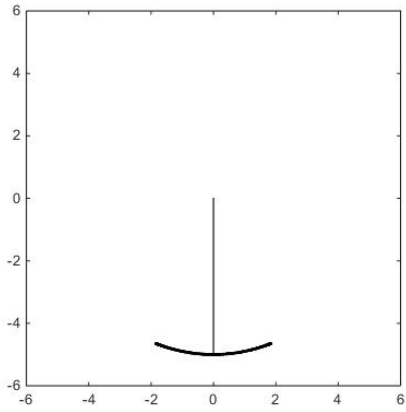
$$\boxed{\ddot{\theta}(t) = -\frac{g}{l}\sin(\theta(t))} \quad (10.0.7)$$

This equation is the same as obtained with the method using Lagrangian mechanics.

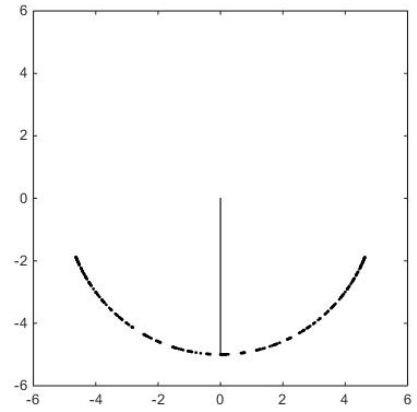
- **Numerical Solution**

The equations of motion found with the above methods, will now solved numerically using a computer. The formulation of the equation of motion found with the Lagrangian and Kane's method is used for this simulation since these are most conveniently solved. Since this equation of motion is a second-order differential equation, two initial conditions have to be specified in order to solve it; $\theta(0)$ and $\dot{\theta}(0)$. Choosing $\theta(0) = 0$ and $\dot{\theta}(0) \in \{0.5, 1.5, 2.5, 3.0\}$, setting $l = 5$ and solving for $t \in [0, 100]$ gives the following figures:

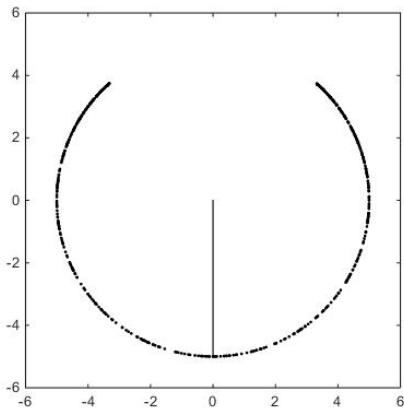
In the simulations, the object attached to the pendulum is considered a point mass with no dimensions.



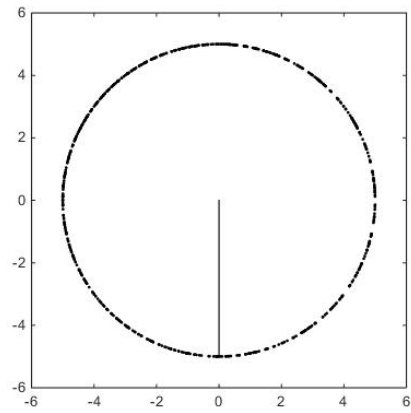
(a) $\dot{\theta}(0) = 0.5$



(b) $\dot{\theta}(0) = 1.5$



(c) $\dot{\theta}(0) = 2.5$



(d) $\dot{\theta}(0) = 3.0$

Figure 10.0.1: Planar pendulum simulation with 0-dimensional object

11. Appendix B

Equation (5.1.3):

$$\begin{aligned}
 \beta_1(\boldsymbol{\theta}) &= 0 \\
 \beta_2(\boldsymbol{\theta}) &= \frac{l}{b'}(c_2c_3(\frac{l}{b'}s_2c_3 + s_4c_5) + c_2s_3(-\frac{b}{b'} + \frac{l}{b'}s_2s_3 + c_4c_5) + s_2(-\frac{l}{b'}c_2 + s_5)) \\
 \beta_3(\boldsymbol{\theta}) &= \frac{l}{b'}(-s_2s_3(\frac{l}{b'}s_2c_3 + s_4c_5) + s_2c_3(-\frac{b}{b'} + \frac{l}{b'}s_2s_3 + c_4c_5)) \\
 \beta_4(\boldsymbol{\theta}) &= c_4c_5(\frac{l}{b'}s_2c_3 + s_4c_5) - s_4c_5(-\frac{b}{b'} + \frac{l}{b'}s_2s_3 + c_4c_5) \\
 \beta_5(\boldsymbol{\theta}) &= s_4s_5(\frac{l}{b'}s_2c_3 + s_4c_5) + c_4s_5(-\frac{b}{b'} + \frac{l}{b'}s_2s_3 + c_4c_5) - c_5(-\frac{l}{b'}c_2 + s_5).
 \end{aligned}$$

Equation (5.1.4):

$$\dot{\theta}_5 = \left(\frac{-I_{45} \boldsymbol{\beta}(\boldsymbol{\theta})}{\mathbf{e}_5^T \boldsymbol{\beta}(\boldsymbol{\theta})} \right)^T I_{45} \dot{\boldsymbol{\theta}}.$$

Define: $\boldsymbol{\gamma}(\boldsymbol{\theta}) = \frac{-I_{45} \boldsymbol{\beta}(\boldsymbol{\theta})}{\mathbf{e}_5^T \boldsymbol{\beta}(\boldsymbol{\theta})}$.

$$\dot{\theta}_5 = \boldsymbol{\gamma}^T(\boldsymbol{\theta}) I_{45} \dot{\boldsymbol{\theta}}.$$

Equation (5.1.5):

$$N_{\mathbf{n}}^{\tilde{\mathbf{n}}}(\boldsymbol{\theta}) = \begin{pmatrix} s_1c_4 + c_1s_4s_5 & c_1c_4 - s_1s_4s_5 & -s_4c_5 \\ -s_1s_4 + c_1c_4s_5 & -c_1s_4 - s_1c_4s_5 & -c_4c_5 \\ -c_1c_5 & s_1c_5 & -s_5 \end{pmatrix}.$$

Equation (5.1.7):

$$N_{\mathbf{n}}^{\mathbf{b}}(\boldsymbol{\theta}) \cdot N_{\mathbf{n}}^{\tilde{\mathbf{n}}}(\boldsymbol{\theta}) = N_{\mathbf{n}}^{\mathbf{b}}(\boldsymbol{\theta})$$

Equation (5.1.9):

$$S_{145} = \begin{pmatrix} 1 & 0 & 0 & 0 & 0 \\ 0 & 0 & 0 & 1 & 0 \\ 0 & 0 & 0 & 0 & 1 \end{pmatrix},$$

such that

$$S_{145} \dot{\boldsymbol{\theta}} = \begin{pmatrix} \dot{\theta}_1 \\ \dot{\theta}_4 \\ \dot{\theta}_5 \end{pmatrix}.$$

Equation (5.1.11): The transformation between the bases N and B has been defined as:

$$B = N_{\mathbf{n}}^{\mathbf{b}}(\boldsymbol{\theta}) N = N_{\mathbf{n}}^{\mathbf{b}}(\boldsymbol{\theta}) N ,$$

using that $N = I_3$. From this it follows that:

$$\begin{aligned} B [\boldsymbol{\omega}]_B &= N [\boldsymbol{\omega}]_N \iff \\ [\boldsymbol{\omega}]_B &= B^{-1} N [\boldsymbol{\omega}]_N \iff \\ &= (N_{\mathbf{n}}^{\mathbf{b}}(\boldsymbol{\theta}))^{-1} N [\boldsymbol{\omega}]_N \iff \\ &= (N_{\mathbf{n}}^{\mathbf{b}}(\boldsymbol{\theta}))^{-1} [\boldsymbol{\omega}]_N \iff \\ &:= N_{\mathbf{b}}^{\mathbf{n}}(\boldsymbol{\theta}) [\boldsymbol{\omega}]_N \iff \end{aligned}$$

Equation (5.1.17):

$$V(\boldsymbol{\theta}) = \begin{pmatrix} v_{11} & \cdots & v_{15} \\ \vdots & \cdots & \vdots \\ v_{31} & \cdots & v_{35} \end{pmatrix} ,$$

where:

$$\begin{aligned} v_{11} &= r s_{\lambda}(c_1 c_4 - s_1 s_4 s_5) \\ v_{12} &= l c_2 c_3 \\ v_{13} &= -l s_2 s_3 \\ v_{14} &= r(s_{\lambda}(-s_1 s_4 + c_1 c_4 s_5) + c_{\lambda} c_4 c_5) \\ v_{15} &= r(-c_{\lambda} s_4 s_5 + s_{\lambda} c_1 s_4 c_5) \\ v_{21} &= -r s_{\lambda}(c_1 s_4 + s_1 c_4 s_5) \\ v_{22} &= l c_2 s_3 \\ v_{23} &= l s_2 c_3 \\ v_{24} &= -r(s_{\lambda} s_4 c_5 + s_{\lambda}(s_1 c_4 + c_1 s_4 s_5)) \\ v_{25} &= r(s_{\lambda} c_1 c_4 c_5 - c_{\lambda} c_4 s_5) \\ v_{31} &= r s_{\lambda} s_1 c_5 \\ v_{32} &= l s_2 \\ v_{33} &= 0 \\ v_{34} &= 0 \\ v_{35} &= r(c_{\lambda} c_5 + s_{\lambda} c_1 s_5) \end{aligned}$$

Equation (5.1.18):

$$\dot{V}(\boldsymbol{\theta}) = \frac{d}{dt} V(\boldsymbol{\theta}) = \begin{pmatrix} \dot{v}_{11} & \cdots & \dot{v}_{15} \\ \vdots & \cdots & \vdots \\ \dot{v}_{31} & \cdots & \dot{v}_{35} \end{pmatrix} ,$$

where:

$$\begin{aligned}
\dot{v}_{11} &= -rs_\lambda((s_1c_4 + c_1s_4s_5)\dot{\theta}_1 + (c_1s_4 + s_1c_4s_5)\dot{\theta}_4 + s_1s_4c_5\dot{\theta}_5) \\
\dot{v}_{12} &= -l(s_2c_3\dot{\theta}_2 + c_2 + s_3\dot{\theta}_3) \\
\dot{v}_{13} &= -l(c_2s_3\dot{\theta}_2 + s_2c_3\dot{\theta}_3) \\
\dot{v}_{14} &= r(-s_\lambda(c_1s_4 + s_1c_4s_5)\dot{\theta}_1 - (s_\lambda s_1c_4 + s_\lambda c_1s_4s_5 + c_\lambda s_4c_5)\dot{\theta}_4 + (s_\lambda c_1c_4c_5 - c_\lambda c_4s_5)\dot{\theta}_5) \\
\dot{v}_{15} &= r(-s_\lambda s_1s_4c_5\dot{\theta}_1 + (s_\lambda c_1c_5 - c_\lambda s_5)c_4\dot{\theta}_4 - (c_\lambda s_4c_5 + s_\lambda c_1s_4s_5)\dot{\theta}_5) \\
\dot{v}_{21} &= -rs_\lambda((c_1c_4s_5 - s_1s_4)\dot{\theta}_1 + (c_1c_4 - s_1s_4s_5)\dot{\theta}_4 + s_1c_4c_5\dot{\theta}_5) \\
\dot{v}_{22} &= l(-s_2s_3\dot{\theta}_2 + c_2c_3\dot{\theta}_3) \\
\dot{v}_{23} &= l(c_2c_3\dot{\theta}_2 - s_2s_3\dot{\theta}_3) \\
\dot{v}_{24} &= -r(s_\lambda(c_1c_4 - s_1s_4s_5)\dot{\theta}_1 + (c_\lambda c_4c_5 - s_\lambda s_1s_4 + s_\lambda c_1c_4s_5)\dot{\theta}_4 + (s_\lambda c_1s_4c_5 - c_\lambda s_4s_5)\dot{\theta}_5) \\
\dot{v}_{25} &= r(-s_\lambda s_1c_4c_5\dot{\theta}_1 + (c_\lambda s_5 - s_\lambda c_1c_5)s_4\dot{\theta}_4 - (s_\lambda c_1c_4s_5 + c_\lambda c_4c_5)\dot{\theta}_5) \\
\dot{v}_{31} &= rs_\lambda(c_1c_5\dot{\theta}_1 - s_1s_5\dot{\theta}_5) \\
\dot{v}_{32} &= lc_2\dot{\theta}_2 \\
\dot{v}_{33} &= 0 \\
\dot{v}_{34} &= 0 \\
\dot{v}_{35} &= r(-s_\lambda s_1s_5\dot{\theta}_1 + (s_\lambda c_1c_5 - c_\lambda s_5)\dot{\theta}_5)
\end{aligned}$$

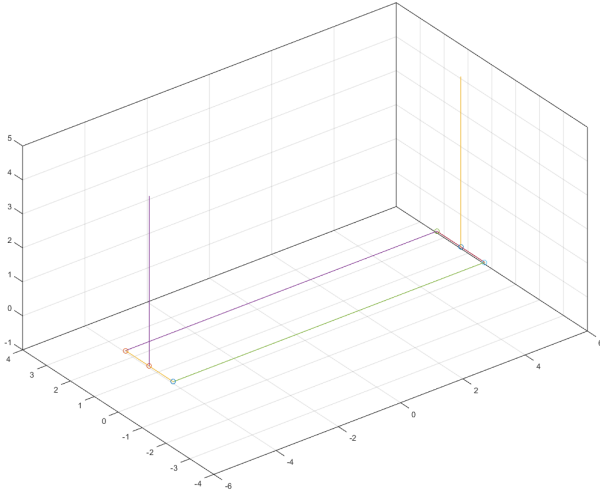
Equation (5.1.25):

$$\mathbf{T} = B [\mathbf{T}]_B = N_n^b(\boldsymbol{\theta}) [\mathbf{T}]_B ,$$

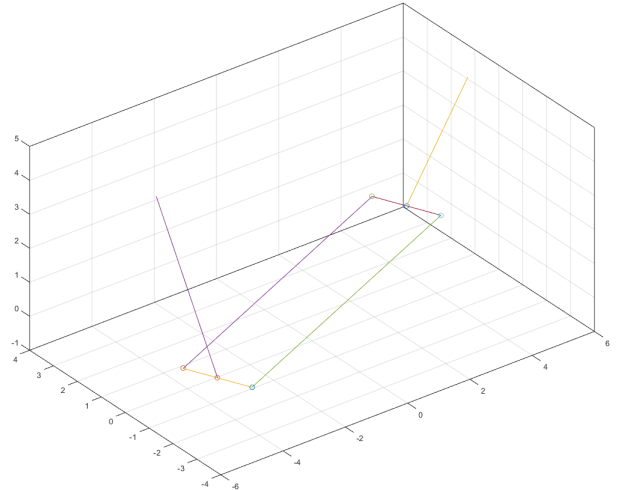
where from Euler's equation it follows $[\mathbf{T}]_B$ can be determined by:

$$[\mathbf{T}]_B = -(\mathbf{I} [\boldsymbol{\alpha}]_B + [\boldsymbol{\omega}]_B \times (\mathbf{I} [\boldsymbol{\omega}]_B)) .$$

Solving equation (5.2.13) numerically for initial values $\theta(0) = 0, \dot{\theta}(0) = 1$ results in the following two figures.



(a) Position at rest



(b) Position at maximum angle θ

Bibliography

- [1] Matt R. Jardin, Eric R. Mueller (2007). *Optimized Measurements of UAV Mass Moment of Inertia with a Bifilar Pendulum*, United States of America: American Institute of Aeronautics and Astronautics
- [2] Patrick Hamill (2014). *A Student's Guide to Lagrangians and Hamiltonians*, United States of America: Cambridge University Press
- [3] T. R. Kane, Gan-Tai Tseng (1966). *Dynamics of the bifilar pendulum*, United States of America: Division of Engineering Mechanics, Stanford University, Stanford, California
- [4] www.cs.cmu.edu/~delucr/kane.doc